Decoding Ankyrin-G Targeting and Function

by

Meng He

Department of Pharmacology and Cancer Biology
Duke University

Date:_____

Approved:

_____
Vann Bennett, Supervisor

_____
Michel Bagnat

_____
Marc Caron

_____
Bernard Mathey-Prevot

_____
Christopher Nicchitta

Dissertation submitted in partial fulfillment of
the requirements for the degree of Doctor
of Philosophy in the Department of
Pharmacology and Cancer Biology in the Graduate School
of Duke University

2014

ABSTRACT

Decoding Ankyrin-G Targeting and Function

by

Meng He

Department of Pharmacology and Cancer Biology
Duke University

Date:_____

Approved:

_____
Vann Bennett, Supervisor

_____
Michel Bagnat

_____
Marc Caron

_____
Bernard Mathey-Prevot

_____
Christopher Nicchitta

An abstract of a dissertation submitted in partial fulfillment of
the requirements for the degree of Doctor
of Philosophy in the Department of
Pharmacology and Cancer Biology in the Graduate School
of Duke University

2014

Abstract

The spectrin-ankyrin network assembles diverse plasma membrane domains including axon initial segments and nodes of Ranvier, cardiomyocyte T-tubules and intercalated discs, epithelial lateral membranes, costameres and photoreceptor inner and outer segments. However the mechanism that targets the spectrin-ankyrin network to those plasma membrane domains is unknown. This thesis identifies two lipid inputs from protein palmitoylation and phosphoinositides that together control the precise localization of the spectrin-ankyrin network. In Chapter 2, we identify a linker peptide encoded by a single divergent exon that distinguishes the subcellular localization of ankyrin-B and -G by selectively suppressing protein binding through autoinhibition. In Chapter 3, we demonstrate that ankyrin-G is S-palmitoylated at a conserved C70 residue which is required to assemble epithelial lateral membranes and neuronal axon initial segments. We continue to interrogate how palmitoylation regulates ankyrin-G activities in Chapter 4, and identify DHHC5 and DHHC8 as the palmitoyltransferases in MDCK cells. We showed that palmitoylated ankyrin-G, in concert with phosphoinositide lipids, determines the polarized localization of beta II spectrin though a co-incidence detection mechanism. This palmitoyltransferases/ ankyrin-G/beta II spectrin pathway determines the cell height of columnar epithelial cells. In Chapter 5, we elucidated the molecular mechanism through which the spectrin-ankyrin network assembles epithelial lateral

membranes. We demonstrated that ankyrin-G and beta II spectrin function by opposing clathrin-mediated endocytosis to build the lateral membrane in MDCK cells. Together, this thesis dissects the mechanisms of how the spectrin-ankyrin network achieves precise membrane targeting and how it assembles lateral membranes to determine the morphogenesis of columnar epithelial cells, and provides the first molecular insight to understand how cells control the assembly of diverse plasma membrane domains.

Dedication

This is dedicated to my parents and my wife Yifan for their endless support and love.

Contents

List of Tables

List of Figures

List of Abbreviations

AnkG	Ankyrin-G
AnkB	Ankyrin-B
AnkR	Ankyrin-R
ABD	Ankyrin-binding domain
MDCK	Madin-Darby canine kidney
HBE	Human Bronchial Epithelial
AIS	Axon initial segment
LDL	Low density lipoproteins
CH	Calponin homology domain
PH	Pleckstrin homology domain
SH3	The SRC Homology 3
ZU5	Domain present in ZO-1 and Unc5-like netrin receptors
PI(4,5)P2	Phosphatidylinositol 4,5-bisphosphate
PI3P	Phosphatidylinositol 3-phosphate
PI4P	Phosphatidylinositol 4-phosphate
STORM	Stochastic optical reconstruction microscopy
SCA5	Spinocerebellar ataxia type 5
SPARCA1	Spectrin-associated Autosomal Recessive Cerebellar Ataxia type 1

CAMKII	Calmodulin-Dependent Protein Kinase II
OHC	Outer hair cells
GFP	Green fluorescent protein
DHHC	Asp-His-His-Cys
MS	Mass spectrometry
FRAP	Fluorescence recovery after photobleaching
ZO-1	Zona occludens protein 1
NEM	N-Ethylmaleimide
FITC	Fluorescein iso- thiocyanate
CHC	Clathrin heavy chain

Acknowledgements

My PhD training at Duke University is a wonderful journey, and what has made this journey even more enjoyable is the scientific and personal support from numerous people. First of all, I want to express my sincere gratitude to my advisor Dr. Vann Bennett. Without his scientific vision, patient mentorship and support, I would never have gone so far in science and achieved so much. I feel extremely lucky to have the opportunity to learn science from someone like him, his guidance over the past 4 years has provided a solid foundation for my professional development. I also want to thank everyone in the Bennett Lab----Jonathan Davis, Janell Hostettler, Damaris Lorenzo, Paul Jenkins, Weichou Tseng, Kathryn Walder, Fangfei Qu, Glenda Johnson and Erica Robinson----for their technical and intellectual support, as well as my committees, Dr. Michel Bagnat, Dr. Marc Caron, Dr. Bernard Mathey-Prevot and Dr. Christopher Nicchittafor for their valuable advice and suggestions. Last but not least, I want to give my special appreciation to my lovely and wonderful wife, Yifan Shang for her endless love and support. Over the past a few years, she has been staying with me to overcome many challenges, I cannot imagine a life without her.

Chapter 1. Background and Overview

1.1 Plasma membrane domains

The plasma membrane provides a structural and functional basis for cells to interact with surrounding environment. The conventional view of plasma membrane was depicted by Singer and Nicolson as the "fluid mosaic" model (Singer and Nicolson, 1972), where membrane proteins are incorporated into lipid bilayers, and are in constant motion. This model provides a biophysical foundation to understand the structure and dynamics of plasma membranes. However, at organismal level, when the cells are integrated into three dimensional tissues, the cellular plasma membranes are precisely organized into unique membrane domains that are enriched in functionally related proteins and lipids (Bennett and Healy, 2008). Even at single cell level, taking the yeast as an example, the plasma membrane is also highly patterned into distinct patches (Berchtold and Walther, 2009; Spira et al., 2012). The "fluid mosaic" model does not explain how the membrane proteins achieve specific segregation patterns in the lipid bilayers and how the patterns are properly maintained and adapted for cellular functions.

Those plasma membrane domains are critical for physiological functions including but not limited to mechanical support, water and salt homeostasis and electrical signaling. Examples include neuronal axon initial segments, epithelial lateral membranes and cardiomyocyte transverse tubules (Bennett and Healy, 2008). In order to

maintain the integrity and identity of those plasma membrane domains, a group of functionally related membrane proteins need to be delivered, segregated and maintained to those membrane regions (Grubb and Burrone, 2010; Nejsum and Nelson, 2009; Rasband, 2011; Salle and Brette, 2007). Even though proteins and lipids that are enriched in those membrane domains have been identified, the molecular mechanisms that control the assembly and maintenance of those domains remain elusive. A few models have been proposed to address these questions, but require further investigation.

1.2 Clathrin-mediated editing in maintaining membrane polarity

Clathrin was identified from purified coated vesicles (Pearse, 1975), and its function was first elucidated in the uptake of plasma low density lipoproteins (LDL) (Anderson et al., 1977; Anderson et al., 1978; Brown and Goldstein, 1976; Goldstein and Brown, 1977). The clathrin lattice is linked to the vesicles through adaptor proteins, which bind directly to the phospholipid components or proteins embedded in the vesicle membrane (Bonifacino and Lippincott-Schwartz, 2003; Kalthoff et al., 2002a; Kalthoff et al., 2002b). The canonical function of clathrin is to coat membrane vesicles at the plasma membrane and transport proteins and lipids into intracellular compartments (Mousavi et al., 2004; Takei and Haucke, 2001). It was also shown that the clathrin-coated vesicles can carry proteins and lipids from the trans-Golgi network to lysosomes

(Hirst and Robinson, 1998; Kirchhausen, 1999), as well as the related vesicular/tubular structures (Bonifacino and Lippincott-Schwartz, 2003).

In contrast to the conventional function of clathrin, the discovery of basolateral targeting motifs which mimic the endocytosis signals recognized by the clathrin adaptors (Casanova et al., 1991; Hunziker et al., 1991; Mostov et al., 1986) has led to the hypothesis that clathrin is required for the establishment of cell polarity through direct protein sorting (Bonifacino, 2014; Bonifacino and Traub, 2003; Deborde et al., 2008; Farias et al., 2012; Folsch et al., 2003). However, many of the studies relied on exogenous proteins such as the LDL receptor, transferrin receptor and VSV-G viral coat protein (Deborde et al., 2008; Gravotta et al., 2012; Rodriguez Boulan and Sabatini, 1978). For the endogenous proteins, loss of clathrin heavy chain in MDCK cells only led to partial mislocalization of E-cadherin or no detectable effect on the Na/K ATPase (Deborde et al., 2008). Moreover, E-cadherin and Na/K ATPase both sort to the lateral membranes of LLC-PK cells lacking AP1B, which was proposed to be an epithelial-specific clathrin AP1 adaptor (Folsch et al., 1999; Ohno et al., 1999), suggesting the existence of an AP1B-independent mechanism (Duffield et al., 2004; Miranda et al., 2001). Knockout of either the mu-1B subunit or Rab8, which regulates AP1B dependent basolateral transport, does not affect epithelial morphology in mouse tissues (Sato et al., 2007; Takahashi et al., 2011). Surprisingly, the μ1B KO mice and AP1-deficient C. elegans also showed

abnormal apical protein sorting (Hase et al., 2013; Shafaq-Zadah et al., 2012; Zhang et al., 2012), which is inconsistent with its proposed function in basolateral sorting.

Given the fact that the initial plasma membrane localization of many proteins is not affected by clathrin/AP knockdown (Bonifacino, 2014), clathrin may function as editing machinery instead of sorting machinery to establish cell polarity. Indeed recent study of E-cadherin polarity in MDCK cells has shown that polarity motif of the cytoplasmic domain of E-cadherin can be recognized by both clathrin adaptors and ankyrin-G which work coordinately to regulate E-cadherin polarity (Jenkins et al., 2013). Part of this thesis will focus on addressing how the ankyrin/spectrin lattice functions as the molecular machinery, opposing clathrin-mediated endocytosis, to build epithelial lateral membranes.

1.3 Lipid rafts

Another model that has been proposed to understand the plasma membrane organization is lipid rafts. This model was introduced to explain the establishment of the glycolipid enriched epithelial apical membranes (Simons and van Meer, 1988). Lipid rafts are defined as sterol and sphingolipid-enriched membrane regions that can organize protein-protein interaction, protein-lipid interaction and lipid-lipid interaction at a nano-scale (Simons and Sampaio, 2011). Those lipid rafts have been proposed to play a role in signal transduction, apoptosis, cell adhesion and migration and synaptic

transmission (Brown and London, 1998; Harris and Siu, 2002; Simons and Toomre, 2000; Tsui-Pierchala et al., 2002).

Due to the technical challenges of detecting lipid rafts, this concept has raised many controversies. At early stage of this field, the most common method used for lipid raft detection was the resistance to cold Triton X-100 solubilization and sensitivity to cholesterol depletion, which now are considered artificial (Brown and Rose, 1992; Edidin, 2003; Heerklotz, 2002; Munro, 2003; Pizzo et al., 2002; Yu et al., 1973). Model membranes such as giant unilamellar vesicle were also widely used to address membrane lipid phase separations (Lentz et al., 1980; Simons and Vaz, 2004). This system was considered non-physiological because it lacks the complexity and many biophysical properties of biological bilayers. For instance, giant unilamellar vesicles normally only contain one or two homogeneous phospholipids, whereas the biological bilayers contains diverse components such as the long acyl lipid chains and integral proteins which can potentially perform self-organization within the bilayer (Munro, 2003).

More recently, with modern imaging technologies, some studies have revealed the existence of cholesterol-dependent sphingolipids and the GPI-anchored protein clusters that mimic the lipid rafts (Roduit et al., 2008; Sezgin and Schwille, 2011). However, there is great inconsistency about the lifetime of those observed nanoscale

assemblies, ranging from milliseconds to seconds (Brameshuber et al., 2010; Kusumi et al., 2004), raising the arguments of the identities of those structures.

The lipid raft model emphasizes the separation and organization of lipid and protein components in the membrane at nanoscale. However, it has also been shown that the proteins on the plasma membrane can be segregated or organized into large scale microdomains. For instance, in yeast, most of the plasma membrane associated proteins are distributed non-homogeneously into distinct patterns (Spira et al., 2012).

1.4 Spectrin- and ankyrin-based membrane domain assembly

The spectrin-ankyrin network forms a membrane skeleton underneath the plasma membrane in erythrocytes and provides mechanical supports for the cells to adapt to environmental stress (Bennett and Baines, 2001; Liu et al., 1987). The micron-scale organization of diverse membrane-spanning proteins such as adhesion molecules and ion channels through the spectrin-ankyrin network also provides a functional support for the cells to sense extracellular signals (Bennett and Healy, 2008; Bennett and Healy, 2009; Bennett and Lorenzo, 2013). The spectrin-ankyrin partnership was first characterized in human erythrocytes (Bennett and Baines, 2001), and subsequently elucidated in organizing multiple membrane domains (Figure 1), including axon initial segments and nodes of Ranvier (Dzhashiashvili et al., 2007; Galiano et al., 2012; Hedstrom et al., 2008; Hedstrom et al., 2007; Jenkins and Bennett, 2001; Sobotzik et al., 2009; Susuki et al., 2013; Zhang and Bennett, 1998; Zhang et al., 1998), unmyelinated

axons (Scotland et al., 1998), cardiomyocyte T-tubules and intercalated discs (Hund et al., 2010; Lowe et al., 2008; Mohler et al., 2005; Mohler et al., 2004c), epithelial lateral membranes (Kizhatil and Bennett, 2004; Kizhatil et al., 2007a; Kizhatil et al., 2007b), costameres (Ayalon et al., 2008; Ayalon et al., 2011), and photoreceptor inner and outer segments (Kizhatil et al., 2009a; Kizhatil et al., 2009b).

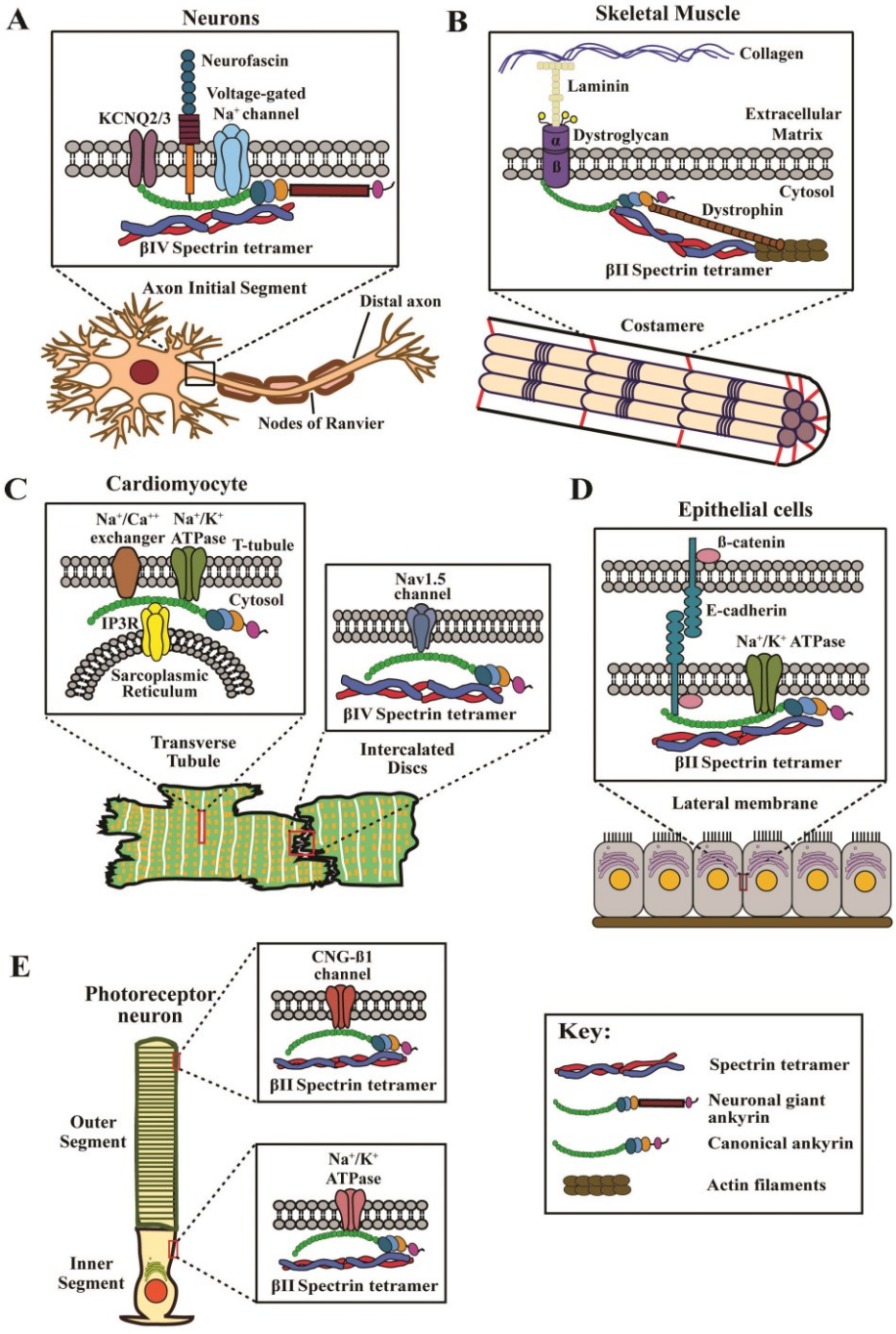

Figure 1: Spectrin-ankyrin-based plasma membrane domains

(From Bennett and Lorenzo, 2013)

1.4.1 Spectrin

Spectrin consists of alpha and beta subunits that assemble side-to-side antiparallely to form a heterodimer which can further form an extended 200nm tetramer through end-to-end interaction (Baines, 2009; Bennett and Baines, 2001; Bennett and Lorenzo, 2013; Shotton et al., 1979). The human genome encodes two alpha-spectrins that contain a calmodulin-related domain at the C-terminus, a series of spectrin repeats, and an SRC Homology 3 (SH3) domain (Bennett and Baines, 2001). Five beta spectrin genes are identified in human genome, the beta spectrins are capable of binding to F-actin through the N-terminal calponin homology (CH) domains (Banuelos et al., 1998; Djinovic Carugo et al., 1997), to ankyrin through the 14th and 15th spectrin repeats (Davis et al., 2009; Ipsaro et al., 2009; Kennedy et al., 1991; Stabach et al., 2009), and to PI(4,5)P2 phosphatidylinositol lipids through a C-terminal pleckstrin homology (PH) domain (Hyvonen et al., 1995; Macias et al., 1994). See Figure 2 for details.

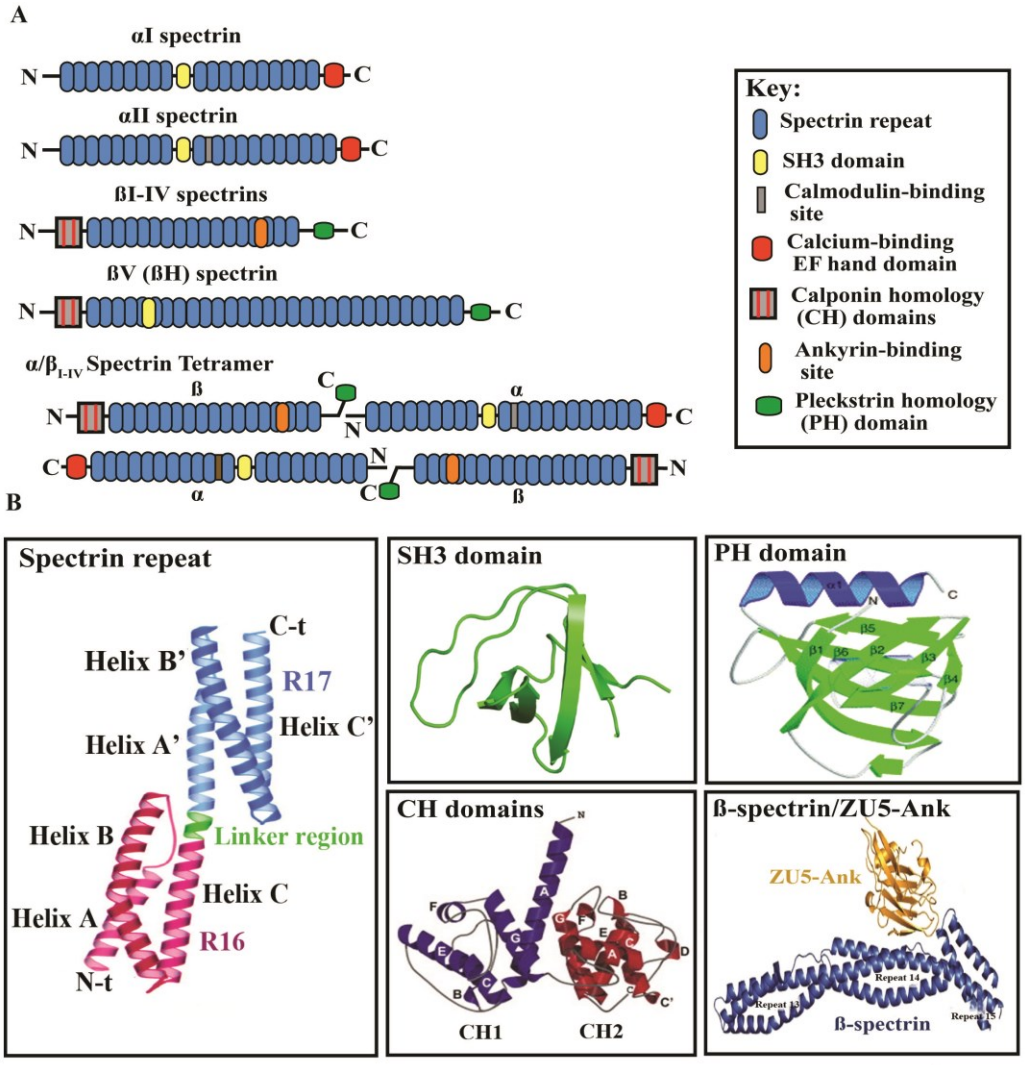

Figure 2: Domain organization of spectrin molecules

(From Bennett and Lorenzo, 2013)

The presence of beta-spectrins in sponge and placozoa genomes suggests its earlier appearance than ankyrin (Baines, 2009; Bennett and Lorenzo, 2013). These spectrins have similar domain organizations as the vertebrate spectrins, but have no

recognizable ankyrin-binding site (Davis et al., 2009; Ipsaro and Mondragon, 2010), indicating that the ankyrin binding appeared later during evolution and may contribute to spectrin activities in more complex tissue. An evident ankyrin binding site on beta spectrin emerged in *Cnidarians*, which also contains ankyrin-like sequences, including a ZU5 domain with a potential spectrin-binding site. Therefore the proto-type of this spectrin-ankyrin network may appear 555 million years ago when the first bilaterian fossil dated to (Baines, 2009; Bennett and Lorenzo, 2013). Given this evidence from evolutional analysis, the spectrin-ankyrin network gained its ability to organize membrane-spanning proteins during the evolution of bilaterians when the multicellular organisms require more complicated tissue.

The cDNA of beta I spectrin was first isolated and characterized in red blood cells, where it lacks the C-terminal PH domain (Winkelmann et al., 1990a). It is the major isoform of beta spectrin lattice in erythrocytes, and relies on ankyrin binding to associate with the plasma membrane (Bennett, 1982; Bennett and Stenbuck, 1979). Deficiency in assembling the spectrin lattice or linking the spectrin lattice to the plasma membrane in red blood cells results in severe hemolytic anemia (Agre et al., 1981; Winkelmann and Forget, 1993).

Beta II spectrin was first isolated from brain tissue, and has been shown to have a broad expression pattern (Bennett et al., 1982; Hu et al., 1992). Knockout of a beta II spectrin/ELF results in embryonic lethality in mice and leads to disruption of TGF-beta

signaling by interfering with the nuclear localization of Smad proteins (Tang et al., 2003; Tang et al., 2005). Recently, it is also shown that the inactivation of TGF-beta signaling pathway by beta II spectrin deficiency is also responsible for the abnormal heart development (Lim et al., 2014). In epithelial cells, beta II spectrin collaborates with ankyrin-G to establish the lateral membrane domain (Kizhatil et al., 2007b). Loss of βII spectrin in neuronal axons also disrupts the paranodal barrier that is required for myelinated axon domain organization (Zhang et al., 2013). Beta II spectrin, together with ankyrin-B and alpha II spectrin, assembles a distal axonal submembranous cytoskeleton that defines a boundary limiting ankyrin-G to the proximal axon (Galiano et al., 2012). Stochastic Optical Reconstruction Microscopy (STORM) recently revealed that the actin-spectrin skeleton in axons formed ring-like structures that were evenly spaced with a periodicity of ~180 to 190 nanometers (Xu et al., 2013).

Beta III spectrin was first identified in brain (Ohara et al., 1998; Stankewich et al., 1998). It is highly expressed in the cerebellum and mutation of this gene in human results in spinocerebellar ataxia type 5 (SCA5) (Ikeda et al., 2006). In addition to its function in the cerebellum, beta III spectrin is also implicated in cortical brain development and cognition, deficiency of this gene leads to a novel recessive ataxic syndrome, Spectrin-associated Autosomal Recessive Cerebellar Ataxia type 1 (SPARCA1) (Lise et al., 2012). A recent study suggests that beta III spectrin is critical for the recruitment and maintenance of ankyrin R at the plasma membrane of Purkinje cell

dendrites. Mutations associated with SCA5 showed a reduced ability to maintain ankyrin-R levels at the cell membrane (Clarkson et al., 2014).

Beta IV spectrin is highly expressed in brain (Berghs et al., 2000) where it colocalizes and interacts with ankyrin-G at axon initial segments and nodes of Ranvier to stabilize the membrane proteins (Jenkins and Bennett, 2001; Komada and Soriano, 2002). Homozygous mice carrying a null mutation in the beta IV spectrin gene exhibit tremors and contraction of hindlimbs (Komada and Soriano, 2002; Parkinson et al., 2001). Beta IV spectrin differs from beta I, II, III spectrins that it has additional sequence between the last spectrin repeat and the C-terminal PH domain (Berghs et al., 2000). This extra sequence can interact with calmodulin-dependent protein kinase 2 (CAM kinase 2) and recruits CAM kinase 2 to cardiac interacalated discs and axon initial segments (Hund et al., 2010).

Beta V spectrin is the most divergent isoform and lacks ankyrin binding activity. The gene for beta V spectrin was first isolated from a human retina cDNA library (Stabach and Morrow, 2000). It is a homolog of the Drosophila and Caenorhabditis elegans beta H (heavy) spectrin, and has up to 30 spectrin repeats (Stabach and Morrow, 2000). This beta spectrin isoform can dimerize with alpha II spectrin and localize to apical domains of epithelial tissues such as small intestine (Glenney et al., 1983). Beta H spectrin lacks ankyrin-binding activity and has been shown to interact with several subunits of the microtubule-based motor proteins, kinesin II and the dynein complex,

therefore contributing to protein transport in photoreceptors (Papal et al., 2013). Moreover, the alpha II-beta V spectrin can directly interact with multiple components of the outer hair cell (OHC) cortical lattice, playing a role in organizing the sound-induced electromotility of OHCs (Legendre et al., 2008).

1.4.2 Ankyrin

The ankyrin family has three members, ankyrin-R, ankyrin-B and ankyrin-G encoded by *ANK1, ANK2* and *ANK3* respectively (Bennett and Baines, 2001; Bennett and Healy, 2008). The three mouse homologs are encoded by distinct genes located in different chromosomes (Peters et al., 1995). It was proposed that the three vertebrate ankyrins originated from a single ankyrin gene from urochordates (Cai and Zhang, 2006). The canonical ankyrins share highly conserved protein sequences and structures (Figure 3). They preserve a well-recognized ankyrin repeats domain, where multiple protein interactions occur (Bennett and Healy, 2009; Michaely et al., 2002) , followed by a spectrin-binding domain which coordinates the biological interactions with spectrin (Davis et al., 2009; Wang et al., 2012). A death domain with unknown function is also present in all three ankyrin members. Following the death domain is a C-terminal regulatory region with the highest sequence variability. Spliced isoforms of 480/270kD ankyrin-G and 440kD ankyrin-B have an large insert between the UPA domain and Death domain (Chan et al., 1993; Kordeli et al., 1990; Kunimoto, 1995; Kunimoto et al., 1991). Previous studies have shown that ankyrin B C-terminal region can

intramolecularly interact with the ankyrin repeat domain. This intramolecular interaction plays critical role in regulating ankyrin-B functions in cardiomyocytes and neurons (Abdi et al., 2006; Galiano et al., 2012). Despite the significant amino acid identity among three ankyrin members, they maintain unique biological functions *in vivo.*

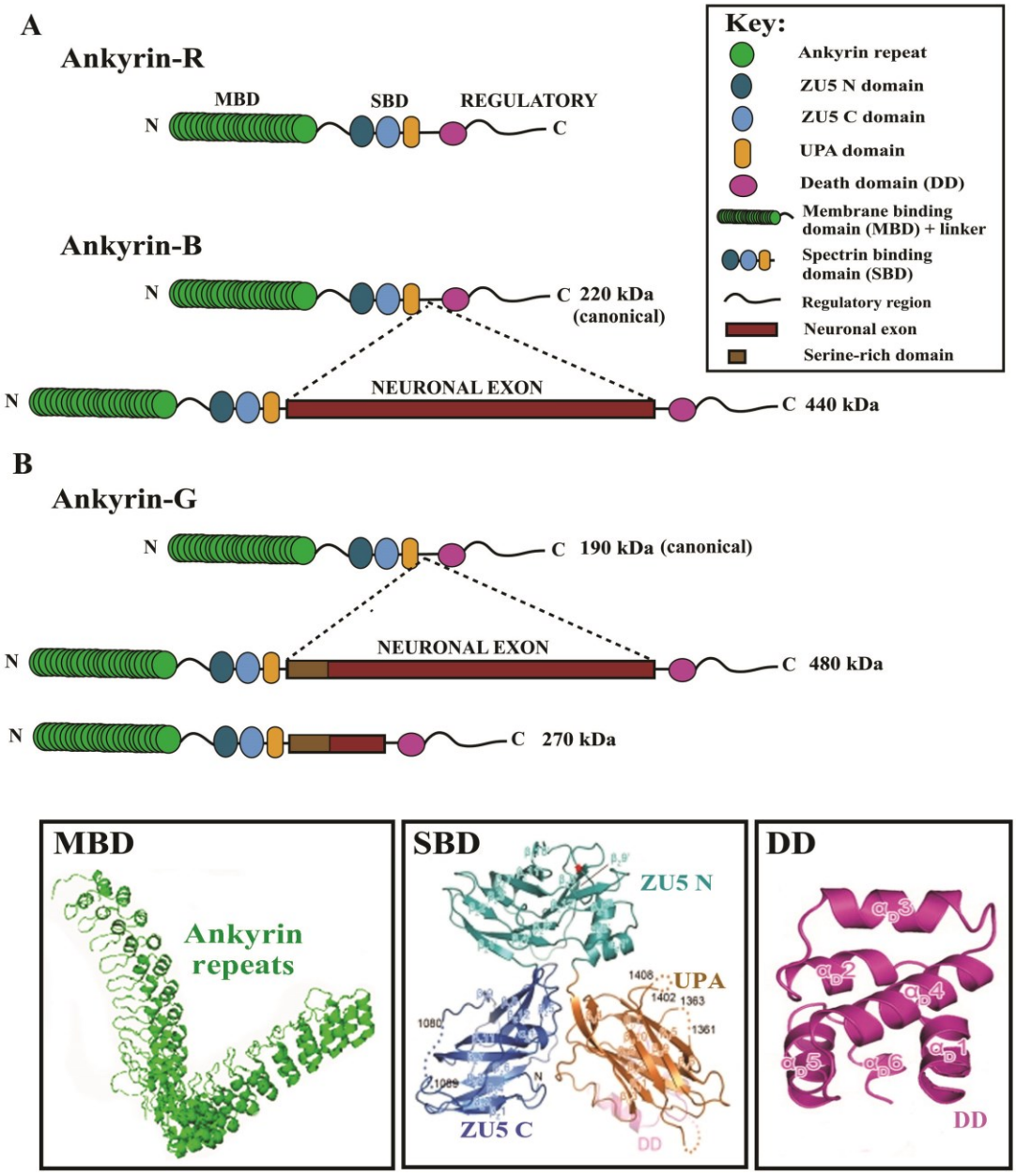

Figure 3: Domain organization of ankyrin molecules

(From Bennett and Lorenzo, 2013)

Ankyrin-R was first identified as the spectrin receptor in erythrocytes (Bennett, 1978; Bennett and Stenbuck, 1979), and is mainly expressed in brain, heart and skeletal muscle (Bennett, 1979; Bennett and Baines, 2001). Ankyrin-R links the underlying spectrin lattice to the plasma membrane in red blood cells by interacting with the transmembrane protein band 3 (anion exchanger 1). Reduction of high affinity membrane binding sites for ankyrin-R was identified in patients with hemolytic poikilocytic anemia (Agre et al., 1981). Genetic studies also indicate that mutations in ankyrin-R are highly responsible for hereditary spherocytosis (Benz, 2010; Edelman et al., 2007; Gallagher et al., 2010; Gundel et al., 2011; Huang et al., 2013; Sangerman et al., 2008).

In contrast, ankyrin-B and ankyrin-G are co-expressed in most, if not all, cell types, but they have no known overlapping functions. Ankyrin-B/-G function in conjunction with spectrin to coordinate plasma membrane domains, and different cells utilize this spectrin-ankyrin interaction differently (Bennett and Healy, 2008; Bennett and Lorenzo, 2013). In rod photoreceptors, ankyrin-G exclusively localizes at the outer segment and plays essential roles in segregating cyclic nucleotide-gated channels, while ankyrin-B is expressed in the inner segment (Kizhatil et al., 2009a). In the costamere of skeletal muscle, the expression and localization of ankyrin-B and ankyrin-G are independent of each other. Ankyrin-B, but not ankyrin-G is required for sarcolemmal localization of dystrophin and dynactin-4 (Ayalon et al., 2008). In neurons, ankyrin-G

and beta IV spectrin colocalize in axon initial segments and nodes of Ranvier and are required to cluster multiple voltage-gated channels and adhesion molecules (Hedstrom et al., 2008; Jenkins and Bennett, 2001; Jenkins and Bennett, 2002; Koticha et al., 2006; Yang et al., 2007), whereas ankyrin-B and beta II spectrin were proposed to assemble a distal axonal cytoskeleton that limits ankyrin-G localization and controls axon initial segment assembly (Galiano et al., 2012).

Though the spectrin-ankyrin network has been widely recognized for its essential roles in organizing plasma membrane domains, the molecular mechanisms underlying the assembly and regulation of this network remains elusive. The main focus of this thesis will address the molecular pathways that ensure the cells to achieve precise subcellular targeting of the spectrin-ankyrin network, and provides mechanistic insights how this network is driving membrane domain assembly.

Chapter 2. A Single Divergent Exon Inhibits Ankyrin-B Association with the Plasma Membrane

2.1 Introduction

As discussed above, the vertebrate ankyrin family contains three members comprised of ankyrin-R, ankyrin-B and ankyrin-G, that are encoded by distinct genes (ANK 1,2,3) with distinct cellular location and functions (Bennett and Baines, 2001). Vertebrate ankyrins evolved from a single ankyrin gene in the invertebrate urochordate *C. intestinalis*, and overall are highly conserved in primary sequence and domain organization (Cai and Zhang, 2006). The N-terminal ANK repeat domain (membrane-binding domain) is involved in diverse protein-protein interactions (Bennett and Healy, 2009). Following the ANK repeat domain, there is a $ZU5_2$-UPA domain module, which includes the beta-spectrin binding site (Davis et al., 2009; Mohler et al., 2004e; Wang et al., 2012). A death domain of unknown function is also present in all three ankyrin members. A C-terminal regulatory domain exhibits the highest diversity among three ankyrins (Bennett and Baines, 2001; Davis et al., 1992; Hall and Bennett, 1987). The ankyrin-B C-terminal region interacts with its ANK repeat domain, and plays a critical role in regulating ankyrin-B functions in cardiomyocytes (Abdi et al., 2006; Mohler et al., 2002a).

Ankyrin-B and ankyrin-G are co-expressed in most tissues, but have distinct cellular localization and function. In rod photoreceptors, ankyrin-G exclusively localizes at the outer segment and is required for segregating cyclic nucleotide-gated channels to

the outer segment (Kizhatil et al., 2009a), while ankyrin-B is expressed in the inner segment where it is required for localization of the sodium/calcium exchanger and Na/K ATPase (Kizhatil et al., 2009b). In skeletal muscle, ankyrin-B is required for delivery of β-dystroglycan to costameres and for a costamere-associated population of microtubules, while ankyrin-G is required to retain β-dystroglycan and dystrophin at costameres (Ayalon et al., 2008). Additionally, ankyrin-G is a master organizer of the axon initial segment and nodes of Ranvier (Hedstrom et al., 2008; Jenkins and Bennett, 2002; Kordeli et al., 1995; Sobotzik et al., 2009), while ankyrin-B localizes to the distal axon together with αII-spectrin and βII-spectrin (Galiano et al., 2012).

The molecular mechanisms underlying distinct functions of ankyrin-B and ankyrin-G remain to be fully elucidated. A previous study showed that the C-terminal region determines the specificity of ankyrin-B function in cardiomyocytes (Mohler et al., 2002a). The ZU5$_2$-UPA module determines the distal axonal localization of ankyrin-B in neurons (Galiano et al., 2012). Here, we adopted a comprehensive domain-substitution strategy to determine effects of exchanging domains or unstructured regions between ankyrin-B and ankyrin-G on their ability to associate with epithelial lateral membranes. This systematic approach led to identification of a heretofore unrecognized ankyrin-B-specific linker peptide connecting the ANK repeats and ZU5$_2$-UPA module that prevents association of ankyrin-B with plasma membranes of epithelial cells and neurons through intramolecular association with ANK repeats.

2.2 Methods and Materials

Reagents

Dynabeads® Protein G for Immunoprecipitation (Catalog Number 10004D) and Lipofectamine® 2000 Transfection Reagent (Catalog Number 11668-027) were purchased from Life Technologies Corporation. QuikChange II XL Site-Directed Mutagenesis Kits (Catalog Number 200522) were purchased from Agilent Technologies. Mouse Monoclonal Anti-HA antibody (Catalog Number H6908) was purchased from Sigma-Aldrich. Rabbit polyclonal anti-GFP antibody was lab-generated. Rabbit polyclonal anti-ankyrin B or -ankyrin G antibody was generated using the C-terminal domain as antigen.

Cloning of Chimeric Ankyrin-B/G constructs

The 1st generation of chimeric GFP tagged Ankyrin-B/G constructs were previously described (Mohler et al., 2002a). In ankyrin-B, the linker region was defined as amino acids 848-960, the ZU5 domains were defined as amino acids 961-1287, the UPA domain was defined as amino acids 1288-1443. In ankyrin-G, the linker region was defined as amino acids 874-984, the ZU5 domains were defined as amino acids 985-1312, the UPA domain was defined as amino acids 1313-1476. Two restriction sites SphI and SpeI were introduced after the linker region and the second ZU5 domain respectively. The corresponding regions in ankyrin-G and ankyrin-B were exchanged using standard cloning protocols.

Transfection and Immunostaining

10^5 MDCK cells were plated on MatTek plates, and the next day the cells were transfected with 50ng of plasmids using lipofectamine® 2000 following the recommended protocol. 24 hours after transfection, cells were washed with cold phosphate-buffered saline (PBS) and fixed with 4% paraformaldehyde at room temperature for 15 minutes, and permeabilized with 0.2% Triton X-100 at room temperature for 10 minutes, followed by a 30-minute blocking in PBS buffer containing 4% bovine serum albumin. Then cells were incubated with primary antibody at 4°C overnight. The next day, cells were washed with PBS buffer three times and then incubated with fluorescence-conjugated secondary antibodies (Alexa Fluor 488, 568 or 663) at room temperature for 2 hours. Fluorescent antibody labeling was visualized using Zeiss LSM 510 or 780 laser scanning microscopes. Images were collected using a 63X NA 1.4 objective lens, and XZ planes were reconstructed from Z stacks with optical sections of 0.5μm.

Membrane recruitment assay

This assay was previously reported (Zhang et al., 1998). Briefly, 10^5 HEK293 cells were plated in collagen-coated MatTek plates. The next day, cells were co-transfected with 100ng HA-tagged neurofascin-186 or E-cadherin plasmids and 80ng GFP-tagged chimeric ankyrin plasmids. 24 hours later, cells were fixed and processed for immunofluorescence as described above.

Co-immunoprecipitation

$6x10^6$ 293T cells were plated in 10cm dishes, and the next day cells were co-transfected with 4μg of plasmid DNA encoding HA-tagged ANK repeat domain of ankyrin-B or ankyrin-G with 2μg of plasmid DNA encoding GFP-tagged B-linker. 48 hours after transfection, cells were collected and lysed in lysis buffer (10mM sodium phosphate, 2mM NaEDTA, 0.32M sucrose and protease inhibitors (10μg/ml AEBSF, 30μg/ml benzamidine, 10μg/ml pepstatin, and 10μg/ml leupeptin), pH=7.4) by passage through a 27G needle. Cell lysates were then centrifuged at 10^5×g for 30 minutes, the supernatant were collected and incubated with protein-G dynabeads preloaded with anti-GFP antibody. Immunoprecipitation samples were then analyzed by SDS-PAGE and western blotting.

Hippocampal neuronal cultures and transfection

Neurons and medium were prepared as described (Baranes et al., 1998). Briefly, hippocampi of P0 mouse pups were isolated, treated with trypsin and then gently triturated through a glass pipette with a fire-polished tip. The dissociated cells were plated onto poly-D-lysine and laminin coated MatTek dishes in Neurobasal-A medium containing 10% fetal bovine serum, B27 supplement, 2mM glutamine and Penicillin/Streptomycin. On the following day, the medium was replaced with fresh serum-free Neurobasal-A medium containing B27, glutamine and Ara-C. Cultured hippocampal neurons at day 5 were transfected with 50ng chimeric ankyrin plasmids

following standard protocol. 48 hours after transfection, cells were fixed in 4% PFA with 4% sucrose, and processed for immunostaining as described above.

Quantification and statistical analysis

The immunofluorescence intensities of plasma membrane or cytoplasmic staining were measured using image J. The intensity ratios were calculated and analyzed using Graphpad Prism6. Student's t-tests or one way ANOVA with Tukey's post-hoc tests were performed for hypothesis testing.

2.3 Results

2.3.1 Ankyrin-B is excluded from the lateral plasma membrane in Human Bronchial Epithelial Cells

Cultured epithelial cells require ankyrin-G for biogenesis of their lateral membranes (Kizhatil and Bennett, 2004). Ankyrin-G in turn requires interaction with βII-spectrin for its function in lateral membrane biosynthesis (Kizhatil et al., 2007b). Ankyrin-B recruits beta-2 spectrin to an intracellular compartment in neonatal cardiomyocytes (Mohler et al., 2004e), but ankyrin-B has not been studied in epithelial cells. Therefore, we used human bronchial epithelial (HBE) cells to compare the localization of ankyrin-G and ankyrin-B.

We first determined the expression and localization of endogenous ankyrin-B and ankyrin-G in HBE cells. An antibody against the C-terminal domain of ankyrin-B detected multiple spliced isoforms, including the 220kDa isoform and a major 55kDa

isoform (Figure 4B). Immunofluorescence showed no ankyrin-B-immunoreactivity on the plasma membrane and instead revealed intracellular vesicles of unknown identity (Figure 4A). Three major ankyrin-G isoforms (one at 210kDa, two at 120kDa) are expressed in HBE cells (Figure 4B), and are mainly concentrated on the plasma membrane, consistent with previous findings (Kizhatil and Bennett, 2004) (Figure 4A). We next compared the localization of transfected 220kDa ankyrin-B-GFP and 190kDa ankyrin-G-GFP in HBE cells. Figure 4C is a scheme showing the structural details of ankyrin proteins, where ankyrin-B domains are highlighted in red and ankyrin-G domains are highlighted in green. 220kDa ankyrin-B-GFP is excluded from the plasma membrane where it is associated with vesicles in a similar pattern as endogenous ankyrin-B, while the 190kDa ankyrin-G predominantly localizes to the lateral membrane (Figure 4D, E).

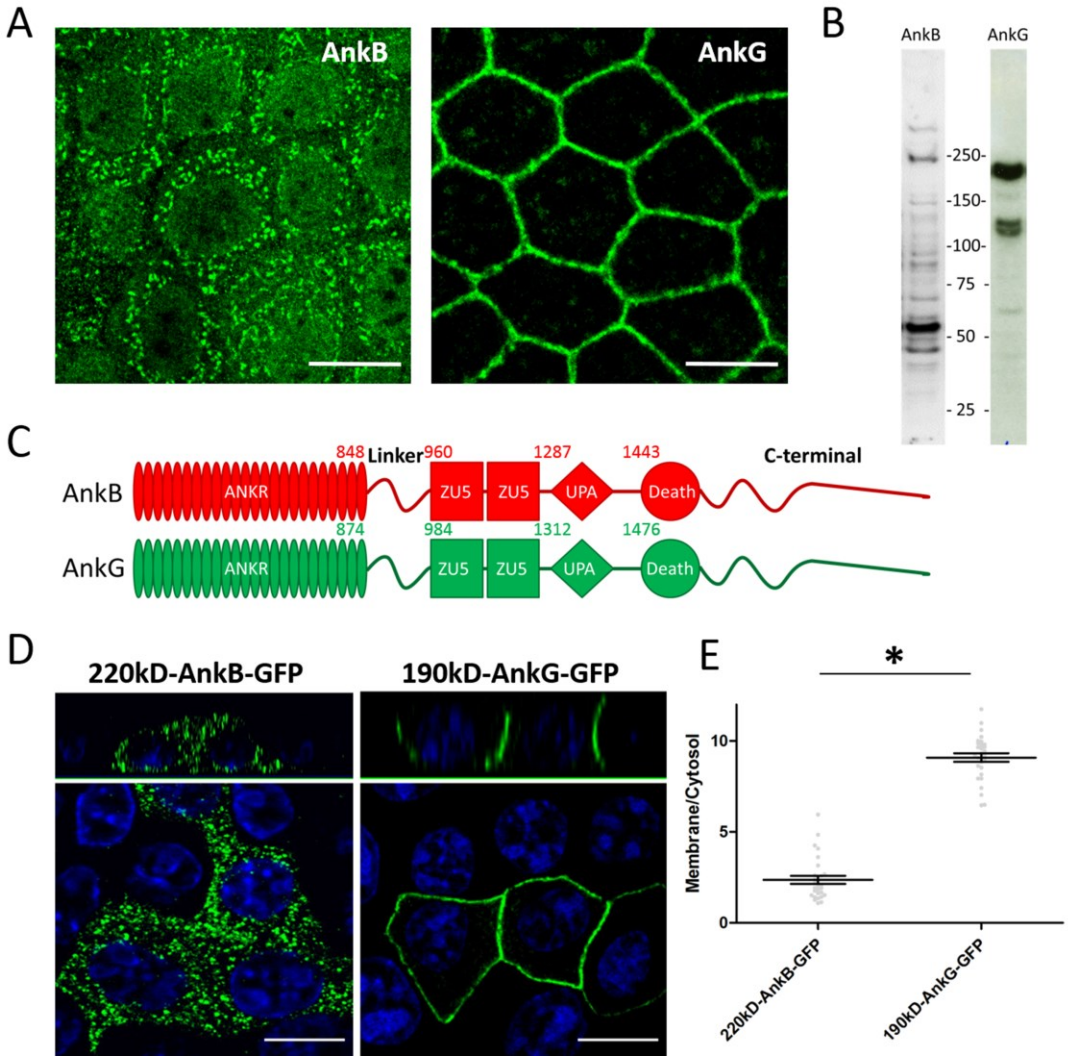

Figure 4: Ankyrin-B is excluded from the lateral membrane of HBE cells

(A), immunofluorescence showing total endogenous AnkB and AnkG in polarized HBE cells. Scale bar, 10μm. (B), immunoblot of total HBE cell lysate showing various AnkB and AnkG isoforms. (C), schematic representation of the canonical 220kDa AnkB (red) and 190kDa AnkG (green) polypeptides. (D), immunofluorescence showing transiently-expressed, GFP-tagged AnkB and AnkG (green, GFP staining; blue, DAPI staining) in polarized HBE cells. Scale bar, 10μm. (E), quantification of the immunofluorescence intensity ratio of plasma membrane vs. cytosolic GFP staining. (Student's t-test, n=23-25, * indicates $p<0.05$).

2.3.2 An ANK repeat-ZU5 linker determines lateral membrane exclusion of ankyrin-B

In order to explore the molecular mechanism for the dramatic difference between plasma membrane localization of ankyrin-B and ankyrin-G, we examined which domain is required for plasma membrane localization using B/G chimeras. We first used the previously generated ankyrin-B/G chimeric proteins containing all 8 combinations of membrane-binding, spectrin-binding, and C-terminal domains (Mohler et al., 2002b). Surprisingly, the C terminal region, which was reported to regulate the activity of ankyrin-B in neonatal cardiomyocytes (Mohler et al., 2002b), is not required for plasma membrane localization of ankyrin-B or ankyrin-G (BBG, GGB, Figure 5A, B and C). Instead, we found that the central spectrin-binding domain determines the specificity of ankyrin localization. Ankyrin-B containing the ankyrin-G spectrin-binding domain (BGB, Figure 5A, B and C), efficiently targets to the lateral membrane. Similarly, ankyrin-G containing the ankyrin-B spectrin-binding domain shows more intracellular localization (GBG, Figure 5A, B and C), even though it did not become completely intracellular.

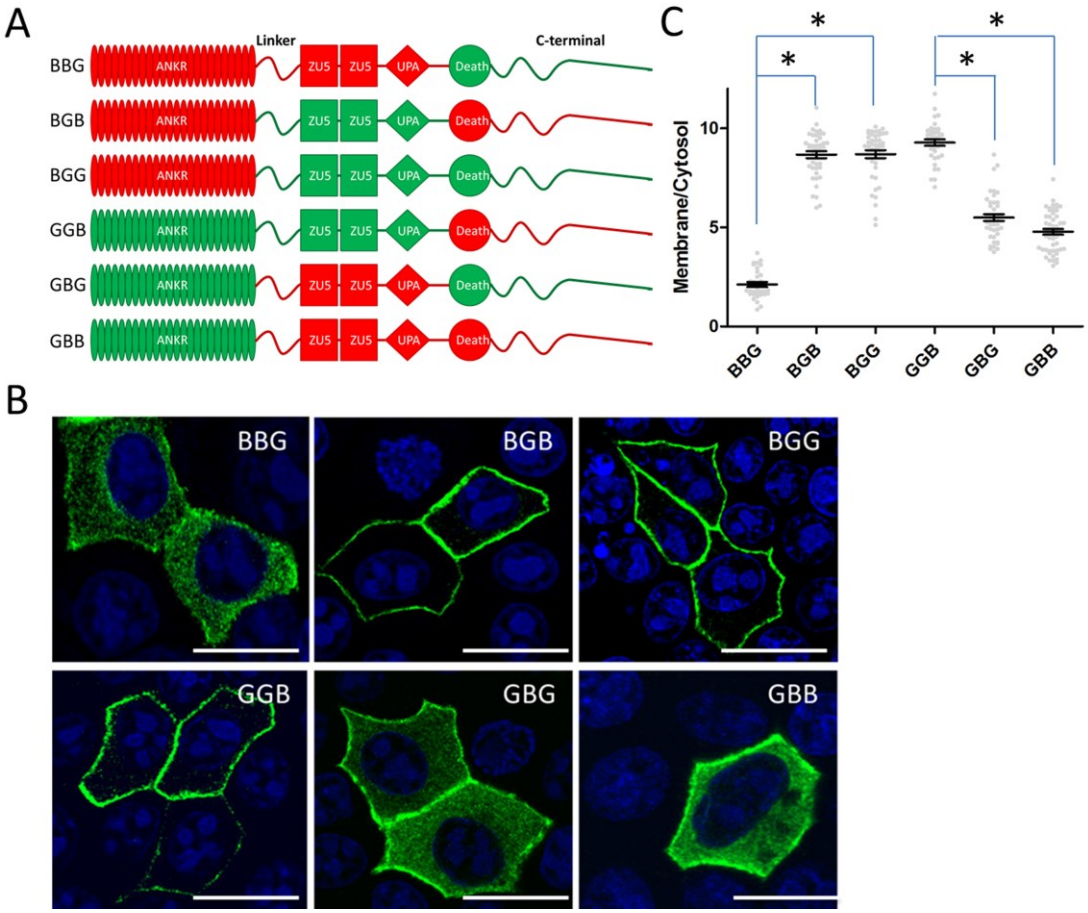

Figure 5: The linker-ZU52-UPA module of ankyrin proteins regulates their subcellular localization.

(A), schematic representation of the AnkB/G chimeric proteins, red represents AnkB counterparts while green represents AnkG counterparts. (B), immunofluorescence showing transiently-expressed, GFP tagged AnkB/G chimeric proteins (green, GFP staining; blue, DAPI staining) in polarized HBE cells. Scale bar, 10μm. (C), quantification of the immunofluorescence intensity ratio of plasma membrane vs. cytosolic GFP staining (One way ANOVA followed by Tukey's post-hoc test, n=27-35, * indicates $p<0.05$)

The spectrin-binding domain consists of a linker peptide, two ZU5 domains, and a UPA domain. The beta spectrin-binding site has been mapped to the first ZU5 domain (Kizhatil et al., 2007b; Mohler et al., 2004b). In order to further explore the structural requirement for ankyrin localization in HBE cells, we made a second generation of ankyrin-B/G chimeric constructs, in which we sequentially exchanged their linker peptides, ZU5 domains, and UPA domains. The sequence boundaries of each region were determined by the structure of the $ZU5_2$-UPA super-domain module of ankyrin-B (Wang et al., 2012). We then compared the cellular localization of chimeras transfected into HBE cells. Interestingly, neither the ZU5 domains nor the UPA domain were required for localization of ankyrin-B or ankyrin-G, since the chimeric proteins ($B/ZU5_G$, B/UPA_G, $G/ZU5_B$, G/UPA_B) behaved the same as their wild type counterparts (Figure 6A, B and C). However, exchange of the linker peptides (hereby referred to as the B-linker and G-linker for ankyrin-B and -G respectively) between ankyrin-B and ankyrin-G resulted in dramatic alteration of cellular localization. Ankyrin-B, containing the G-linker (B/L_G) gained lateral membrane localization, while ankyrin-G containing the B-linker (G/L_B) showed increased intracellular staining (Figure 6A, B and C). The residual membrane staining of G/L_B may indicate that B-linker is not sufficient to block all the potential protein interactions with ankyrin-G, or the lipid modification described in the next chapter.

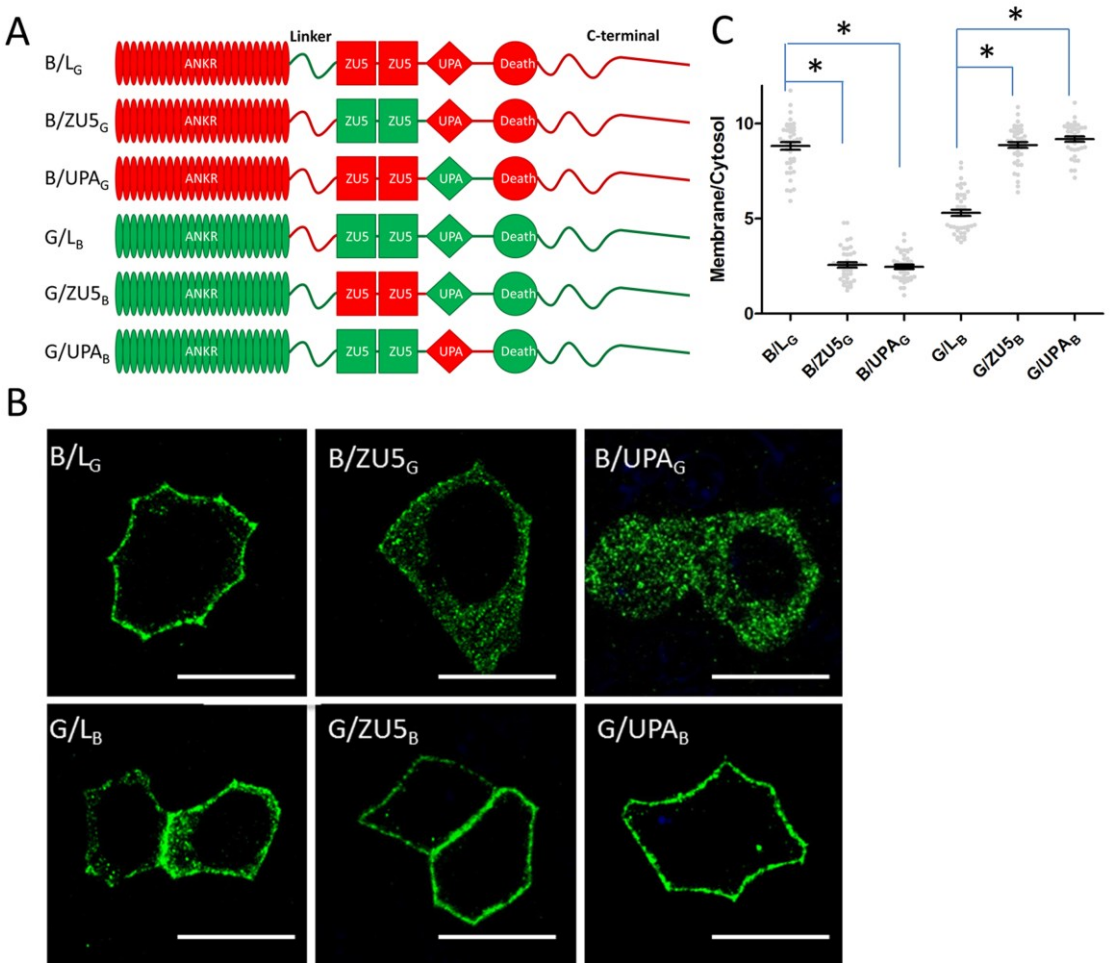

Figure 6: An ANK repeat-ZU5 linker contains the information regulating AnkB or AnkG subcellular localization.

(A), schematic representation of the second generation AnkB/G chimeric proteins, red represents AnkB counterparts while green represents AnkG counterparts. (B), immunofluorescence showing transiently-expressed, GFP-tagged 2nd AnkB/G chimeric proteins in polarized HBE cells. Scale bar, 10μm. (C), quantification of the immunofluorescence intensity ratio of plasma membrane vs. cytosolic GFP staining. (One way ANOVA followed by Tukey's post-hoc test, n=30-37, * indicates $p<0.05$).

2.3.3 The B-linker acts through an autoinhibitory mechanism

Since ankyrin-B targets to the plasma membrane when its linker region was replaced with the G-linker, we initially hypothesized that the G-linker itself independently associates with the plasma membrane. To test this hypothesis, GFP-tagged G-linker was expressed in HBE cells. However, the G-linker alone showed no membrane localization (Figure 7A). We next generated truncated constructs only including the ANK repeat domain and the linker region (Figure 7B). Surprisingly, the ANK repeat domain of either ankyrin-B or ankyrin-G was sufficient for lateral membrane targeting ($ANKR_B$, $ANKR_G$), and this membrane localization was not affected by addition of the G-linker ($ANKR_B/L_G$, $ANKR_G/L_G$) (Figure 7C and D). However, fusion of the B-linker to the C terminus of the ANK repeat domain efficiently blocked the lateral membrane binding activity of the ANK repeat domains of both ankyrin-B and ankyrin-G ($ANKR_B/L_B$, $ANKR_G/L_B$, Figure 7C and D).

Given the fact that B-linker inhibits the lateral membrane targeting of the ANK repeat domain, the B-linker may directly interact with ANK repeats. To test this hypothesis, we performed a co-immunoprecipitation assay, in which GFP-tagged B-linker was co-expressed with HA-tagged ANK repeat domain of ankyrin-B or -G. After immunoprecipitating GFP-B-linker, we detected robust HA immunoreactivity, which indicated a strong interaction between the B-linker and the ANK repeat domain (Figure 7E). Interestingly, an atomic structure of the C-terminal twelve ankyrin repeats of

ankyrin-R solved by Michaely and colleagues showed that the ankyrin repeat solenoid contains an extended groove which associates with the endogenous C-terminal peptide corresponding to the B-linker (Figure 7F) (Michaely et al., 2002). This model suggests an autoinhibitory mechanism where an unstructured B-linker polypeptide represses the activity of ANK repeat domain through association with the ANK repeat groove thus competing with membrane partners.

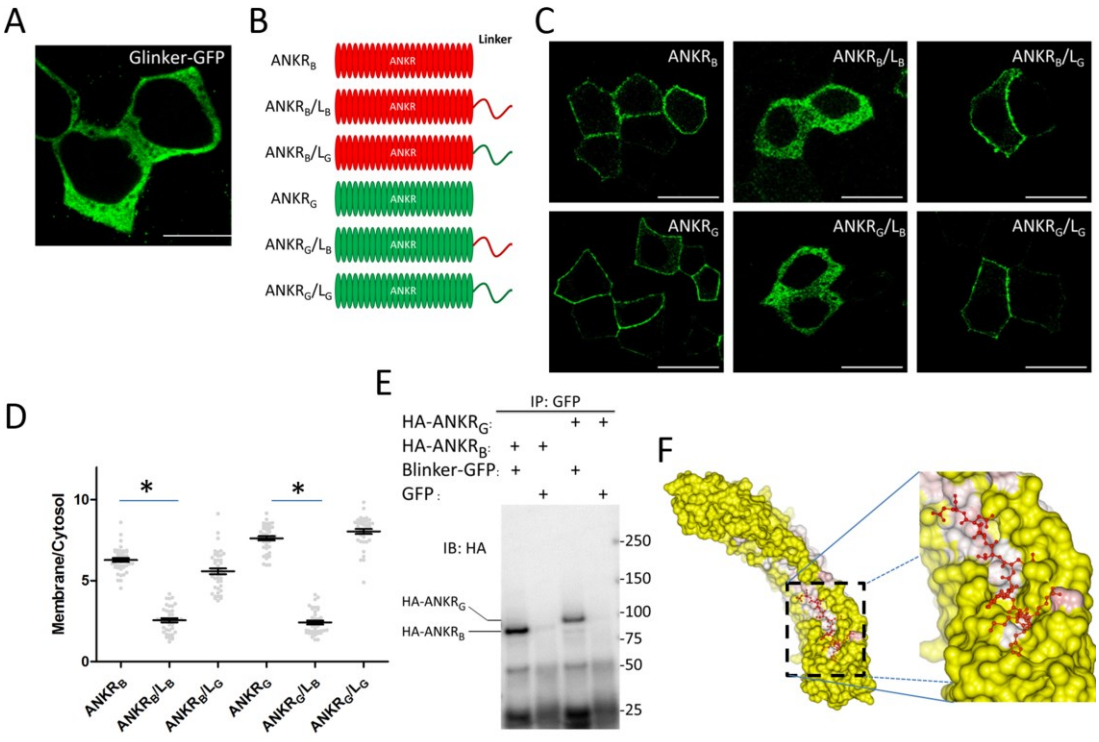

Figure 7: The ANK repeat-ZU5 linker regulates AnkB localization through autoinhibition.

(A), the linker region of AnkG (G-linker) was tagged with GFP, and transiently expressed in HBE cells. Cells were fixed and stained against GFP to visualize G-linker localization. Scale bar, 10μm. (B), schematic representation of the truncated AnkB/G chimeric proteins, red represents AnkB counterparts while green represents AnkG counterparts. (C), immunofluorescence showing transiently-expressed, GFP-tagged truncated AnkB/G chimeric proteins. Scale bar, 10μm. (D), quantification of the immunofluorescence intensity ratio of plasma membrane vs. cytosolic GFP staining (One way ANOVA followed by Tukey's post-hoc test, n=33-36, * indicates $p<0.05$). (E), co-immunoprecipitation of B-linker and the ANK repeat domain. HA-tagged ANK repeat domain of AnkB (HA-ANKRB) or AnkG (HA- ANKRG) was co-expressed with GFP-tagged B-linker (or GFP only, as a negative control) in 293T cells. Samples were then immunoprecipitated with anti-GFP antibody and blotted with anti-HA antibody. (F), structure of the human AnkR C-terminal 12 ankyrin repeats with a following peptide. Image was generated using CCP4MG software. The surface of the ankyrin repeats was colored by temperature factor, and the peptide was colored red.

2.3.4 The B-linker prevents interaction of ankyrin-B with E-cadherin and neurofascin-186

Ankyrin-G is the native partner for neurofascin-186 and binds to E-cadherin with a much higher affinity than ankyrin-B (Davis et al., 1996; Kizhatil et al., 2007a; Scotland et al., 1998). Therefore, we were interested in testing whether the B-linker functions by regulating the interaction of ankyrin-B with E-cadherin or neurofascin-186. We addressed this question using a previously reported cellular recruitment assay where co-expression of ankyrin-G with a membrane partner in HEK 293 cells results in recruitment of ankyrin-G from the cytoplasm to the plasma membrane (Zhang et al., 1998). Ankyrin-B, when co-expressed with neurofascin-186 or E-cadherin, which both target to the plasma membrane in HEK293 cells, remained in the cytoplasm, indicating no interaction between ankyrin-B and neurofascin-186 or E-cadherin (Figure 8A and B). However, the chimeric ankyrin-B with the G-linker (B/L_G) was efficiently recruited to the plasma membrane by both neurofascin-186 and E-cadherin (Figure 8A and B). These results implied that the B-linker suppressed the binding activity of ankyrin-B with neurofascin-186 and E-cadherin, probably through autoinhibition, as noted above.

In contrast to its effects on ankyrin-B, the B-linker, when substituted for G-linker, did not completely block the recruitment of ankyrin-G by neurofascin-186 or E-cadherin (Figure 8C and D). This result is consistent with the cellular localization results where B-linker only partially prevents ankyrin-G from targeting to the lateral membrane in HBE cells (Figure 6B and C). One explanation for the different sensitivities of ankyrin-B and -

G may be that B-linker requires specific regions in the ANK repeat domain of ankyrin-B for an efficient intramolecular interaction and repression. Consistent with this interpretation, the co-immunoprecipitation assay shows greater binding between B-linker and the ANK repeat domain of ankyrin-B than of ankyrin-G (Figure 7E).

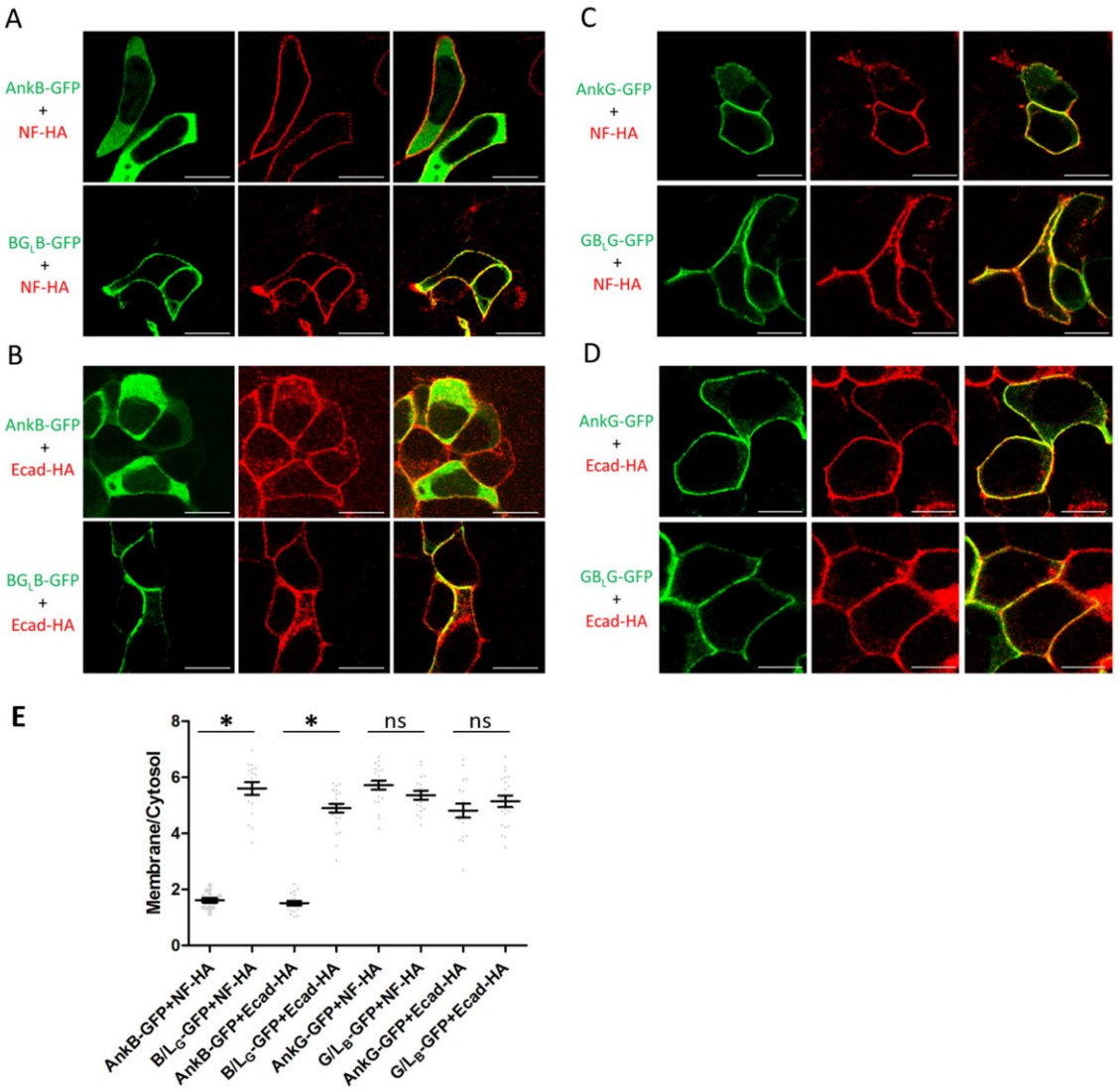

Figure 8: The B-linker inhibits the interaction between AnkB and E-cadherin and neurofascin-186.

(A,B), AnkB-GFP or B/LG-GFP, or (C,D), AnkG-GFP or G/LB -GFP were co-expressed with HA-tagged neurofascin-186 (NF-HA) or Ecadherin (Ecad-HA) in HEK293 cells. Cells were then fixed and co-stained with anti-GFP (green) and anti-HA (red). Scale bars, 10μm. (E), quantification of the immunofluorescence intensity ratio of plasma membrane vs. cytosolic GFP staining (One way ANOVA followed by Tukey's post-hoc test, n=17-24, * indicates $p<0.05$)

2.3.5 Multiple sites in the B-linker are required for its inhibitory function.

To identify critical regions required for the autoinhibition activity of the B-linker, we first truncated the C-terminal half (residues 891-960) of the B-linker, and found that it still maintained its inhibitory activity (data not shown). Then we performed NAAIRS-scanning mutagenesis on the N-terminal portion (residue 848-890) of the B-linker (Marsilio et al., 1991). The NAAIRS (Asp-Ala-Ala-Ile-Arg-Ser) hexapeptide was identified in diverse secondary structures (Wilson et al., 1985). This peptide thus is able to adopt a flexible conformation based upon the local protein structural context, and has been widely used for efficient scanning mutagenesis by replacing six amino acids at a time, without perturbing overall protein folding (Armbruster et al., 2001; Banik et al., 2002; Lonergan et al., 1998; Mosher et al., 2006; Sellers et al., 1998).

We identified three regions (amino acids 848-853, 878-883 and 885-890) within the B-linker that are required for lateral membrane exclusion of ankyrin-B. When those amino acids were mutated into NAAIRS, transiently expressed ankyrin-B-GFP predominantly localized on the lateral membrane in polarized HBE cells (Figure 9). Considering our co-immunoprecipitation result showing that the B-linker interacts with ANK repeat domain (Figure 7E), this finding implies that the B-linker requires multiple contact sites for full interaction and repression of interactions.

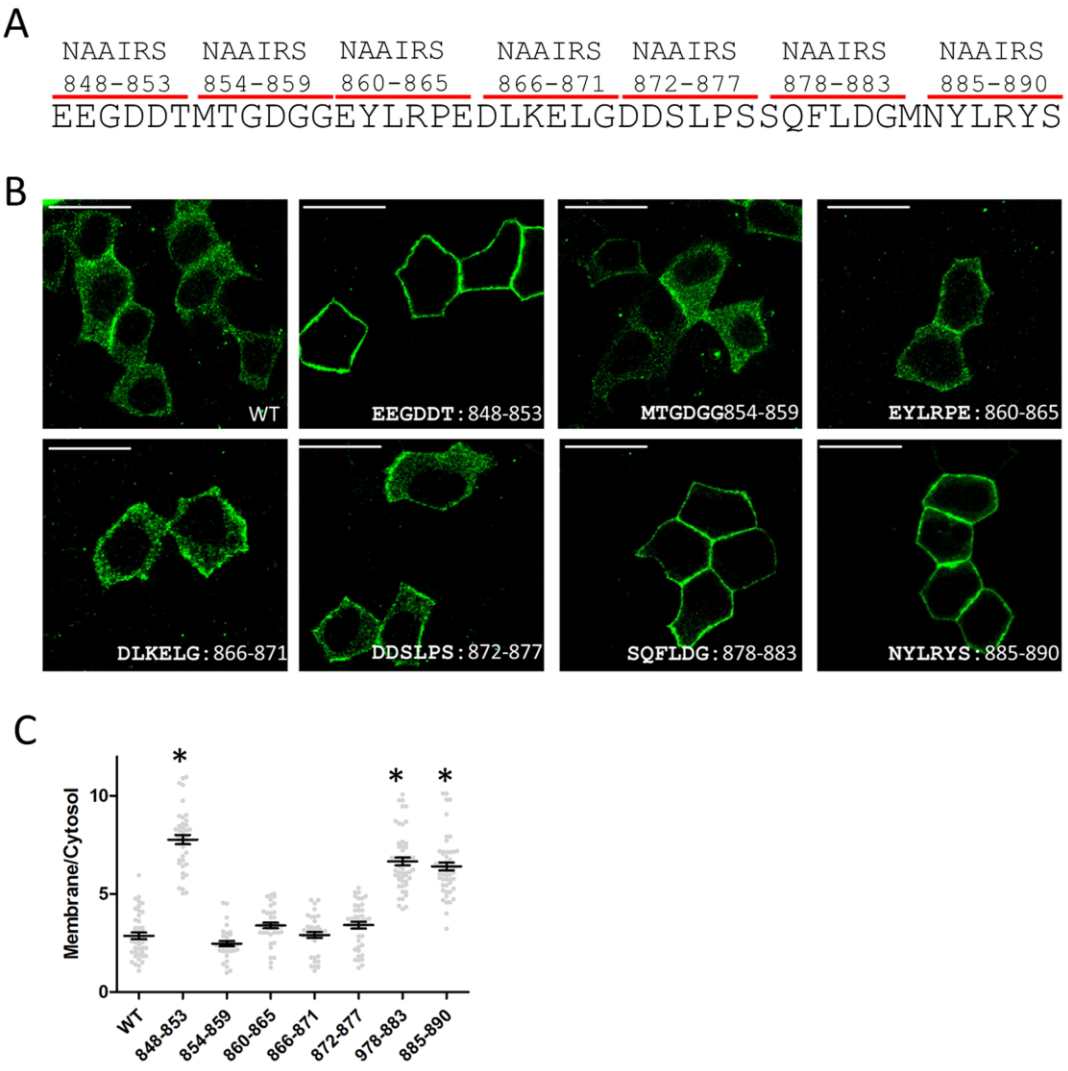

Figure 9: Multiple sites are required for the inhibitory activity of the B-linker.

(A), every six amino acids were mutated into NAAIRS to scan through B-linker region. (B), immunofluorescence showing transiently-expressed, GFP-tagged AnkB mutants. Scale bar, 10μm. (C), quantification of the immunofluorescence intensity ratio of plasma membrane vs. cytosolic GFP staining. (One way ANOVA followed by Tukey's post-hoc test, n=32-39, * indicates $p<0.05$).

2.3.6 The B-linker prevents membrane localization of ankyrin-B in cultured hippocampal neurons

We next investigated whether the B-linker autoinhibition mechanism extends to neurons. We transfected wildtype 220 kDa ankyrin-B-GFP, 190 kDa ankyrin-G-GFP, and their linker chimeras into cultured hippocampal neurons, and compared their membrane localization in soma and primary dendrites. We were unable to resolve the plasma membrane from cytoplasm in axons due to their small size. However, consistent with results in HBE cells, we found that 190kDa ankyrin-G-GFP was able to target to the plasma membrane of soma and primary dendrites (Figure 10A, AnkG panel, and 10B), whereas 220kDa ankyrin-B predominantly localized in the cytoplasm in these cells (Figure 10A, AnkB panel, and 10B). However, ankyrin-G with the B-linker showed increased cytoplasmic staining (Figure 10A, G/L_B panel, and 10B), while ankyrin-B with the G-linker conversely exhibited a robust membrane staining (Figure 10A, B/L_G panel, and 10B).

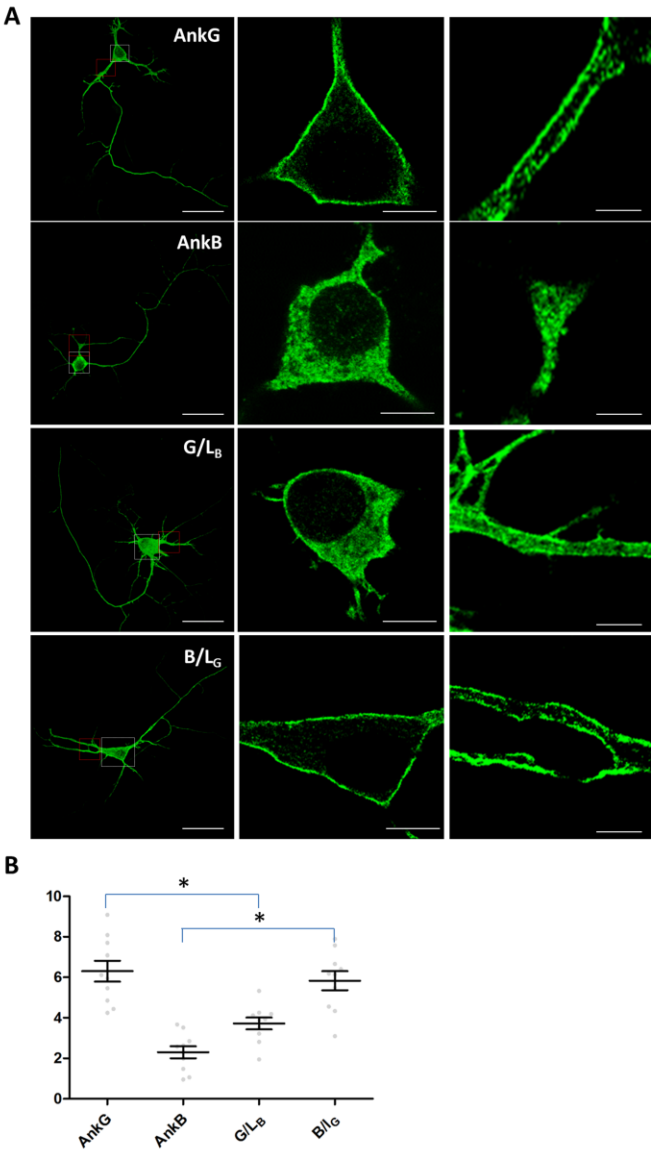

Figure 10: The B-linker regulates ankyrin protein localization in the same way in neurons as in HBE cells.

(A), immunofluorescence showing transiently-expressed, GFP-tagged 2nd generation AnkB/G chimeric proteins (see Figure 4) in hippocampal neurons. The first column show the profile of entire transfected neurons, scale bar, 100μm. The cell body (shown in the second column, scale bar, 5μm) was boxed in while, while the primary dendrite (shown in the third column, scale bar, 2μm) was boxed in red. (B), quantification of the immunofluorescence intensity ratio of plasma membrane vs. cytosolic GFP staining. (One way ANOVA followed by Tukey's post-hoc test, n=10, * indicates $p<0.05$).

2.3.7 The active region of the B-linker evolved from a single highly divergent exon

The similar role of B-linker in regulating plasma membrane localization in both HBE cells and hippocampal neurons suggests that the autoinhibition mechanism may contribute to functional differences between ankyrin family members. The three vertebrate ankyrins evolved from a single ankyrin gene present in the urochordate *C. intestinalis* ((Cai and Zhang, 2006), Figure 11A). Surprisingly, the critical region of B-linker (Figure 9A) required for restricting membrane localization is encoded by a single exon in all three vertebrate ankyrins (Figure 11B). The B-linker exon is highly conserved within the Ank2 family across multiple species from humans to fish (H.sapiens, M.musculus, Xenopus and D.rerio, Figure 11B), especially in the regions identified to be critical for its inhibitory function (highlighted in red, Figure 11B). On the other hand, the linker exons are divergent among Ank1, Ank2, and Ank3 (H. sapiens Ank1, Ank2 and Ank3, Figure 11B), although conserved core elements indicate a common evolutionary origin (highlighted in yellow, Figure 11B).

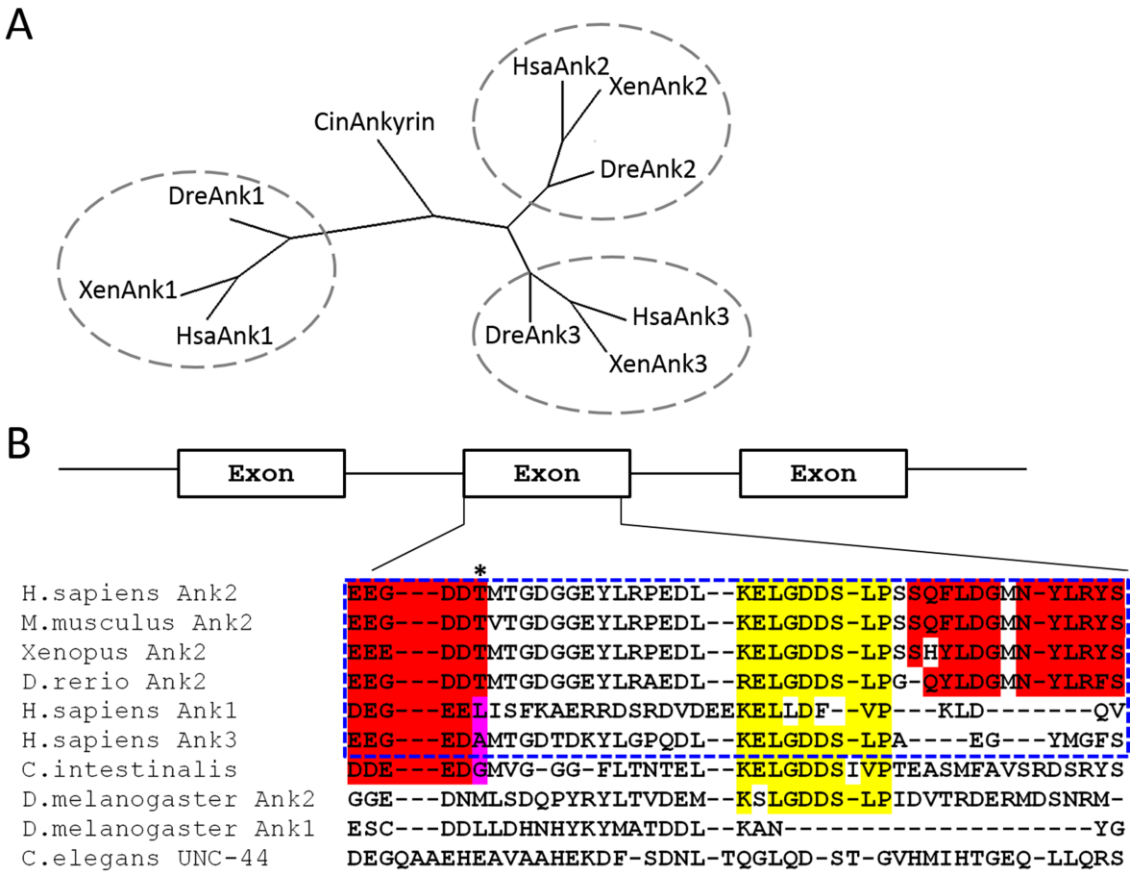

Figure 11: The B-linker region is encoded by a single exon evolutionarily-conserved in the ankyrin-B lineage.

(A), a phylogenetic tree showing the evolutionary lineage of ankyrin proteins. (B), sequence alignment of the linker region in AnkB across multiple species and other ankyrin isoforms. Regions highlighted in red represent the critical regions for the linker's inhibitory activity, regions highlighted in yellow represent conservation back to ancient ankyrin molecules in Drosophila.

2.4 Discussion

Ankyrin-B is primarily associated with an intracellular compartment(s) while ankyrin-G localizes to plasma membranes in epithelial cells (Figure 4) as well as cardiomyocytes (Mohler et al., 2004a; Mohler et al., 2004e). Here, we identify an ankyrin-B-specific linker peptide connecting the ANK repeat domain to the $ZU5_2$-UPA module that inhibits binding of ankyrin-B to membrane protein partners E-cadherin and neurofascin-186, and prevents association of ankyrin-B with epithelial lateral membranes as well as neuronal plasma membranes. The active region of the B-linker is encoded by a small exon that is highly divergent between different ankyrin family members but conserved in the ankyrin-B lineage. We show that the ankyrin-B linker can suppress activity of the ANK repeat domain through an intramolecular interaction, likely with a groove on the surface of the ANK repeat solenoid, thereby regulating the affinities between ankyrin-B and its binding partners. Scanning mutagenesis revealed three regions in the ankyrin-B linker that are required for its full autoinhibition. These results provide a simple evolutionary explanation for how ankyrin-B and -G have acquired striking differences in their plasma membrane association while maintaining overall high levels of sequence similarity.

Deficiency of ankyrin-B causes a constellation of traits termed as "ankyrin-B syndrome" (Healy et al., 2010; Mohler et al., 2007a; Mohler et al., 2007b; Mohler et al., 2004d). Previous research have identified multiple human genetic ankyrin-B variants

(E1425G, L1622I, T1626N, R1788W, E1813K) (Healy et al., 2010; Mohler et al., 2007b; Mohler et al., 2004c; Mohler et al., 2003) which are associated with this syndrome. Interestingly, a search of the Exome Variant Server (http://evs.gs.washington.edu/EVS/) revealed a human genetic variant in this linker region of ankyrin-B (NM_020977.3). This variant causes a Glutamine (aa 879) to Arginine mutation, which happens to locate in one of the three critical regions of B-linker that we identified through scanning mutagenesis (Figure 9). Therefore, it will be interesting to test whether this mutation causes any cellular or physiological defects in future experiments. Additionally, a study conducted by Cunha and the colleagues revealed multiple new exons in the ANK2 gene, and one of those exons is immediately 5′ to the B-linker exon (Cunha et al., 2008). This new exon encodes a short peptide, which can potentially alter the relative position between the ANK repeat domain and the B-linker. Similar alternative exons were also identified 5′ to the G-linker exon (Peters et al., 1995), which may affect membrane protein interactions of ankyrin-G polypeptide.

Here we show that endogenous ankyrin-G localizes to the plasma membrane while ankyrin-B exists in some intracellular vesicles with unknown identity in HBE cells. However membrane association may be cell type specific, since in some cases both ankyrin-B and ankyrin-G localize to the plasma membrane, although in different subdomains. For example, in myelinated neurons, ankyrin-G targets to the nodes of Ranvier while ankyrin-B localizes to the paranode (Galiano et al., 2012). Another

example is the cardiac T-tubules membrane where ankyrin-B localizes together with Na/K ATPase, Na/Ca exchanger, and $InsP_3$ receptor (Mohler et al., 2005), while ankyrin-G localizes to both intercalated disc and T-tubules, and is required for targeting of $Na_v1.5$channels (Lowe et al., 2008). These specific localization patterns may be achieved through ankyrin-B and -G interactions unaffected by the B-linker peptide, and likely involve additional proteins.

Ankyrins recognize their membrane partners through natively unstructured peptides in their cytoplasmic domains (Table 1) (Bennett and Healy, 2009). A structure of the C-terminal half of the ankyrin-R ANK repeat domain revealed a groove-like surface, which provides a potential binding site for unstructured peptides (Michaely et al., 2002). The linker we identified here may function as a native competitor or regulator for determining binding affinities with different partners. To further confirm this hypothesis, it will be important in the future to determine atomic structures of ANK repeats of ankyrin-B with membrane partners and with the B-linker.

Ankyrins and their partner spectrin have from their initial discovery exhibited association with both plasma membranes and intracellular organelles (Beck et al., 1994; Bennett et al., 1982; Levine and Willard, 1981; Lin et al., 1994). Our discovery of a mechanism for preventing association of ankyrin-B with plasma membranes through intramolecular competition for membrane binding partners provides a molecular clue as to how closely related ankyrins can direct spectrin to both cytoplasmic compartments

and the plasma membrane. Given that ankyrin-B and ankyrin-G originated from a single ancestral ankyrin, it is possible that pre-chordate ankyrin had both intracellular and plasma membrane-related functions. The identity of the ankyrin-B-associated intracellular structures in cardiomyocytes (Mohler et al., 2004e) or HBE cells (Figure 4A) remains unknown. Therefore, it will be intriguing to identify the composition and function of ankyrin-B-positive organelles and their cellular functions.

Table 1: Diversity of ankyrin-binding motifs.

	Ankyrin Binding Site
NaV	VPIAGESDFE
KCNQ2	PYIAEGESDTDSD
E-cadherin	KEPLLPPEDDTRDNVYY-YDEEGGGEED
Neurofascin/ L1CAMs	QFNEDGSFIGQY
RhBG	KLPFLDSPP
Dystroglycan	GVPIIFAD ELDDSK
AE1	PAVLTRSGDPS

(From Bennett and Healy, 2009)

Chapter 3. Cysteine 70 of Ankyrin-G is S-palmitoylated and Required for Function of Ankyrin-G in Membrane Domain Assembly

3.1 Introduction

In the last Chapter, we identified a molecular diversity that explains how ankyrin-B is excluded from the plasma membrane of epithelial cells and neurons. However, it is still unclear how ankyrin-G localizes to the epithelial lateral membrane and other specialized membrane domains. Multiple protein domains are required to direct AnkG to the AIS of dorsal root ganglion neurons and lateral membranes of cultured epithelial cells (Kizhatil and Bennett, 2004; Zhang and Bennett, 1998). Elimination of the AnkG binding partners, β4-spectrin or neurofascin, does not prevent localization of AnkG at the AIS (Boiko et al., 2007; Dzhashiashvili et al., 2007; Hedstrom et al., 2007). Recent work has shown that ankyrin-B is critical to confine AnkG to the AIS, though the mechanism for axonal localization remains unclear (Galiano et al., 2012). In epithelial cells, a DAR999AAA mutant AnkG, which specifically loses interaction with β2-spectrin, still efficiently localizes to the lateral membrane, even though this mutant AnkG lacks activity in membrane biogenesis (Kizhatil et al., 2007b). Therefore, additional features mediated by interactions with unidentified proteins or membrane phospholipids may contribute to targeting of AnkG to specialized membrane domains.

Covalent modification of proteins with lipids can contribute to micro-patterning of plasma membranes (Levental et al., 2010). Interestingly, ankyrin-R (AnkR) purified

from erythrocyte membranes exhibited hydrophobicity intermediate between a cytosolic protein and an integral protein (Bennett and Stenbuck, 1980). Moreover, AnkR is palmitoylated in a reversible fashion (Staufenbiel, 1987). In this chapter, we report that AnkG is S-palmitoylated at a cysteine conserved among all three ankyrin family members and located in their membrane-binding domains. We also find that the same cysteine, possibly due to its S-palmitoylation, is required for targeting as well as the biological functions of AnkG in epithelial cells and neurons.

3.2 Methods and Materials

Reagents, plasmids and antibodies

N-Ethylmaleimide and hydroxylamine were from Sigma, EZ-Linker Biotin-BMCC from Thermo, activated Thiol Sepharose 4B from GE Healthcare, Dynabeads with protein-G and Lipofectamine 2000 transfection reagent were from Invitrogen, QuikChange II XL Site-Directed Mutagenesis Kit from Agilent Technologies, palmitic Acid, [9,10-^{3}H] from PerkinElmer. Rat wild-type 190kDa AnkG cDNA was previously described (Kizhatil and Bennett, 2004). Rabbit polyclonal antibody targeting the C-terminal domain of AnkG, and rabbit polyclonal antibody against β2-spectrin were previously described (Kizhatil et al., 2007b), Mouse monoclonal antibodies against human E-cadherin and ZO-1 were from Invitrogen, mouse monoclonal anti-sodium

channel pan antibody was from Sigma, and rabbit polyclonal antibody against biotin was from Abcam.

MDCK stable cell lines

The ViraPower Lentiviral Expression System based on the pLenti6/V5-DEST Gateway Vector from Invitrogen was used to generate stable MDCK cell lines expressing wild-type or C70A AnkG-GFP. For lentivirus generation, 293T cells were grown in Dulbecco's modified Eagle's medium (DMEM) supplemented with 10% fetal bovine serum. 15 million cells were plated in 100mm dishes and transfected the next day with 16μg cDNA (4μg pMDLg/pRRE, 4μg pRSV-Rev, 4μg pMD2.G, and 4μg transfer plasmid) using Lipofectamine 2000 following the manufacturer's protocol. 48 hours later, 25 ml culture medium were collected and centrifuged at 25000rpm for 2 hours to collect the virus. Half a million MDCK cells were plated in a 6-well plate and infected with the virus for 16 hours. Blasticidin S was used to select infected cells and establish a stable cell line.

Calcium switch assay

MDCK cells were maintained in DMEM supplemented with 10% FBS until they formed a polarized monolayer. Cells were then trypsinized, and $2x10^6$ cells were plated on 14mm coverslip inserts of MatTek plates in calcium-free Minimum Essential Medium supplemented with 5% dialyzed low calcium FBS. 16 hours later, cells were washed with PBS to remove unattached cells, and then fed with normal growth medium. Cells were

fixed and processed for immunofluorescence to visualize protein localization at multiple time points.

Membrane recruitment assay

This assay was previously reported (Zhang and Bennett, 1998). Briefly described, $1x10^5$ HEK293 cells were plated in 14mm insert, collagen-coated MatTek plates. The next day, cells were co-transfected with 100ng HA-tagged neurofascin or E-cadherin cDNA and 80ng GFP-tagged 190kDa AnkG cDNA using Lipofectamine 2000. 24 hours later, cells were fixed and processed for immunofluorescence as described below.

Biotin switch assay

The biotin switch assay was previously described for testing protein S-acylation (Drisdel et al., 2006). Since endogenous AnkG is resistant to Triton X-100 extraction we developed a protocol for solubilizing AnkG from MDCK cells in a state compatible with immuno-precipitation. A polarized MDCK monolayer in 150mm dish was washed and suspended in ice-cold PBS buffer with protease inhibitors; cells were then collected by centrifugation at 1000 x g for 5 minutes. The cell pellet was homogenized in lysis buffer (10mM sodium phosphate, 2mM NaEDTA, 0.32M sucrose, 50mM N-Ethylmaleimide and protease inhibitors (10μg/ml AEBSF, 30μg/ml benzamidine, 10μg/ml pepstatin, and 10μg/ml leupeptin), pH=7.4) using a 27G needle, and incubated at 4^oC for 6 hours to pre-block free sulfhydryl groups. SDS was then added to the lysates at a final concentration of 1% (w/v) and mixed well immediately. Lysates were sonicated for 30 seconds on ice

followed by centrifugation at 100,000xg for 30min. Triton X-100 was then added to a final concentration of 1%, (v/v), then mixed well and incubated on ice for 30 minutes followed by rotation at 4°C for another 30 minutes to quench SDS. 60 μl of Dynabeads preloaded with 10μg AnkG antibody were then incubated with the lysates overnight rotating at 4°C. The beads were washed 3 times with cold wash buffer (10mM sodium phosphate, 2mM NaEDTA, and protease inhibitors, pH=7.4), and then incubated with hydrolysis-labeling buffer (1M hydroxylamine, 80μM biotin-BMCC, 10mM sodium phosphate, 2mM NaEDTA, and protease inhibitors, pH 7. As a control, 1M Tris-HCl was substituted for hydroxylamine) at room temperature for 2 hours. Beads were then washed 3 times with wash buffer and incubated with 5X loading buffer (5% SDS, 20% sucrose, 40mM Tris-HCl, 150mM NaCl, 2mM NaEDTA, 200mM DTT with bromophenol blue) at 70°C for 15 minutes to elute proteins. Samples were analyzed by SDS-PAGE and western blotting. A biotin antibody was used to detect S-acylation.

Mass spectrometry

HEK293 cells transfected with WT AnkG-GFP were homogenized in lysis buffer (10mM sodium phosphate, 2mM NaEDTA, 0.32M sucrose, 50 mM N-Ethylmaleimide and protease inhibitors (10μg/ml AEBSF, 30μg/ml benzamidine, 10μg/ml pepstatin, and 10μg/ml leupeptin), pH=7.4) and incubated at 4°C for 6 hours to pre-block free sulfhydryl groups. Triton X-100 was then added at 1% final concentration, and lysates were sonicated for 20 seconds. Dynabeads preloaded with GFP antibody (GFP antibody

was blocked with NEM) were then added to immunoprecipitate AnkG-GFP overnight. The following day, the beads were washed 3 times and incubated with elution buffer (1% SDS, 10mM sodium phosphate, 2mM NaEDTA, 0.32M sucrose) at 50°C for 5 minutes to selectively release AnkG-GFP. Eluted samples were divided into two equal portions: one treated with 1M hydroxylamine the other with 1M Tris-HCl (as a control) at neutral pH with the presence of activated thiol sepharose 4B. After two-hour incubation at 24°C, sepharose beads were washed with 20mM ammonium bicarbonate 3 times and digested in 0.1% Rapigest. After trypsin digestion, the beads were incubated with 20 mM DTT at 24°C for 45 minutes to elute cysteine-containing peptides. Eluted samples were alkylated with 40 mM iodoacetamide and analyzed by LC-MS/MS.

[3H]-palmitic acid labeling

8×10^6 stable MDCK cells of WT or C70A AnkG-GFP were plated on 100mm dishes and grown in 37°C, 5% CO_2 overnight. The next day, cells were rinsed with PBS buffer and incubated with 5ml serum-free medium for 4 hours, and then the medium was replaced with 5ml of fresh DMEM containing 100μCi/ml [3H]-palmitic acid. Following a 4-hour incubation, AnkG-GFP was immunoisolated using the protocol previously described, and divided into two equal portions: one treated with 1M hydroxylamine, the other treated with 1M Tris-HCl at room temperature for 2 hours. Proteins were then eluted, separated by SDS-PAGE and transferred to a nitrocellulose membrane, which was then exposed for 6 weeks in -80°C to detect tritium radioactivity.

Immunostaining and fluorescence recovery after photobleaching

MDCK cells on MatTek plates were first washed with cold PBS and fixed with 4% paraformaldehyde at room temperature for 15 minutes, and then cells were permeabilized with 0.2% Triton X-100 at room temperature for 10 minutes. Following a 30-minute blocking in PBS buffer containing 2% bovine serum albumin, cells were incubated with primary antibody in 4^{o}C overnight. Cells were next washed with PBS buffer three times and then incubated with fluorescence-conjugated secondary antibodies (AlexaFluor 488, 568 or 663, Molecular Probes) at room temperature for 2 hours. Fluorescent antibody labeling was visualized using a Zeiss LSM 510 laser scanning microscope. Images from figure 11 and 17 were collected using the 63X NA 1.4 objective lens, and XZ planes were reconstructed from Z stacks with optical sections of 0.5μm. Images from figure 14 and 16 were collected using a 100X NA 1.45 objective lens, and XZ planes were reconstructed from Z stacks with optical sections of 0.37μm. Volocity 3D image analysis software was used to measure the fluorescence intensity of plasma membrane and cytoplasm. Data were analyzed using Graphpad Prism5. For fluorescence recovery after photobleaching (FRAP) measurements, MDCK cells grown on MatTek plates were transfected with 300ng WT, C70A, DAR999AAA or C70A/DAR999AAA double mutation AnkG-GFP plasmids. 24 hours later, cells were analyzed using a Zeiss LSM 780 laser scanning confocal system. The selected membrane region was bleached for 5 seconds, and the fluorescence recovery was monitored for the

following 500 seconds. An unbleached region was also monitored during the measurements, and was used to normalize the FRAP data. Graphpad Prism5 was used to analyze the data by fitting them to the one-phase association equation $\mathbf{y = y_0 + Ae^{-k \times t}}$.

Doxycycline-inducible shRNA cell lines and rescue experiments

The Tet-pLKO-puro vector was originally obtained from Addgene (Plasmid 21915). We replaced the puromycin-resistance gene with mCherry to allow isolation of transfected cells by fluorescence activated cell sorting (FACS), while the IRES region was replaced with the Foot & Mouth Disease Virus 2A peptide (GSGATNFSLLKQAGDVEENPGP) to facilitate higher expression levels of mCherry. Oligos encoding a shRNA hairpin targeting canine AnkG in the ankyrin repeats domain (gctagaagtagctaatctcct) were cloned into Tet-pLKO-2A-mCherry, with hairpin targeting luciferase gene (ggagatcgaatcttaatgtgc) as a negative control. Lentivirus was generated using the second generation packaging system from Addgene (psPAX2 and pMD2.G) following the recommended protocol. Two days after MDCK cells were infected, cells were trypsinized and fractionated by FACS to establish a stable cell line. To evaluate AnkG knockdown efficiency, stable cells were induced by 5μg/ml doxycycline for 24 and 48 hours. Total RNA was extracted following standard protocol and applied for real time quantitative PCR using Power SYBR Green Master Mix from Life Technology. For rescue experiments, cells were pre-induced for 12 hours using 5μg/ml doxycycline, and

re-plated on 14mm insert MatTek plates with the presence of doxycycline at a density of 1600/mm^2. 6 hours later, cells were transfected with 80ng WT or C70A AnkG-GFP using Lipofectamine 2000. Cells were supplemented with fresh medium 4 hours post-transfection and fixed for immunofluorescence after 36 hours.

Hippocampal neuronal cultures

Hippocampi were dissected from neonatal C57bl/6 mice (P0-P1) and incubated in 2mg/mL papain in Hibernate A with 100μg/mL DNase at 37°C for 20 minutes. Hippocampi were washed twice in plating medium (Neurobasal A plus 2% B-27 supplement, 2mM Glutamax, and 10% horse serum) and triturated first with a P200 pipette tip and then with a fire-polished Pasteur pipette until dissociated. Cells were resuspended in plating medium and plated in poly-L-lysine-coated MatTek plates for 3-4 hours. Media was gently aspirated and replaced with growth medium (Neurobasal A plus 2% B-27 supplement and 2mM Glutamax) for 4-5 days. Transfections were carried out with Lipofectamine 2000. In one tube, 1μg total cDNA was mixed with 100μL Neurobasal A, and in a second tube, 3μL Lipofectamine 2000 was mixed with 100μL Neurobasal A. After 15 minutes tubes were mixed. Growth medium was removed from neurons and set aside, and transfection mixture was added to cells. After 1 hour at 37°C the transfection mix was aspirated and cells were fed with original growth medium supplemented with 5μM cytosine arabinoside. After 48 hours (7 DIV), cells were fixed with 4% paraformaldehyde for 15 minutes at room temperature and ice-cold methanol

for 7 minutes at -20°C and processed for immunostaining. For quantification, confocal Z-stack images were collapsed, and the fluorescence intensities from the first 60μm portion of axons and dendrites were measured using ImageJ software. The intensity ratios of axon to dendrite were quantified and analyzed using Graphpad Prism5.

3.3 Results

3.3.1 AnkG remains on the plasma membrane in MDCK cells grown in low calcium

MDCK cells are well known to require extracellular calcium to maintain transepithelial resistance and apical-basal polarity (Martinez-Palomo et al., 1980). Adherens junction proteins (E-cadherin), tight junction proteins (zonula occludens-1 (ZO-1)), desmosomal proteins (desmoplakin), and components of the spectrin-based membrane skeleton all depend on extracellular calcium for their localization at lateral membrane domains of MDCK cells (Gumbiner et al., 1988; Kaiser et al., 1989; Mattey and Garrod, 1986; Siliciano and Goodenough, 1988). Here we determined effects of low calcium on localization of AnkG and its binding partners, E-cadherin and β2-spectrin. MDCK cells grown in low-calcium medium lacked cell-cell contacts and exhibited a spherical morphology (Figure 12*A*, *B*). As previously reported, E-cadherin is intracellular in unpolarized MDCK cells, and accumulates at the region of cell-cell contact only after addition of calcium (Busche et al., 2010; Gumbiner et al., 1988). β2-spectrin also exhibits a similar pattern and associates with the plasma membrane only

following addition of calcium ((Nelson and Veshnock, 1987); Figure 12B). However, we were surprised to observe a substantial fraction of AnkG that remained associated with the plasma membrane in low calcium and in the absence of cell-cell contacts (Figure 12A, B). Following elevation of calcium, AnkG re-organized and concentrated at the lateral membrane to achieve polarized localization (Figure 12A, B). As far as we are aware, AnkG is the only lateral membrane-associated protein identified so far that remains on the plasma membrane in MDCK cells following depletion of calcium.

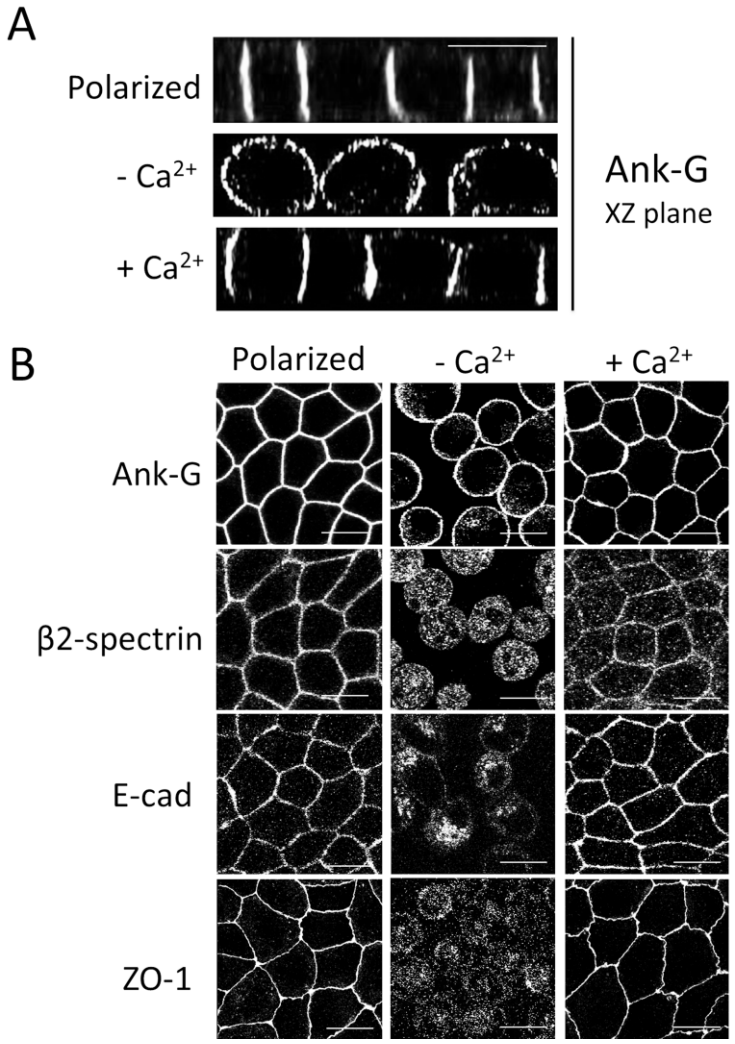

Figure 12: AnkG remains membrane-associated in MDCK cells following calcium switch.

(A and B), fully-polarized MDCK cells (polarized) were trypsinized and re-plated in Ca^{2+} free medium with 5% FBS overnight to reach a steady state. Cells were then either fixed (-Ca^{2+}) or allowed 24 hours to recover in normal growth medium (+Ca^{2+}) then fixed, and processed for immunofluorescence to stain against AnkG, β2-spectrin, E-cadherin and ZO-1. *A*, the XZ planes showing AnkG staining in MDCK cells following calcium switch described above. (B), the XY planes showing immunostaining of AnkG, β2-spectrin, E-cadherin and ZO-1 (a marker of tight junction) in MDCK cells following calcium switch. (Scale bars, 10μm, images are representative of at least three independent repeated experiments).

3.3.2 AnkG is S-palmitoylated at cysteine 70

The finding that AnkG associates with the plasma membrane in non-polarized MDCK cells in the absence of β2-spectrin and E-cadherin suggested the possibility of a protein-independent mode of membrane interaction though lipidation. S-acylation plays critical roles in membrane interactions, intracellular sorting, protein stability and signaling (Salaun et al., 2010). It is pertinent in this regard that AnkR was reported to undergo palmitoylation, although amino acid site(s) were not identified (Staufenbiel, 1988). We therefore explored possible S-acylation of AnkG in MDCK cells using a biotin-switch assay (Drisdel et al., 2006). In this assay, proteins with free sulfhydryl groups were first blocked by N-ethylmaleimide (NEM), and then treated with hydroxylamine (or Tris as a negative control), which selectively cleaves thioester bonds and releases new sulfhydryl groups for labeling using sulfhydryl-reactive biotinylation reagent (BMCC-Biotin). We found that 210kDa AnkG was S-acylated in MDCK cells (Figure 13A). Two smaller AnkG polypeptides with molecular weights of 100 and 120 kDa, which lack ankyrin repeats (Peters et al., 1995), were not S-acylated (Figure 13A).

We next identified the principal S-acylated cysteine(s) of AnkG by mutagenesis. Considering that only full-length AnkG is S-acylated, we created cysteine to alanine mutants of all of cysteines in the membrane-binding domain (C70A, C315A, C357A, C385A, C416A, and C746A). These AnkG mutants were expressed in HEK293 cells, and processed for the biotin switch assay to detect protein S-acylation. As shown in Fig 13B,

WT AnkG as well as C315A, C357A, C385A, C416A, C746A mutants are all S-acylated in HEK293 cells, demonstrating that this modification is not limited to epithelial cells. However, the C70A mutation completely abolished the specific biotin signal (Figure 13B),

In separate experiments we employed mass spectrometry as an independent approach to identify S-acylated peptides in AnkG. We isolated S-acylated AnkG by first blocking free SH groups in cells with NEM followed by removal of thioester groups with hydroxylamine as described above for the biotin switch assay. We then isolated S-acylated AnkG using activated thiol sepharose 4B (Forrester et al., 2011). Following proteolysis, the S-acylated peptide(s) were eluted with dithiothreitol and then alkylated with iodoacetamide. Using liquid chromatography and mass spectrometry we identified a single AnkG peptide, KNGVDVNI**C**NQNGLNALHLASKE, which contains C70, confirming that cysteine 70 was indeed S-acylated (Figure 13C). Figure 13C shows the selected ion chromatograms of the identified peptide from both control (-NH_2OH) and experimental (+NH_2OH) samples.

Protein S-acylation can occur by modification with multiple fatty acids (Jennings and Linder, 2012). We therefore next tested whether AnkG S-acylation is mediated by palmitic acid. MDCK stable cells expressing WT or C70A AnkG-GFP were metabolically labeled with tritiated palmitic acid, followed by immunoisolation of AnkG-GFP. We found that palmitic acid was incorporated into wild type AnkG-GFP, but not the C70A

mutant, and that palmitoylation was reversed by hydroxylamine but not by Tris-HCl (Figure 13D). These results provide direct evidence that palmitic acid is coupled to cysteine 70 of AnkG through a thioester bond.

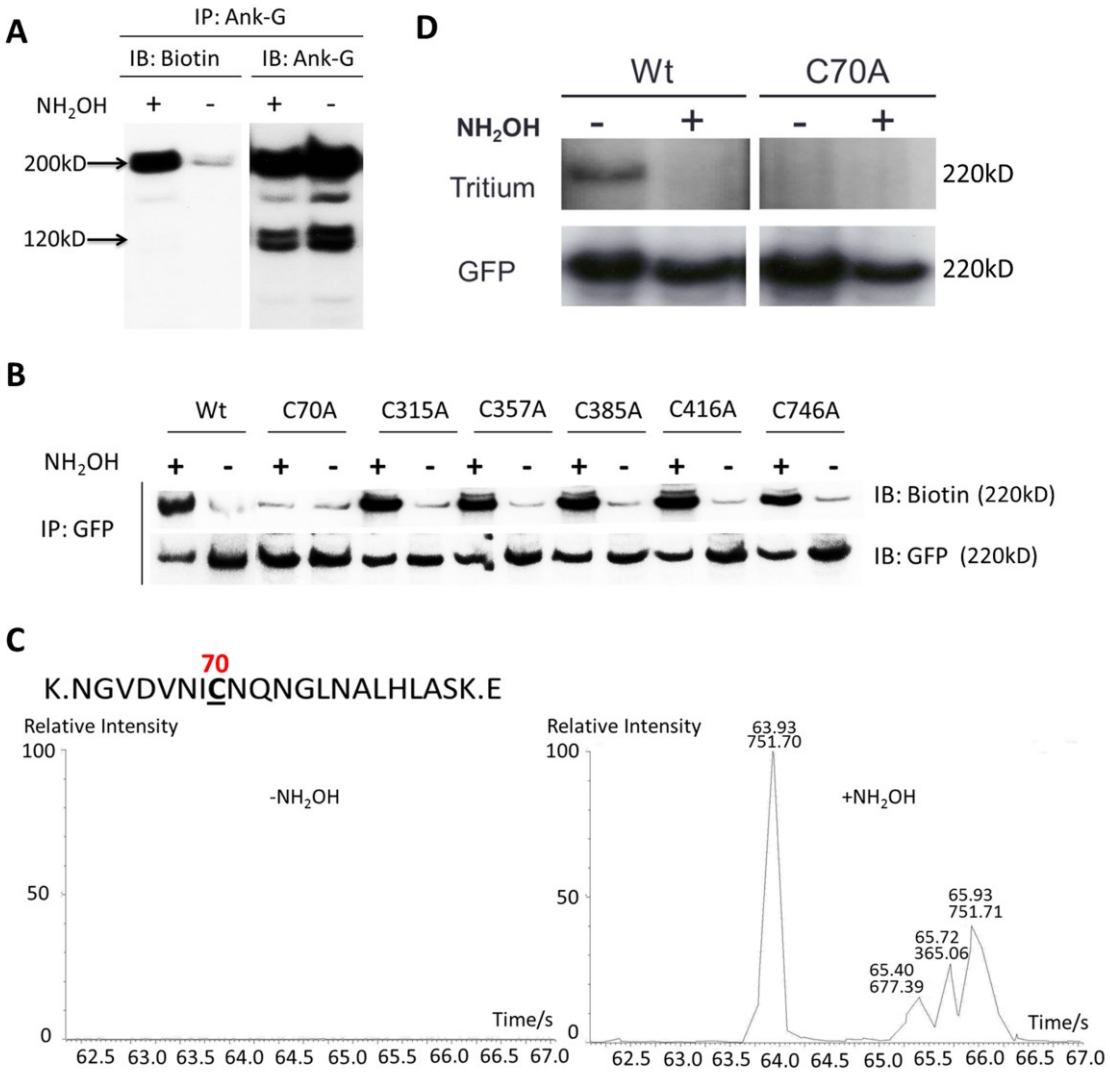

Figure 13: AnkG is S-palmitoylated at Cysteine 70.

(A), The blot shows that only the ~200kDa isoform, which has ankyrin repeats, is S-acylated. (B), The blot shows that C70A completely abolishes AnkG S-acylation. (C), MS identified an S-acylated AnkG peptide KNGVDVNICNQNGLNALHLASKE containing cysteine70, Figure 2C is a mass chromatogram of the selected AnkG peptide. (D), stable MDCK cell lines of WT or C70A AnkG-GFP were labeled with 100μCi/ml [3H]-palmitic acids. AnkG was then immunoprecipitated and analyzed by SDS-PAGE. The blot shows that radioactive palmitic acids can be incorporated into WT AnkG but not C70A in a hydroxylamine-sensitive way.

C70 is located in a loop of the first ankyrin repeat in the membrane-binding domain of AnkG (Figure 14A). Interestingly, C70 is conserved among all three human ankyrin members as well as all vertebrate ankyrins. Interestingly, Drosophila ankyrin isoform 1 also has a cysteine at the comparable position, while the single C. elegans ankyrin and Drosophila ankyrin isoform 2 both contain a serine instead of cysteine (Figure 14B). These results suggest strong evolutionary pressure and a conserved function(s) shared between the three vertebrate ankyrins and one of the Drosophila ankyrin genes.

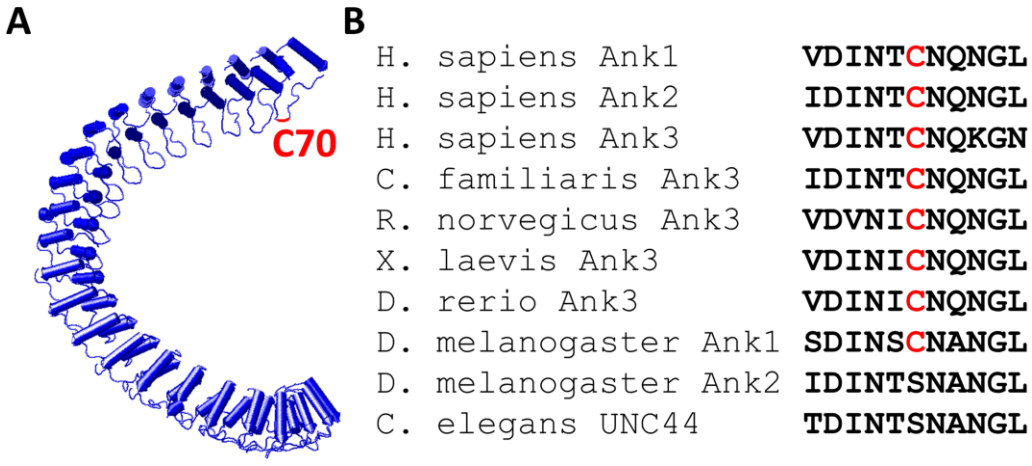

Figure 14: The conservation of Cysteine70 and its position in predicted ankyrin repeats structure

(A), a predicted structure of ankyrin repeats shows that Cysteine 70 locates in the loop connecting the first two repeats, highlighted in red. (B), cysteine70 is conserved among three human ankyrin members, and also conserved in AnkG across different species.

3.3.3 AnkG requires C70 for membrane association in MDCK under low calcium conditions

We next explored the role of cysteine 70 in targeting of AnkG to the plasma membrane of MDCK cells grown in low calcium where other known ankyrin-G protein partners are absent (Figure 12). We evaluated the localization of WT or C70A AnkG-GFP in MDCK cells grown in low calcium medium by measuring the fluorescence intensity ratios of membrane to cytosolic staining. A majority of WT AnkG-GFP remains on the plasma membrane, as observed with native AnkG (Figure 12A). In contrast the C70A mutant was mainly distributed in the cytoplasm (Figure 15A, 4D). WT and C70A AnkG-GFP show average intensity ratios between plasma membrane and cytoplasm of 8.3±0.3 and 2.7±0.2 respectively, ($p<0.001$). This observation indicates that C70 is required for targeting AnkG to the plasma membrane in the absence of E-cadherin and β2-spectrin. Interestingly, WT AnkG-GFP also associates with internal structures that are currently uncharacterized.

One interpretation of loss of C70A AnkG association with plasma membranes of unpolarized MDCK cells (Figure 15A) is that C70 is required for stable folding or protein-protein interactions. We therefore examined membrane localization of C70A AnkG in polarized MDCK cells, which display normal localization of AnkG binding partners (Figure 12B). In contrast to unpolarized MDCK cells, WT and C70A AnkG associate equivalently with the lateral membrane in polarized MDCK cells (Figure 15B,

4D; WT and C70A AnkG-GFP show indistinguishable average intensity ratios between plasma membrane and cytoplasm of 10±0.5 and 8.9±0.5 respectively, p=0.1248).

In order to compare effects of C70A mutation with a loss of spectrin-binding mutation we utilized a DAR999AAA mutant AnkG that lacks spectrin-binding activity (Kizhatil et al., 2007b). We compared the plasma membrane targeting of WT, C70A, DAR999AAA and C70A/DAR999AAA double mutated AnkG expressed by transient transfection of MDCK cells. Both the DAR999AAA mutant and C70A/DAR999AAA double AnkG mutant exhibited plasma membrane localization. However, more of the double mutant remained cytosolic than with either mutation alone (Figure 15C, 15E). WT, C70A, DAR999AAA and C70A/DAR999AAA double mutated AnkG show average intensity ratios between plasma membrane and cytoplasm of 8.5±0.4, 8.1±0.5, 7.8±0.5 and 5.4±0.3 respectively ($p<0.001$).

To evaluate the possibility that C70A mutation interferes with AnkG binding to known membrane-spanning proteins, we directly evaluated ability of C70A mutant AnkG-GFP to interact with E-cadherin and neurofascin using a membrane-recruitment assay in 293 cells. This assay takes advantages of the fact that WT AnkG, when expressed at high levels, exists in the cytoplasm, but can be recruited to the plasma membrane if co-expressed with a membrane partner. Detailed information of this assay can be found in previous publications (Kizhatil et al., 2007a; Zhang and Bennett, 1998). WT and C70A/DAR999AAA double mutant AnkG both were cytosolic when over-

expressed in 293 cells, but were equivalently recruited to the plasma membrane when co-transfected with either E-cadherin or neurofascin (Figure 16). C70A mutation thus has no effect on association of AnkG with at least two of its known protein partners. These results taken together are consistent with a role of palmitoylation of C70 in membrane targeting of ankyrin-G to the membrane of unpolarized MDCK cells (Figure 15A).

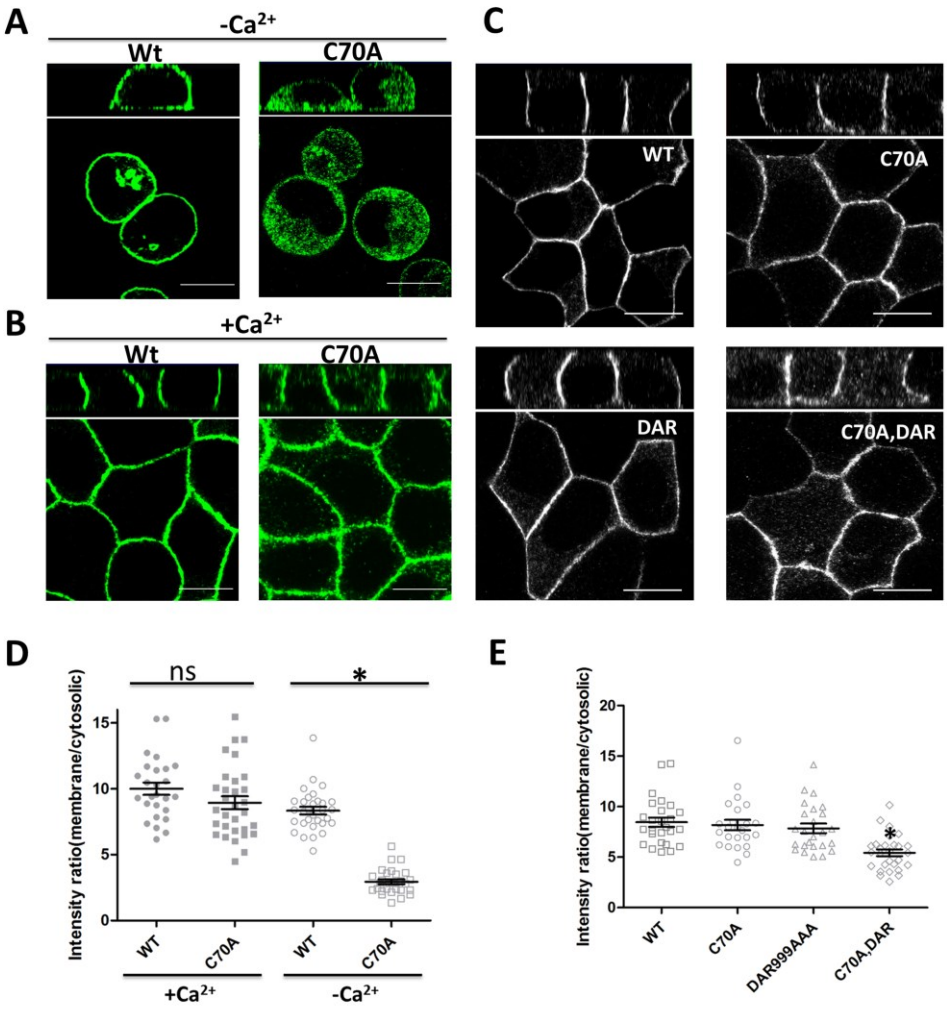

Figure 15: C70A mutation prevents AnkG retention in MDCK cells grown in low calcium.

(A, B), stable MDCK cells expressing WT or C70A AnkG-GFP were grown in low calcium medium or normal medium, then fixed and immunostained against GFP. (C), WT, C70A, DAR999AAA (DAR) and DAR999AAA, C70A double mutant (C70A, DAR) AnkG-GFP cDNA were transfected into MDCK cells, Scale bars, 10μm for A, B and C. (D), Quantitative results of the fluorescence intensity ratio of plasma membrane vs. cytoplasmic staining in AnkG stable MDCK cell lines. ($p<0.001$ for ANOVA, n=26-31 from two independent experiments). (E), Quantitative results of the fluorescence intensity ratio of plasma membrane vs. cytoplasmic staining of WT, C70A, DAR999AAA (DAR) and DAR999AAA, C70A double mutant (C70A, DAR) ($p<0.001$ for ANOVA, n=26-28 from three independent experiments). * indicates $p<0.05$.

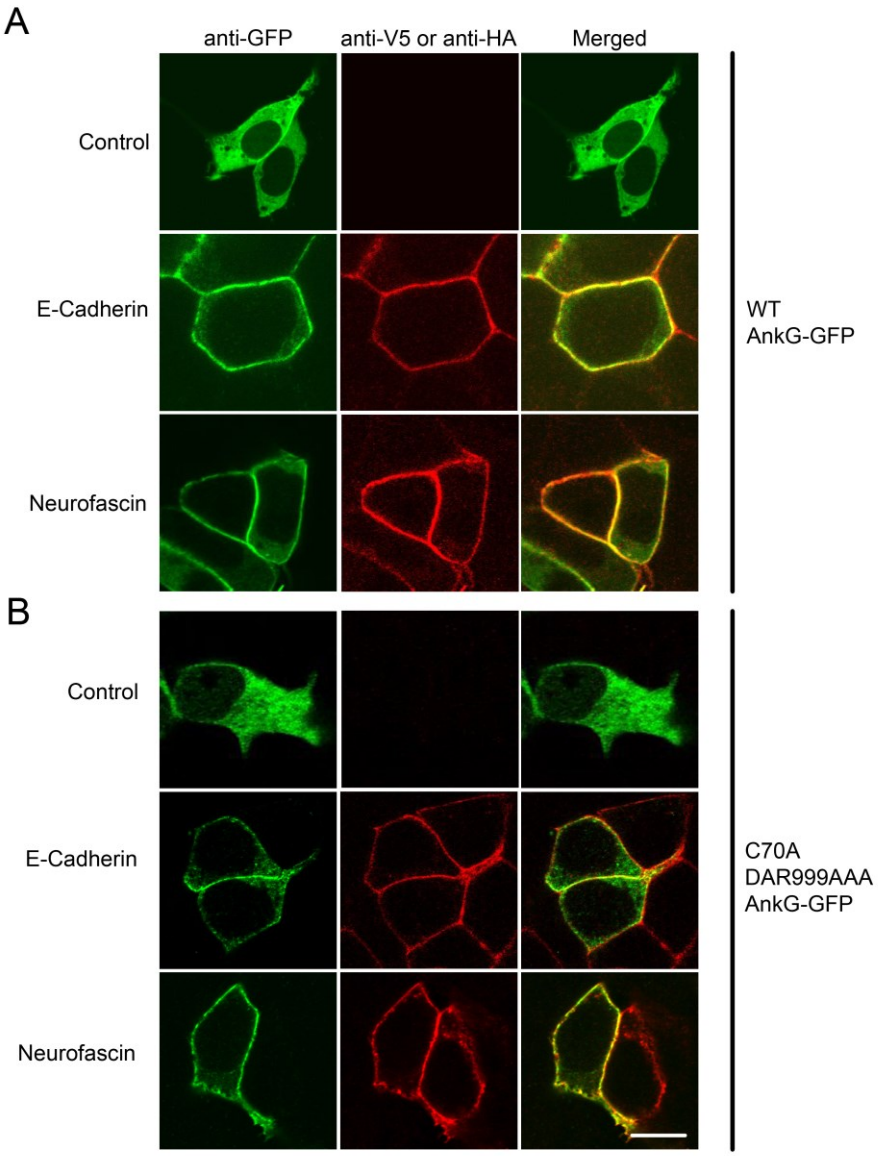

Figure 16: C70 mutation does not affect AnkG interactions with E-cadherin or neurofascin.

The membrane recruitment assay was used to monitor AnkG interactions with the interacting partners, E-Cadherin and Neurofascin. 80ng WT AnkG-GFP (*A*) or C70A/DAR999AAA AnkG-GFP (*B*) was transfected into HEK293 cells with or without (control) 100ng binding partner (V5-E-Cadherin or HA-Neurofascin). Cells were then fixed and double stained with anti-HA or -V5 (red) and anti-GFP (green) antibodies (scale bar, 10 μm).

3.3.4 Effect of C70A and DAR999AAA mutations on AnkG membrane dynamics

It is known that palmitoylation can alter membrane protein dynamics and intracellular trafficking (Henis et al., 2006). Here, we used Fluorescence recovery after photobleaching (FRAP) to examine whether C70A and DAR999AAA mutations affect mobility of GFP-tagged 190 kDa AnkG within the lateral membrane of polarized MDCK cells. WT AnkG exhibited rapid recovery to about 40 percent of its pre-bleach intensity in the first 100 seconds following photobleaching. However, WT AnkG exhibited little further recovery in the remaining 400 seconds, demonstrating a substantial immobile fraction of around 60 percent in the time scale of these measurements. In order to exclude the possibility that the partial recovery is an artifact resulting from total fluorescence loss, we analyzed our data by normalizing to an unbleached region (see experimental procedures for detail). We found that C70A mutation showed no significant increase in the mobile fraction or the initial rate of AnkG recovery within 5 minutes (Figure 17A, B). However, loss of β2-spectrin interaction through the DAR999AAA mutation further increased the mobile fraction by more than 30%, indicating that AnkG is restricted by association with β-2 spectrin (Figure 17A, B). The double mutant C70A/DAR999AAA AnkG showed no further increase in recovery compared to DAR999AAA mutation alone (Fig. 17A, B). These FRAP data demonstrate that a substantial fraction of lateral membrane-associated AnkG is immobile over a 5

minute measurement, and that loss of interaction with β2-spectrin but not C70A mutation increases the mobile fraction of AnkG.

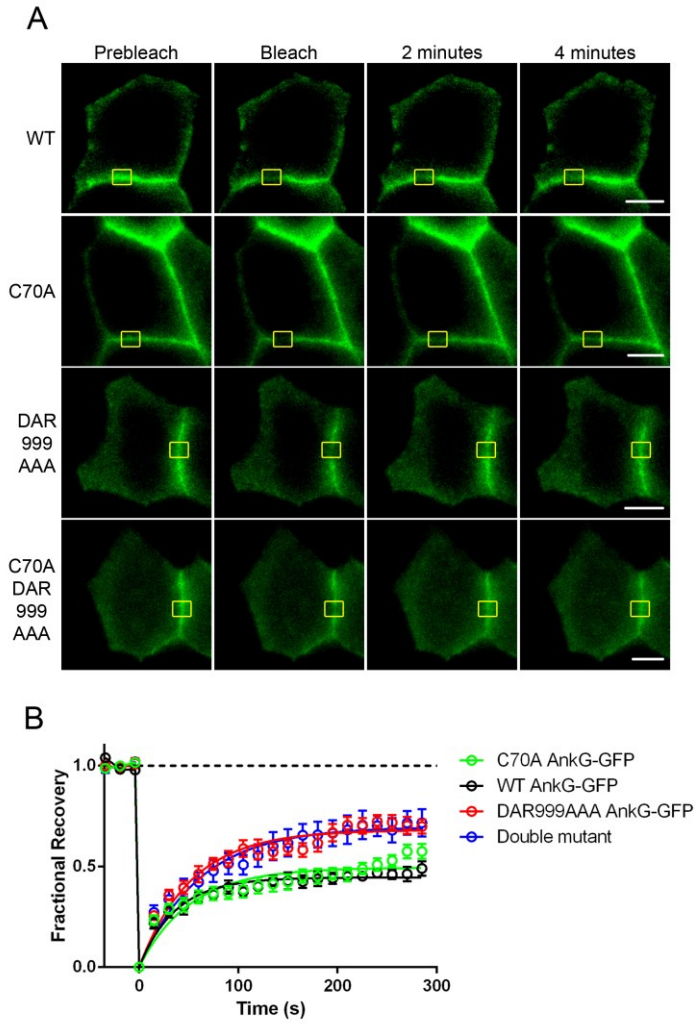

Figure 17: Effects of C70A mutation on AnkG dynamics at the lateral membrane

(A), 300ng WT, C70A , DAR999AAA and C70A/ DAR999AAA double mutant AnkG-GFP were transfected into MDCK cells. Fluorescence recovery after photobleaching (FRAP) was performed using LSM780 confocal microscope. The representative graphs show the fluorescence recovery within 5 minutes, yellow boxes indicate the regions bleached. B, quantitative results of N=10 repetitive measurements. The normalized fluorescence intensities were plotted against time and regressed against the one phase exponential equation $\mathbf{y = y_0 + Ae^{-k \times t}}$, using Graphpad Prism5 (scale bar, 10μm).

3.3.5 C70A mutation abolishes AnkG function in lateral membrane biosynthesis

AnkG collaborates with β2-spectrin in biogenesis of the lateral membrane in human bronchial epithelial cells (Kizhatil and Bennett, 2004; Kizhatil et al., 2007b). We evaluated effects of the C70A mutation on this AnkG function by knocking down endogenous AnkG in MDCK cells followed by rescue with GFP-tagged wild-type or mutant AnkG. We generated a doxycyclin-inducible AnkG shRNA MDCK stable cell line with a hairpin sequence targeting the ankyrin repeat domain. The targeting vector included the fluorescent protein mCherry which allowed isolation of infected cells by fluorescence activated cell sorting (FACS). RT-PCR and immunoblotting showed that 48 hour induction by doxycyclin diminished 210 kDa AnkG by more than 90% at both mRNA and protein levels without affecting the 100 and 120 kDa isoforms (Figure 18A). We observed that when AnkG is silenced by 90 percent, lateral membrane height is reduced from 10 microns to 3 microns (Figure 18B, C) (Kizhatil and Bennett, 2004). When cells depleted of endogenous AnkG were transfected with WT 190 kDa AnkG-GFP, the lateral membrane was restored to its normal height, as previously reported (Kizhatil and Bennett, 2004). However, expression of C70A 190 kDa AnkG failed to rescue lateral membrane height, and resulted in further intracellular accumulation of AnkG-GFP (Figure 18B). Of note, we found that rescue of lateral membrane height was dependent on expression of the rescue plasmid in adjacent cells, since cells that shared a cell-cell contact with a non-transfected cell demonstrated much lower cell heights.

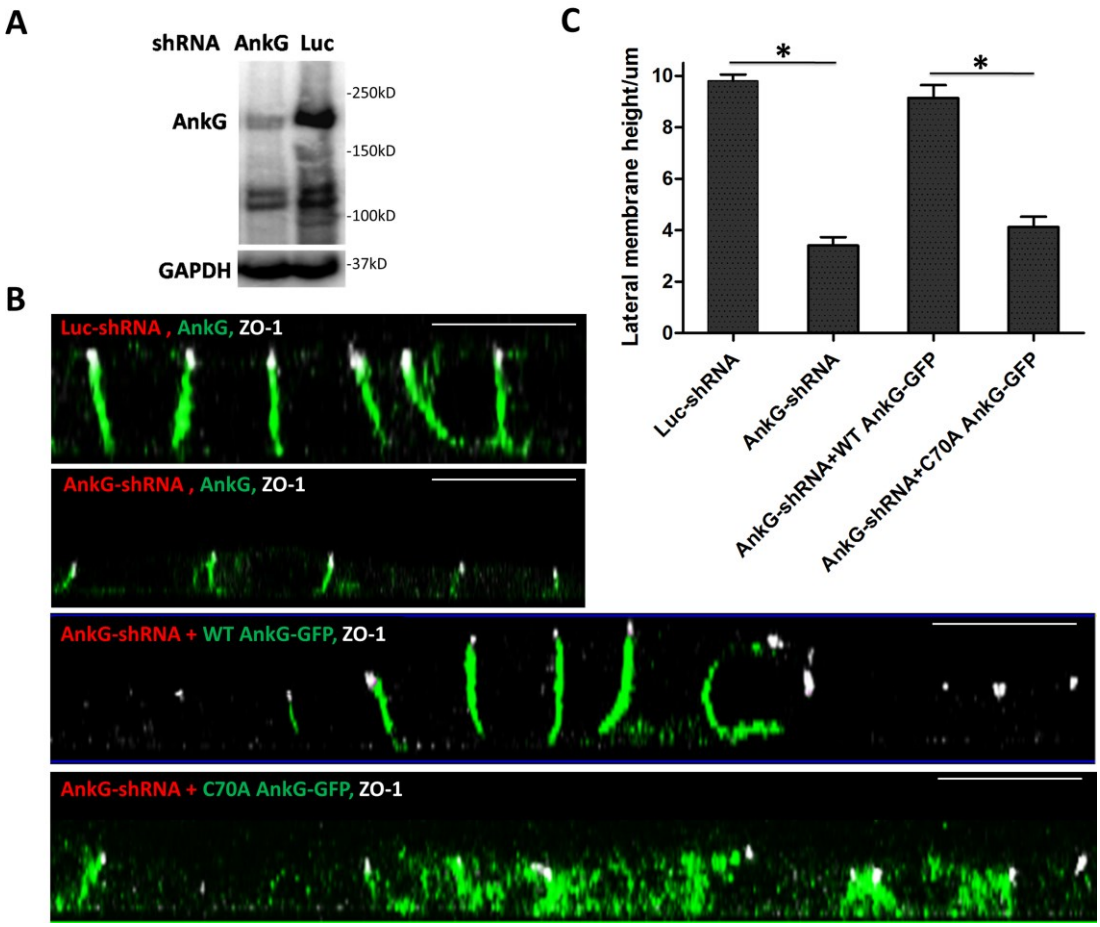

Figure 18: C70A mutation abolishes AnkG function in lateral membrane biosynthesis.

(A), doxycycline-inducible AnkG-shRNA MDCK cell line was generated using an engineered Tet-pLKO-mCherry vector. Two days doxycycline induction could selectively knock down 90% ~200kDa AnkG. (Blot is representative of at least three independent experiments). (B), XZ planes of lateral membrane under different conditions (green, AnkG; white, ZO-1, scale bar, 10μm). AnkG knockdown cells show defect in lateral membrane height compared to luciferase-shRNA cells. WT AnkG, but not C70A mutant is able to restore the height of lateral membrane. (C), quantitative results of the height of lateral membrane. The height was defined as the distance between the bottom of ZO-1 staining and the end of lateral membrane. Mean lateral membrane height was 9.8±0.3μm for Luciferase shRNA, 3.4±0.4μm for AnkG shRNA, 9.1±0.6μm for WT-AnkG rescue, and 4.1±0.5μm for rescue with C70A AnkG-GFP. Conditions were compared using one-way ANOVA followed by a Tukey Post-hoc test ($p<0.001$ for ANOVA, n=24-30 per condition). * indicates $p<0.05$.

3.3.6 C70A mutation abolishes function of 270kDa AnkG at the axon initial segment

270/480kDa AnkG concentrates at the AIS of neurons throughout the peripheral and central nervous system and recruits β4-spectrin and neurofascin (Jenkins and Bennett, 2001; Kordeli et al., 1995; Zhou et al., 1998). None of the known binding partners for AnkG are sufficient for its localization to the AIS (Hedstrom et al., 2007; Zhang and Bennett, 1998). We determined whether C70 plays a role in targeting of 270kDa AnkG to the AIS of cultured hippocampal neurons using a similar knockdown and replacement strategy as used in MDCK cells. By transfecting cells at 4-5 days in vitro, we are able to rescue AnkG expression during AIS formation to test the function of the mutant proteins. C70A 270kDa AnkG-GFP concentrated normally at the AIS in hippocampal neurons containing endogenous AnkG and intact AIS (Figure 20). However, if endogenous AnkG was depleted by shRNA, C70A AnkG was unable to cluster at the AIS region, and instead distributed evenly in the soma, dendrites and axon of transfected neurons (Figure 19A, B). Similarly, interaction with spectrin is also critical for formation of the initial segment, since DAR999AAA was also unable to cluster at the AIS (Figure 19A, B). Moreover, C70A 270kDa AnkG also lost ability to cluster neurofascin and sodium channels to the AIS (Figure 19D, E, F). This loss of ability to recruit neurofascin to the AIS is not a result of a loss of neurofascin binding since the AnkG double mutant (C70A/DAR999AAA) still interacts with neurofascin in the membrane recruitment assay in 293 cells (Figure 16). These results are consistent with a

requirement for palmitoylation for function of AnkG at the AIS as well as epithelial lateral membranes.

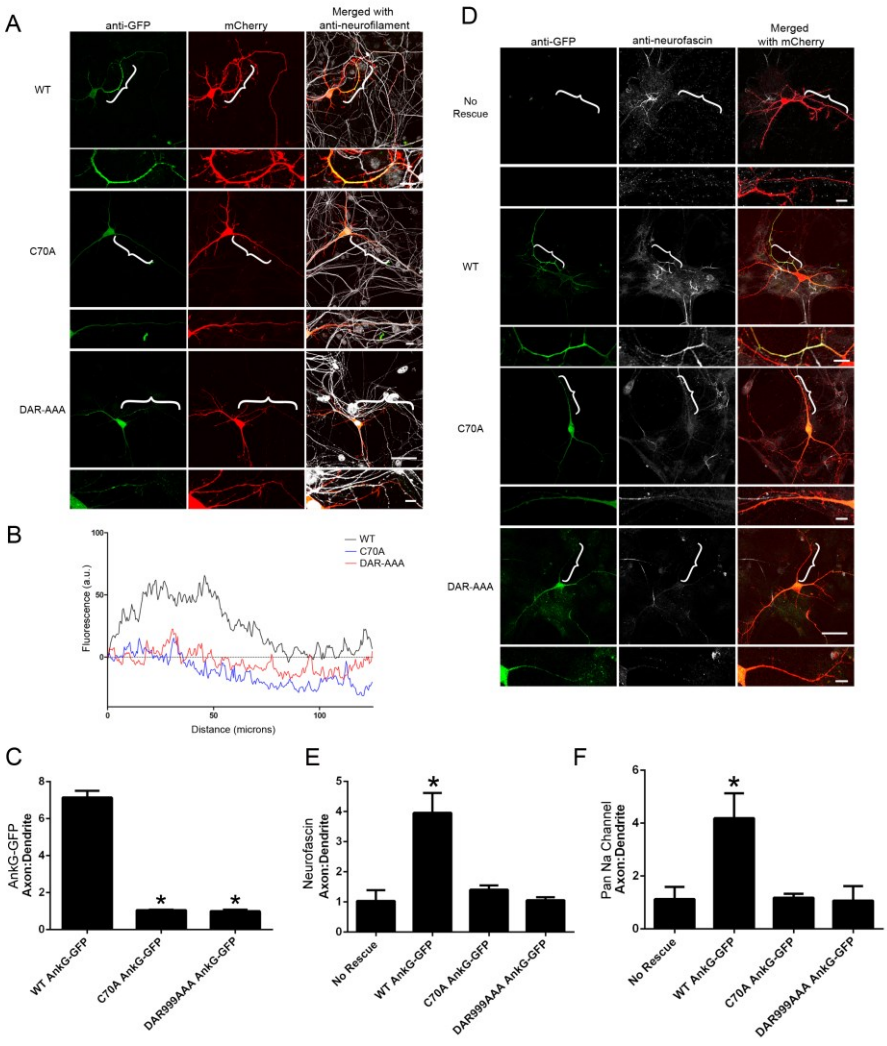

Figure 19: C70A mutation abolishes 270 kDa AnkG clustering and function at axon initial segments in hippocampal neurons.

(A, D), anti-GFP staining for 270kDa AnkG-GFP shown in green, mCherry marking transfected neurons shown in red and the axonal marker neurofilament shown in white (scale bar 50 μm). Brackets mark the axon initial segment, which is shown at higher magnification below each image (scale bar, 10 μm). (B), quantification of fluorescence intensity along the axons. (C), quantification of the anti-GFP fluorescence intensity ratio of axons to dendrites (n=3, * indicates $p<0.05$). (E, F) quantification of the anti-endogenous neurofascin or pan sodium channel fluorescence intensity ratio of axons to dendrites in cells depleted of endogenous 270kDa AnkG and rescued with mock, WT, C70A or DAR999AAA AnkG-GFP (n=3-4, * indicates $p<0.05$).

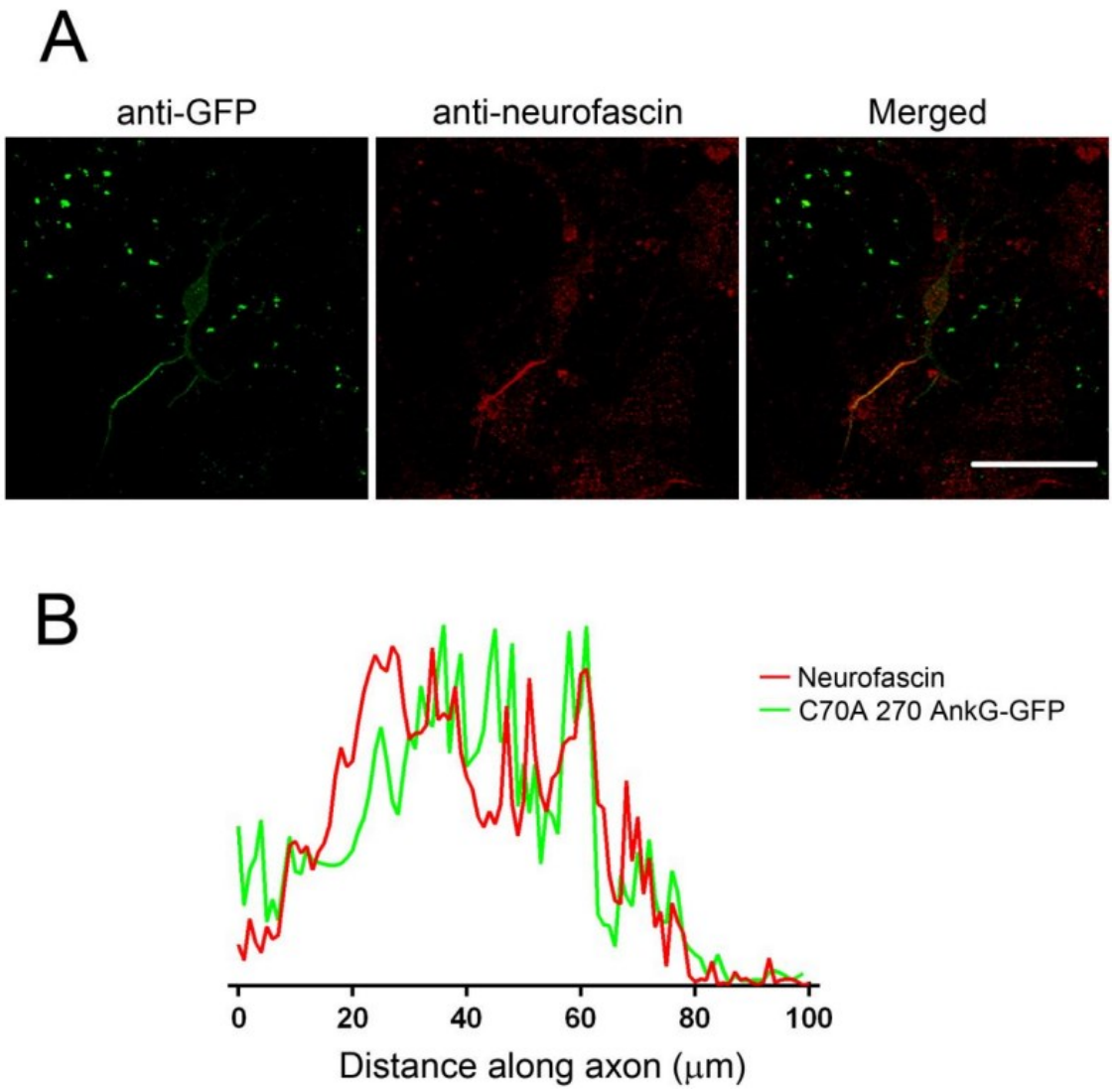

Figure 20: C70A 270kDa AnkG-GFP localizes at axon initial segments in wild type hippocampal neurons.

Hippocampal neurons were transfected with C70A 270kD AnkG-GFP, and fixed at day 7. (A), anti-GFP staining for C70A 270kD AnkG-GFP shown in green, anti-neurofascin shown in red (scale bar 100um). (B), measurements of fluorescent intensity along the axons.

3.4 Discussion

Here we demonstrate that AnkG is S-palmitoylated at cysteine 70 in MDCK cells, and that C70A mutation abolishes activity of AnkG in biogenesis of epithelial lateral membranes and assembly of the AIS in neurons. We also find that C70A mutation prevents association of AnkG with the plasma membrane of unpolarized MDCK cells. The C70A mutation is unlikely to result in loss of folding of AnkG since this residue is located in a predicted solvent-exposed loop of an ankyrin repeat (Figure 14A). Moreover, C70A mutation has no effect on interaction of AnkG with polarized MDCK cell lateral membranes or on interaction with E-cadherin or neurofascin. Effects of C70A mutation therefore are consistent with requirement of S-palmitoylation for function of AnkG at epithelial lateral membranes and the AIS. However, it is important to note that we cannot exclude other interpretations such as requirement of cysteine 70 for interaction with unidentified proteins.

A critical step in developing the palmitoylation hypothesis will be to identify which of the 24 palmitoyl-transferases are responsible for modification of AnkG. These enzymes exhibit specific expression and localization patterns and determine protein subcellular targeting, protein stability and membrane micropatterning (Aicart-Ramos et al., 2011; Greaves and Chamberlain, 2010). C70 is conserved among three ankyrin isoforms and across vertebrate species as well as one of the Drosophila ankyrin genes (Figure 14B). Therefore, it will be important to evaluate palmitoylation of other ankyrin

members and to determine if there is a conserved palmitoylation-dependent targeting mechanism shared by the ankyrin family.

FRAP measurements of WT AnkG-GFP motility on the lateral membrane in MDCK cells surprisingly shows a limited mobile fraction, which can be increased by 30% upon loss of β2-spectrin interaction but not palmitoylation (Figure 17A, B). The increased recovery with loss of spectrin binding is unlikely to result from plasma membrane-cytoplasm protein exchange, since WT AnkG-GFP reaches a steady plateau at only 40% fractional recovery. Our findings, for the first time, suggest the existence of membrane subdomains or compartments which may coordinate AnkG, β2-spectrin and probably other proteins. Those domains could play important roles in limiting AnkG dynamics on the lateral membrane. Even though the C70A mutation shows no effect on AnkG mobility, palmitoylation could be involved in organizing those subdomains. Interestingly, it has been reported that palmitoylated proteins are targeted to "lipid rafts" membrane subdomains (Delint-Ramirez et al., 2011; Fragoso et al., 2003; Linder and Deschenes, 2007). Furthermore, neurofascin, an AnkG binding partner, is palmitoylated at a site in the transmembrane domain conserved among the L1CAM family (Ren and Bennett, 1998). It will be of interest to study how the doubly palmitoylated AnkG-neurofascin complexes alter the properties of membrane domains in neurons. It also will be important in future experiments to directly visualize the

distribution of AnkG and other palmitoylated proteins at those membrane domains using high-resolution 3D microscopy.

A striking finding that stimulated our discovery of S-palmitoylation of AnkG was the retention of AnkG at the plasma membrane of unpolarized MDCK cells grown in low calcium (Figure 12A). AnkG is the only lateral membrane-associated protein that we are aware of that persists under low calcium conditions, and this behavior depends on C70 (Figure 15A, B). Residual AnkG is not associated with its partners β2-spectrin or E-cadherin, which are located in the cytoplasm, and may function as a template during reassembly of these proteins on the lateral membrane following restoration of calcium. It is tempting to speculate that residual AnkG remains membrane-associated through its C70-palmitate modification. In this case, lipid-based patterning of AnkG and other palmitoylated proteins may play important roles in determining lateral membrane identity.

Interestingly, in Chapter 2 we found that fusion of the B-linker to the ANK repeat domain of ankyrin-G or ankyrin-B reduces their lateral membrane targeting. One explanation may be that B-linker interferes with S-palmitoylation, since protein S-palmitoylation is mediated by a group of palmitoyltransferases, which can transiently associate with their substrates and transfer palmitic acids to target cysteine(s). Another possibility is that palmitoylation follows association of ANK repeats with membrane

proteins. In this case, the B-linker prevents ANK repeat domains from binding to plasma membrane compartments where they are subsequently palmitoylated.

Chapter 4. Ankyrin-G Palmitoylation and βII-spectrin Binding to Phosphoinositides Drive Lateral Membrane Assembly

4.1 Introduction

A common organizational principle shared by the spectrin-ankyrin-based plasma membrane domains, as presented in reviews and cartoons, is straightforward: membrane-spanning proteins, including cell adhesion proteins capable of responding to extracellular cues as well as membrane transporters, are "anchored" within the fluid bilayer by association with ankyrin, which in turn is coupled to an extended spectrin-actin network that is tightly associated with the plasma membrane. However, these protein-based models, while descriptive of steady state protein composition, do not provide an explanation for how membrane domains are actually assembled and precisely localized in cells.

In Chapter 3, we found that ankyrin-G is S-palmitoylated at a conserved cysteine 70, which is required for its function in assembling membrane domains, suggesting the essential roles of lipids in membrane domain assembly. Indeed, membrane lipids and lipid modifications play important roles in determining plasma membrane identity. For example, phosphoinositide lipids are increasingly recognized as critical determinants of plasma membrane organization in addition to their roles in intracellular organelles (Hammond et al., 2012; Johnson et al., 2012; Martin-Belmonte et al., 2007; Nakatsu et al., 2012; Shewan et al., 2011). In addition, the aspartate-histidine-histidine-cysteine (DHHC)

family of 23 protein palmitoyltransferases, first discovered in yeast, now are known to function in vertebrates in targeting and trafficking of membrane proteins (Bartels et al., 1999; Fukata et al., 2004; Fukata and Fukata, 2010; Greaves and Chamberlain, 2011; Roth et al., 2002). Beta-spectrins contain a pleckstrin homology domain with preference for phosphatidylinositol 4, 5-bisphosphate (PI(4,5)P2) (Das et al., 2008; Trave et al., 1995). Moreover, as described in the last chapter, different from any known polarized lateral membrane proteins, ankyrin-G remains on the plasma membrane of unpolarized MDCK cells through the palmitoylated cysteine 70 (Figure 11 and 15A), suggesting ankyrin-G as a candidate to function as a template to assemble lateral membranes. Together, these considerations suggest the membrane lipid environment and in particular phosphoinositides and protein palmitoylation, are likely to work in concert with ankyrin- and spectrin-based protein interactions in establishing and/or regulating membrane domains.

In this Chapter, we identifies DHHC 5 and 8 as the only DHHC family members localized to the lateral membrane of MDCK cells and the two palmitoyltransferases responsible for palmitoylation and targeting of ankyrin-G. We also find that βII-spectrin requires binding to both ankyrin-G as well as phosphoinositide lipids in order to localize and function at lateral membranes. βII-spectrin thus operates as a co-incidence detector that ensures high spatial fidelity in its polarized targeting to the lateral membrane. Together these findings demonstrate a critical requirement of palmitoylation and

phosphoinositide recognition in addition to protein-protein interactions for precise assembly of ankyrin-G and βII-spectrin at the lateral membrane of epithelial cells.

4.2 Methods and Materials

Plasmids

The 23 HA tagged mouse DHHC constructs were a kind gift from Dr. Masaki Fukata (National Institute for Physiological Sciences, Japan). DHHC5 was subcloned into peGFP-C1 vector using SacII and BamHI cut sites; DHHC8 was subcloned into peGFP-C1 vector using SalI and BamHI cut sites; DHHC14 was subcloned into peGFP-N1 using HindIII and EcoRI cut sites. The wild type ankyrin-G-GFP and mutants C70A and DAR999AAA were previously described (Kizhatil et al., 2007b). The human βII-spectrin cDNA was subcloned into peGFP-C3 vector using HindIII and SacII cut sites, the mutations Y1874A and K2207Q were introduced by mutagenesis. For βII-spectrin purification, a prescission protease site (LEVLFQGP) was introduced between the GFP and start codon. The pleckstrin homology domain of human βII-spectrin (PH domain: amino acids 2200-2305) was subcloned into peGFP-N1 using XhoI and SacII cut sites.

Reagents and antibodies

Palmitic Acid, [9,10-3H(N)] (PerkinElmer); N-Ethylmaleimide and hydroxylamine (Sigma); EZ-Link BMCC-Biotin, 1-Biotinamido-4-[4′-(maleimidomethyl)cyclohexanecarboxamido]butane (Thermo Scientific); Dynabeads

with protein-G and Lipofectamine 2000 transfection reagent (Invitrogen); QuikChange II XL Site-Directed Mutagenesis Kit (Agilent Technologies). Mouse α-HA monoclonal antibody (Santa Cruz); rabbit α-GFP polyclonal antibody (lab generated); chicken α-GFP polyclonal antibody, rat α-E-cadherin monoclonal antibody (Abcam); rabbit α-ankyrin-G polyclonal antibody (lab generated using the C terminal domain as epitope); rabbit α-biotin polyclonal antibody, rabbit α-DHHC5 polyclonal antibody, rabbit α-DHHC8 polyclonal antibody (Abcam); mouse α-GAPDH monoclonal antibody (sigma); mouse α-ZO-1 monoclonal antibody (Invitrogen).

Metabolic radiolabeling

This assay was performed following the protocol previously described with a few modifications (Fukata et al., 2006). In brief, 10^6 HEK293T cells were plated in the 6-well plates and transfected with 2μg HA-DHHC plasmids plus 3μg ankyrin-G-GFP plasmids. 20 hours after transfection, the cells were incubated with DMEM supplemented with 5% dialyzed FBS for 1 hour, then [^{3}H]palmitic acid was added to the final concentration of 200μCi/ml. After 4 hours incubation, the cells were washed with PBS and lysed directly using 0.5ml SDS-PAGE buffer (62.5mM Tris–HCl pH 6.8, 10% glycerol, 2% SDS, 0.001% bromophenol blue and 10mM DTT) and heated for 5 minutes at 70^{o}C. The proteins were separated in 3.5%-17.5% gradient polyacrylamide gels. For western blotting, samples were transferred onto nitrocellulose membrane and probed with α-GFP, or α-HA antibody. For autoradiography, the gels were treated with amplify

fluorographic reagent, dried using cellophane membrane and exposed to X-ray film at -80°C.

Generation of doxycycline-inducible shRNA MDCK cell lines

The original pLKO-Tet-on lentiviral vector (Addgene) was modified by replacement of the puromycin resistant gene with fluorescent TagBFP, and the IRES (internal ribosome entry site) with P2A peptide (GSGATNFSLLKQAGDVEENPGP), which mediates co-translational cleavage. After cloning the shRNA hairpin targeting genes of interest to the vector, lentivirus was generated following standard protocol (Wiederschain et al., 2009). On the day of infection, 0.5-1×10^6 MDCK cells were mixed with virus and 8μg/ml polybrene and plated in 6-well dishes. 16 hours later, the cells were extensively washed to remove viral particles and then grown in DMEM, 10% FBS. The next day, cells were trypsinized and sorted for the brightest TagBFP population (~1%), which can be maintained as a stable cell line. Hairpins used to target genes of interest: luciferase control (ggagatcgaatcttaatgtgc); dog ankyrin-G (gctagaagtagctaatctcct); dog βII-spectrin (ggtgctattactatctcaaga); dog DHHC5 (gtgtcagatgggcagataact); dog DHHC8 (acctgtccaggaccatcatgg); dog DHHC5/8 (tgggtgaacaactgtatcg).

rtPCR

To examine the native transcription of DHHC5 and DHHC8 in MDCK cells, total RNA was isolated using standard TRIzol-based protocol, and cDNA was generated

using SuperScript® III First-Strand Synthesis System (Life technology). Primers used for gene amplification: dog GAPDH (F: ggtgatgctggtgctgagtatgttg; R: agtggaagcagggatgatgttctgg); dog DHHC5 (F: ggaggatgaagacaaggaagatgac; R: gctacagggatgaagaataagccag); dog DHHC8 (F: gatgaggacgaggataaggaggac; R: gatgacagggatgaagaagaggc).

Acyl-biotin exchange assay

This assay was described in the last chapter. Briefly, Luc-, DHHC5-, DHHC8- or DHHC5/8-shRNA cells were induced by 4μg/ml doxycycline for 3 days and then homogenized in the presence of 50mM N-Ethylmaleimide. 1% SDS was added to the lysates to increase ankyrin-G solubility. After sonication and centrifugation, Triton X-100 was added to a final concentration of 1% (v/v) to quench SDS. 60 μl of dynabeads preloaded with 10μg α-ankyrin-G antibody were then incubated with the lysates overnight. The beads were then washed and incubated with hydrolysis-labeling buffer (1M hydroxylamine/Tris as a control, 80μM biotin-BMCC, 10mM sodium phosphate, 2mM NaEDTA, pH=7) at room temperature for 2 hours. Beads were then washed and incubated with loading buffer (2% SDS, 10% glycerol, 40mM Tris-HCl, 150mM NaCl, 2mM NaEDTA, 200mM DTT with bromophenol blue). Samples were analyzed by SDS-PAGE and probed by immunoblotting with α-ankyrin-G or α-biotin antibodies. The total cell lysates were also collected and analyzed to confirm the knockdown efficiency of DHHC5 and 8.

Transfection and Immunofluorescence

To examine the subcellular localization of the 23 DHHC palmitoyltransferases, 1×10^5 MDCK cells were plated in the insert of MatTek plates. The next day, cells were transfected with 80ng plasmids encoding HA- or GFP-DHHC using Lipofectamine. 48 hours later, the cells were fixed by 4% paraformaldehyde for 15 minutes, permeabilized by 0.4% Triton-X100 for 10 minutes, blocked by 5% BSA, and incubated with primary antibody overnight at 4°C. Alexa Fluor 488, 568 were used for secondary antibody. To study the localization of ankyrin-G after silencing DHHC5, DHHC8 or DHHC5/8, cells were induced by 4μg/ml doxycycline for one day and then re-plated on MatTek plates in the presence of doxycycline for another 2 days before fixation. Parallel samples were collected for western blotting to study ankyrin-G levels.

Calcium switch assay and lateral membrane re-assembly

The calcium switch assay was described in the last chapter. Here we used this assay to study lateral membrane re-assembly. Luc-, Ankyrin-G- or DHHC5/8-shRNA cells were induced by 4 μg/ml doxycycline for 3 days, then trypsinized and plated in calcium-depleted medium (DMEM, 5% dialyzed FBS, 4 μg/ml doxycycline, 10^6 cells in MatTek plates). The next day, washed the plates slightly to remove un-attached cells and then switched to regular medium (DMEM, 10% FBS, 4 μg/ml doxycycline). Cells were then fixed at different time points (2 hours, 4 hours, 8 hours, 16 hours and 24 hours). To examine the localization of transfected GFP-DHHC5 and 8 in unpolarized MDCK cells,

100ng DNA was transfected into MDCK cells following standard protocol. 6 hours later, the cells were trypsinized and re-plated in calcium-depleted medium and kept for 24 hours before fixation.

Lateral membrane rescue

10^7 Ankyrin-G-shRNA or βII-spectrin-shRNA cells were induced in 10cm dishes in the presence of 4 μg/ml doxycycline for 16 hours. Then 1.5×10^5 pre-induced cells were re-plated in MatTek plates. 8 hours later, cells were washed and transfected them with 100ng rescue plasmids (GFP, Ankyrin-G-GFP or GFP-βII-spectrin) using the standard protocol. Cells were maintained in 4 μg/ml doxycycline and fixed 48 hours after transfection.

Microscopy

Imaging for fixed samples was performed at room temperature using a Zeiss LSM780 confocal microscope with either a 63×, NA 1.40 or 100×, NA 1.45 objective lens. Secondary antibodies were conjugated with Alexa fluor 488, 568 or 647. XZ planes were reconstructed from Z stacks with optical sections of 250nm using ZEN 2012 software. For live imaging, the incubation chamber was maintained at 37°C, 5% CO_2, and cells were maintained in growth medium (DMEM, 10% FBS). For 3D deconvolution microscopy, images were collected at room temperature using the 100×, NA 1.45 objective lens with optical sections of 250nm, and subjected to 3D deconvolution in Volocity 3D Image Analysis Software (PerkinElmer) with a point spread function (Axial

Spacing In Z: 0.25 μm, Lateral Spacing In X-Y: 0.0277 μm, Medium Ref. Index: 1.52, Numerical Aperture: 1.45, Detector Pinhole Size: 1 Airy unit(s)).

Expression and purification of βII-spectrin:

βII-spectrin was cloned into peGFP-C3 along with a prescission protease site (LEVLFQGP) between the GFP and ATG of βII-spectrin. Mutations were made into the βII-spectrin sequence using site-directed mutagenesis (Stratagene). WT-βII-spectrin and mutants were transfected into 293T17 cells in 10 cm dishes using lipofectamine (Invitrogen). After 36 hours lysates were produced from each transfection and GFP-βII-spectrin was isolated using a rabbit anti-GFP antibody and pulled down using protein-G dynabeads (Invitrogen). After extensive washing using high salt and TritonX-100, βII-spectrin was released from dynabeads using prescission protease enzyme (GE Life Sciences).

Ankyrin-G-βII-spectrin binding assay

His-tagged ankyrin-G expressed in S9 cells was purified as previously described (Kizhatil et al., 2007a). GFP-βII-spectrin WT and GFP-βII-spectrin Y1874A expressed and purified from HEK293 cells were immobilized using antibody against GFP on protein-G dynabeads and increasing concentrations of ankyrin-G-His were added to a final reaction volume of 200μl in binding buffer (10 mM sodium phosphate, 75 mM NaCl, 1mM DTT, 1mM EDTA, 5% sucrose and 4% BSA, pH 7.3). Bound and free ankyrin-G-His were separated by pelleting beads through a 20% sucrose cushion. The amount of

bound ankyrin-G-His was determined through immunoblotting with α-His antibody followed by phosphor image analysis. Data points were generated after normalization for βII-spectrin levels and nonspecific binding of ankyrin-G.

Fluorescence recovery after photobleaching

300ng plasmids encoding GFP-βII-spectrin WT or Y1874A were transfected into βII-spectrin-silenced MDCK cells as described above. The GFP signals were collected every 5 seconds for a 3-minute period, at each time point three regions were monitored: region 1 is the photobleached membrane area; region 2 is a membrane area of an adjacent transfected cell, which can be used to control the signal variability; region 3 is a non-transfected cell region, which is used to correct the background noise. The signal from region 1 was double-normalized to that from region 2 and 3, and then fitted to the exponential equation $y = y_0 + Ae^{-k \times t}$.

Phosphatidylinositol binding assay

We purchased phosphatidylinositol labeled liposomes that contained a biotin tag from Echelon Biosciences. Liposomes for PIP2(3,4), PIP2(4,5), PIP3(3,4,5) and PIPN(control) were used at 10 μM concentration and incubated with purified βII-spectrin WT and βII-spectrin K2207Q in interaction buffer (50 mM Tris, 100 mM NaCl, 1mM DTT, 5% sucrose and 3% fatty-acid free BSA, pH 7.4). Bound βII-spectrin was separated from free βII-spectrin through pull down of liposomes using streptavidin-

labeled dynabeads. Levels of protein binding were determined by immunoblotting using α-βII-spectrin antibody and quantified through phosphor imager.

Data analysis

ImageJ was used to measure the fluorescence intensity of confocal microscopy images, and a typhoon-9200 phosphor imager and Imagequant software were used to quantify the intensity of western blots. Student's t-test was used to analyze two-group comparison, and one-way ANOVA followed by Tukey's tests were used to perform multiple group comparison. The tests were performed using GraphPad Prism 5 software.

4.3 Results

4.3.1 DHHC5 and 8 are the physiological ankyrin-G palmitoyl-transferases in MDCK cells.

We previously demonstrated that cysteine 70 of ankyrin-G is palmitoylated, and is required for ankyrin-G function in formation of epithelial lateral membranes of MDCK cells as well as axon initial segments of hippocampal neurons (He et al., 2012). We next sought to identify the palmitoyltransferase(s) responsible for modifying ankyrin-G. A screening assay using metabolic labeling with tritiated-palmitate in cells co-transfected with substrate and individual member of the DHHC family of 23 palmitoyltransferases has been widely used to determine enzyme specificity (Fernandez-Hernando et al., 2006; Fukata et al., 2004; Fukata et al., 2006; Iwanaga et al.,

2009; Tsutsumi et al., 2009). Using this assay in HEK 293T cells, we observed a dramatic increase of palmitoylation of ankyrin-G-GFP when co-expressed with either DHHC5 or DHHC8, but not with the other 21 DHHC family members (Figure 21A).

A phylogenetic comparison of the 23 mouse DHHC proteins shows that DHHC5 and DHHC8 are closely related (Figure 21B). DHHC5 and DHHC8 use GRIP1b as a substrate in neurons and play critical roles in regulating AMPA-R trafficking (Thomas et al., 2012). Additionally, DHHC5 also directly palmitoylates flotillin-2 and is required for flotillin-2 oligomerization (Li et al., 2012). However, no study has characterized the biological functions of DHHC5 and 8 palmitoyltransferases in epithelial cells.

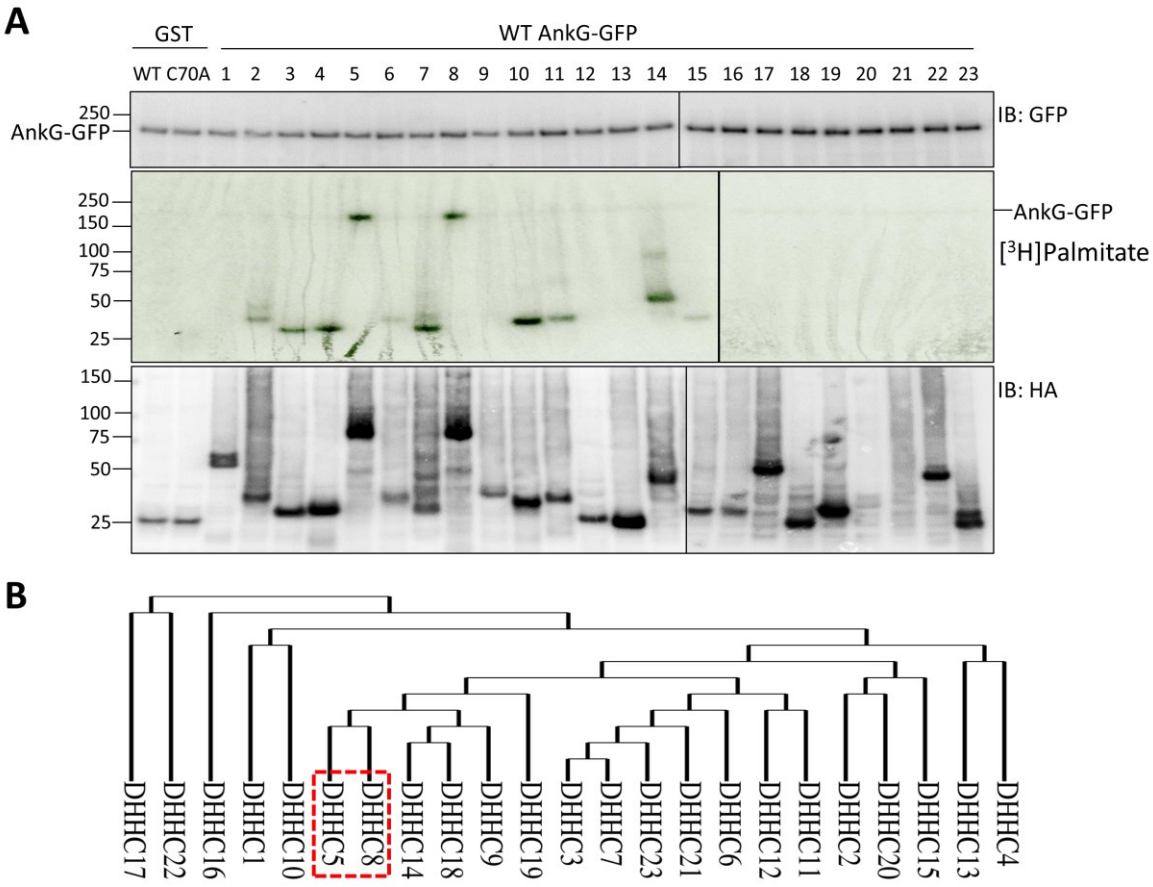

Figure 21: Ankyrin-G is palmitoylated by palmitoyltransferases DHHC5 and DHHC8.

(A) DHHC5 and DHHC8 increase the palmitoylation level of ankyrin-G. Ankyrin-G-GFP was co-transfected into HEK293 cells with each of the 23 HA-DHHC. After metabolic labeling with [3H]-palmitic acid, cells were lysed and analyzed by SDS-PAGE. (Top) the expression level of ankyrin-G-GFP probed by α-GFP antibody; (middle) autoradiograph showing the extent of protein labeling in cell extracts; (bottom) the expression level of the co-transfected HA-DHHC probed by α-HA antibody. (B) The phylogenetic tree of the 23 mouse DHHC shows that DHHC5 and DHHC8 are closely related.

We next asked where DHHC5 and 8 are localized in MDCK cells, and whether these particular palmitoyltransferases exhibit a distinct pattern compared to the other 21 DHHC family members. Tagged DHHC proteins exhibit specific localization patterns in non-polarized HEK 293T cells (Ohno et al., 2006). However, the localization of DHHC proteins in epithelial cells has not been reported. 20 of the HA-DHHC constructs transfected into MDCK cells localized to intracellular compartments, most likely the Golgi/ER network as previously described (Ohno et al., 2006). However, DHHC5, DHHC8 and DHHC14 predominantly localized to the plasma membrane when viewed in XY sections (Figure 22A). The plasma membrane localization of DHHC8 and DHHC14 in MDCK cells was unexpected since these proteins are primarily intracellular in HEK 293T cells (Ohno et al., 2006). 3D confocal imaging in MDCK cells revealed that DHHC5 and DHHC8 are polarized and confined to the lateral membrane together with ankyrin-G (Figure 22B, 22C). DHHC14, in contrast to DHHC 5 and 8, localizes equally to both lateral and apical membranes (Figure 22D). DHHC5 and 8 thus are the only family members that co-localize with ankyrin-G on the lateral membranes of MDCK cells.

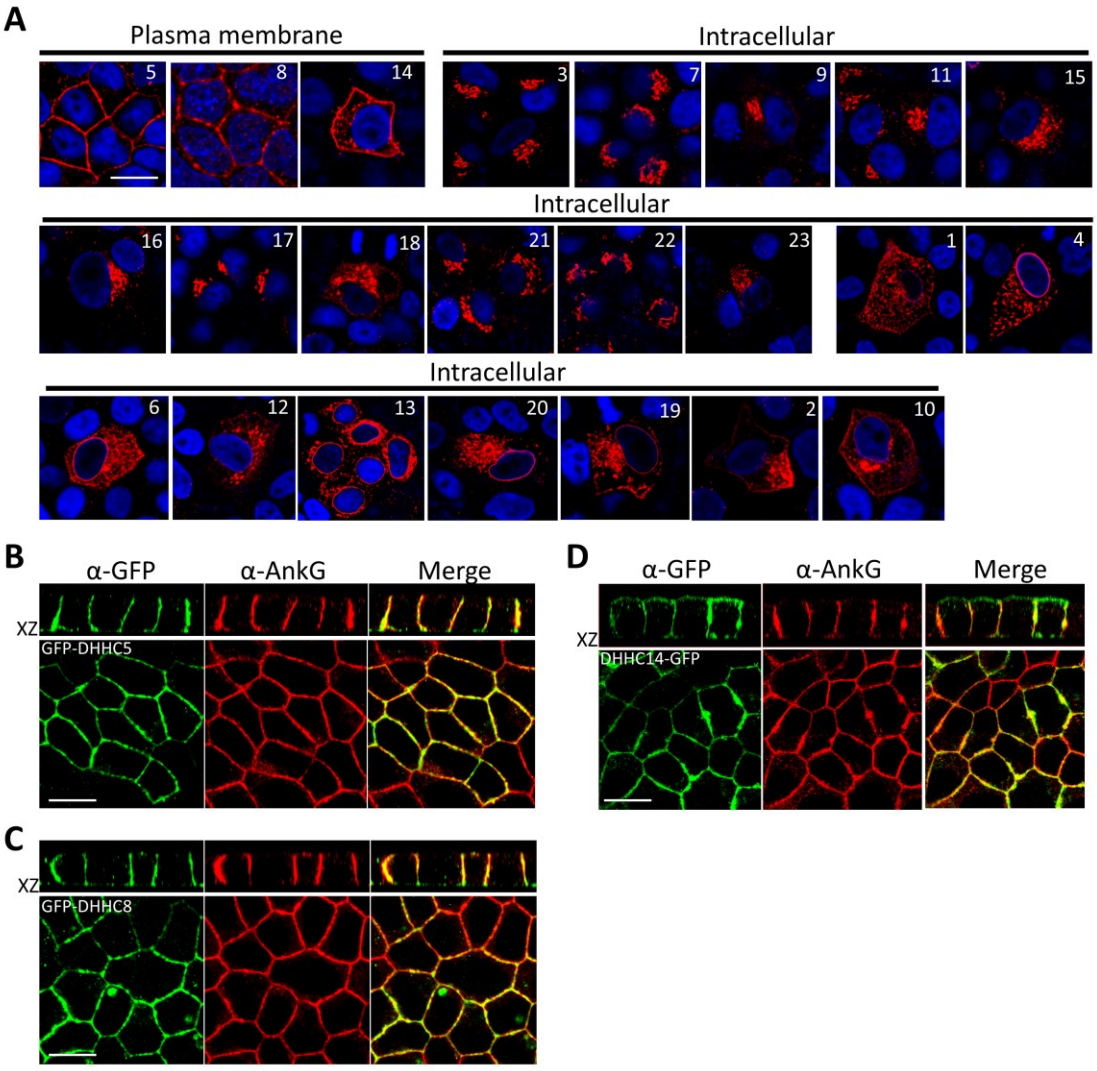

Figure 22: DHHC5 and DHHC8 colocalize with ankyrin-G at lateral membranes of MDCK cells.

(A) HA-DHHC family members target to different membrane structures. HA-DHHC 1-23 were expressed separately in MDCK cells, and visualized by immunofluorescence (red, α-HA; blue, DAPI). HA-DHHC5, 8 and 14 are primarily localized to the plasma membrane, while the others exist in intracellular compartments. Scale bar, 10 μm. (B, C and D) GFP tagged DHHC5, 8 and 14 were transfected into MDCK cells, after achieving complete polarization, the cells were fixed for immunofluorescence (green, α-GFP; red, α-ankyrin-G), the XZ planes were reconstructed from confocal Z-stacks. Scale bar, 10μm.

A critical test of whether ankyrin-G is a physiological substrate for DHHC5 and 8 was to determine if knockdown of these enzymes resulted in loss of ankyrin-G palmitoylation. We first confirmed that both DHHC5 and DHHC8 are natively transcribed in cultured MDCK cells using RT-PCR (Figure 23A). Then we developed a cell-sorting strategy for generating doxycycline-inducible shRNA stable cell lines in order to study effects of knockdown of DHHC 5 and 8, either separately or together. We modified the single lentiviral vector Tet-inducible shRNA system (pLKO-Tet-On) (Wiederschain et al., 2009) in two ways: 1. The puromycin resistance gene was replaced with DNA encoding the fluorescent protein TagBFP (excite 402; emit 457) to allow fluorescent cell sorting without interfering with other fluorescent tags such as GFP or mCherry; 2. The internal ribosome entry site (IRES) was replaced with a 2A "self-splicing" peptide linker to ensure that stimulation of shRNA expression also efficiently stimulated expression of TagBFP (Figure 23B). Through cell sorting, we were able to select a small population of MDCK cells with similar high levels of shRNA expression (Figure 23C).

DHHC5 and DHHC8 genes of *Canis lupus familiaris* share identical genomic sequences in multiple regions, which allow individual knockdown as well as selection of a single hairpin simultaneously targeting both genes in MDCK cells. An acyl-biotin exchange assay was used to assess ankyrin-G palmitoylation (Drisdel et al., 2006). Single knockdown of either DHHC5 or DHHC8 had no effect on palmitoylation of ankyrin-G

(Figure 23D, E, F and J). However, silencing both DHHC5 and DHHC8 markedly reduced ankyrin-G palmitoylation (Figure 23G, H, I and J). In summary, DHHC 5 and 8 are the physiological palmitoyltransferases responsible for palmitoylating ankyrin-G in MDCK cells based on their unique behavior compared to the other 21 DHHC family members in palmitoylating ankyrin-G in heterologous cells, their co-localization with ankyrin-G at the lateral membranes of MDCK cells, as well as loss of ankyrin-G palmitoylation following their knockdown in MDCK cells.

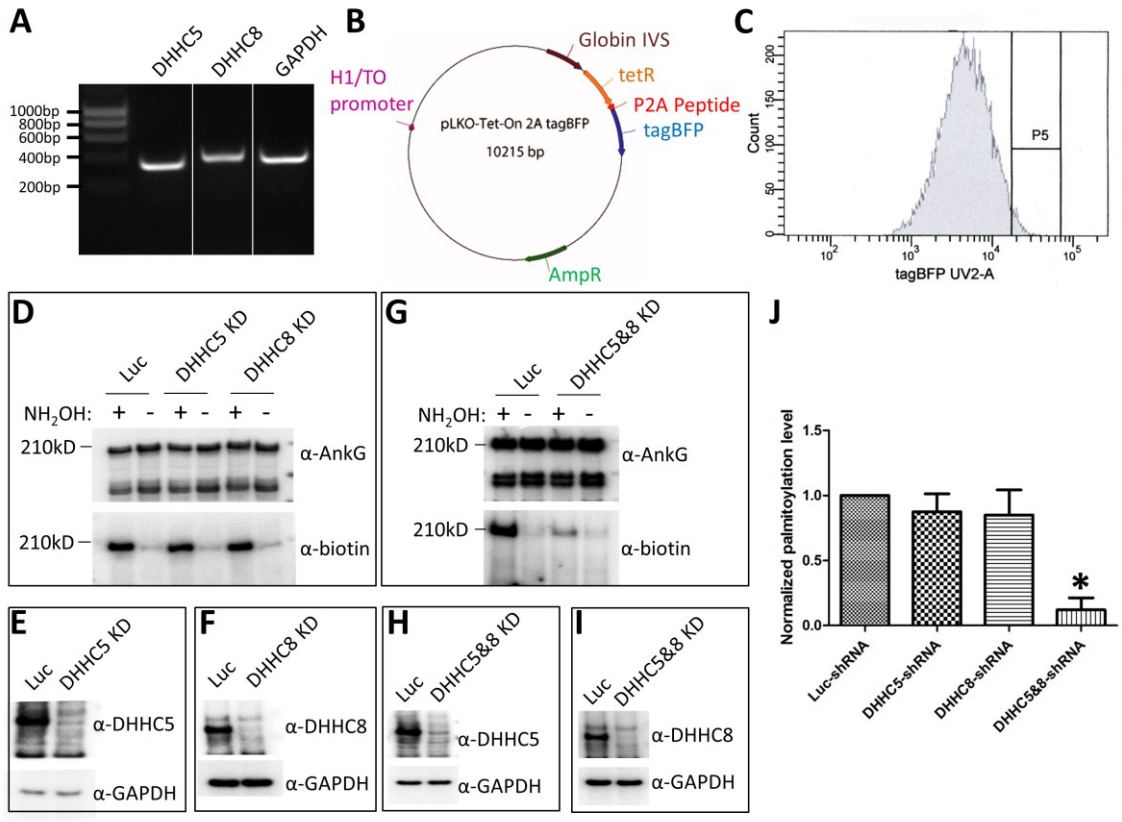

Figure 23: DHHC5 and DHHC8 exhibit functional redundancy in palmitoylation of ankyrin-G.

(A) The rtPCR shows that both DHHC5 and 8 are natively transcribed in MDCK cells. (B and C) The cell sorting based strategy for making inducible shRNA cell lines. (D, E and F) Single knockdown of DHHC5 or DHHC8 shows no reduction of ankyrin-G palmitoylation. Endogenous ankyrin-G was immunoprecipitated and analyzed using acyl biotin exchange assay (D). The silencing efficiency of DHHC5 (E) or DHHC8 (F) was also verified. Luc is a control cell line which targets the luciferase gene. (G, H and I) Double knockdown of DHHC 5 and 8 causes significant reduction of ankyrin-G palmitoylation. (J) Quantification of the normalized ankyrin-G palmitoylation level, mean±SEM. Results were analyzed using one-way ANOVA and Tukey's tests, $p<0.001$, $n=3$-5.

4.3.2 DHHC5/8 double knockdown phenocopies loss of ankyrin-G in MDCK cells

We next examined effects of knockdown of DHHC5 and 8 on subcellular localization of endogenous ankyrin-G and on cell height. In the DHHC5/8 double knockdown cells, ankyrin-G staining spread from the plasma membrane to the cytosol, in contrast to the single knockdown or control cells where ankyrin-G was confined to the lateral membrane (Figure 24A and 24D). Residual ankyrin-G staining remaining on the lateral membrane may result from residual palmitoylation which was only 90 percent complete, and/or interaction with E-cadherin and/or βII-spectrin. In addition, 110 and 120 kDa cross-reacting polypeptides (Figure 24B) likely resulting from alternative splicing lack ANK repeats and are not subject to palmitoylation (He et al., 2012; Hoock et al., 1997; Peters et al., 1995). The loss of membrane staining was not caused by reduction of ankyrin-G expression level based on immunoblots of control and DHHC5/8 double knockdown cells (Figure 24B and C). Interestingly, the DHHC5/8 double knockdown cell monolayer exhibited a markedly reduced lateral membrane height (Figure 24A, the XZ plane; 24E), thus phenocopying loss of ankyrin-G (Kizhatil and Bennett, 2004; Kizhatil et al., 2007b). This result is consistent with previous findings that ankyrin-G requires its palmitoylated cysteine 70 to restore the lateral membrane in ankyrin-G-depleted MDCK cells (He et al., 2012).

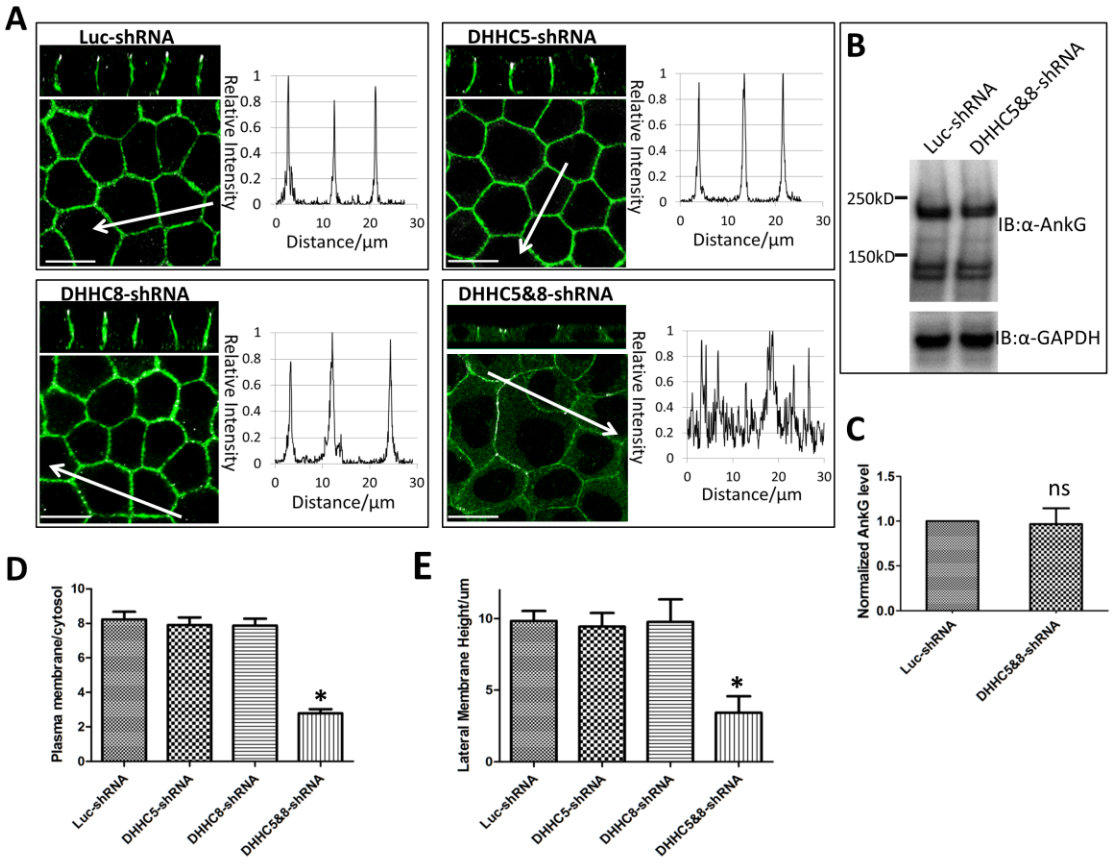

Figure 24: Double knockdown of DHHC5 and 8 in MDCK cells causes disassociation of ankyrin-G from the plasma membrane and reduces lateral membrane height.

(A) The inducible shRNA cell lines were treated with doxycycline to knockdown indicated genes, and then fixed for immunofluorescence (green, α-ankyrin-G; white, α-ZO-1). The profiles represent the α-ankyrin-G fluorescence intensities across the regions of interest indicated by the white arrows. Scale bar, 10μm. (B) Representative western blot showing ankyrin-G levels after silencing DHHC5 and 8. (C) Quantification of the normalized ankyrin-G level in DHHC5/8-silenced cells, mean±SEM, student's t-test, p=0.8, n=4. (D) Quantification of the α-ankyrin-G fluorescence intensity ratio of plasma membrane to cytosol. Results were analyzed using one-way ANOVA and Tukey's tests, p<0.001, n=47-53. (E) Quantification of the lateral membrane height. Results were analyzed using one-way ANOVA and Tukey's tests, p<0.001, n=47-53.

MDCK cells require millimolar concentrations of calcium to achieve apical-basolateral polarity, and reversibly lose their polarity when transferred to a low calcium medium (Martinez-Palomo et al., 1980). We previously reported that ankyrin-G remains on the plasma membrane in un-polarized MDCK cells exposed to low calcium, while its binding partners E-cadherin and βII-spectrin re-locate to intracellular sites (Figure 25A. (He et al., 2012)). In contrast, C70A ankyrin-G mutant, which is resistant to palmitoylation, also exhibited loss of plasma membrane staining in un-polarized MDCK cells (He et al., 2012). Under the same low calcium condition, DHHC5 and DHHC8 remain localized to the plasma membrane together with ankyrin-G (Figure 25B). Moreover, double knockdown of DHHC5 and 8 abolished the plasma membrane localization of ankyrin-G in un-polarized MDCK cells (Figure 25C). These results together with loss of membrane association by the C70A ankyrin-G mutant demonstrate that palmitoylation of ankyrin-G by DHHC5/8 drives its association with the plasma membrane in un-polarized MDCK cells.

We next compared effects of knockdown of either DHHC5/8 or 210 kDa ankyrin-G on lateral membrane re-assembly following restoration of calcium. Control cells (Luc-shRNA) experienced rapid biosynthesis of the lateral membrane, and grew from about 2 to 8 microns in height within 24 hours. In contrast, cells depleted of either 210 kDa ankyrin-G or DHHC5/8 failed to restore lateral membrane height and grew from 2 to only 3 microns over the same period (Figure 25D and E) (see Figure 26 for extent of 210

kDa ankyrin-G knockdown). However, loss of 210 kDa ankyrin-G or DHHC5/8 did not affect the establishment of cell polarity, indicated by unaltered tight junction staining for ZO-1 and lateral membrane staining for E-cadherin (Figure 25D). Cells depleted of either ankyrin-G or DHHC5/8 still maintained a residual lateral membrane of about 3μm. The remaining lateral membrane may result from incomplete knockdown as detectable levels of ankyrin-G as well as DHHC5/8 persist in shRNA-expressing cells (Figure 23, 26). Alternatively, the residual height of 2-3 microns may represent lateral membrane that is independent of the ankyrin-G-DHHC5/8 pathway.

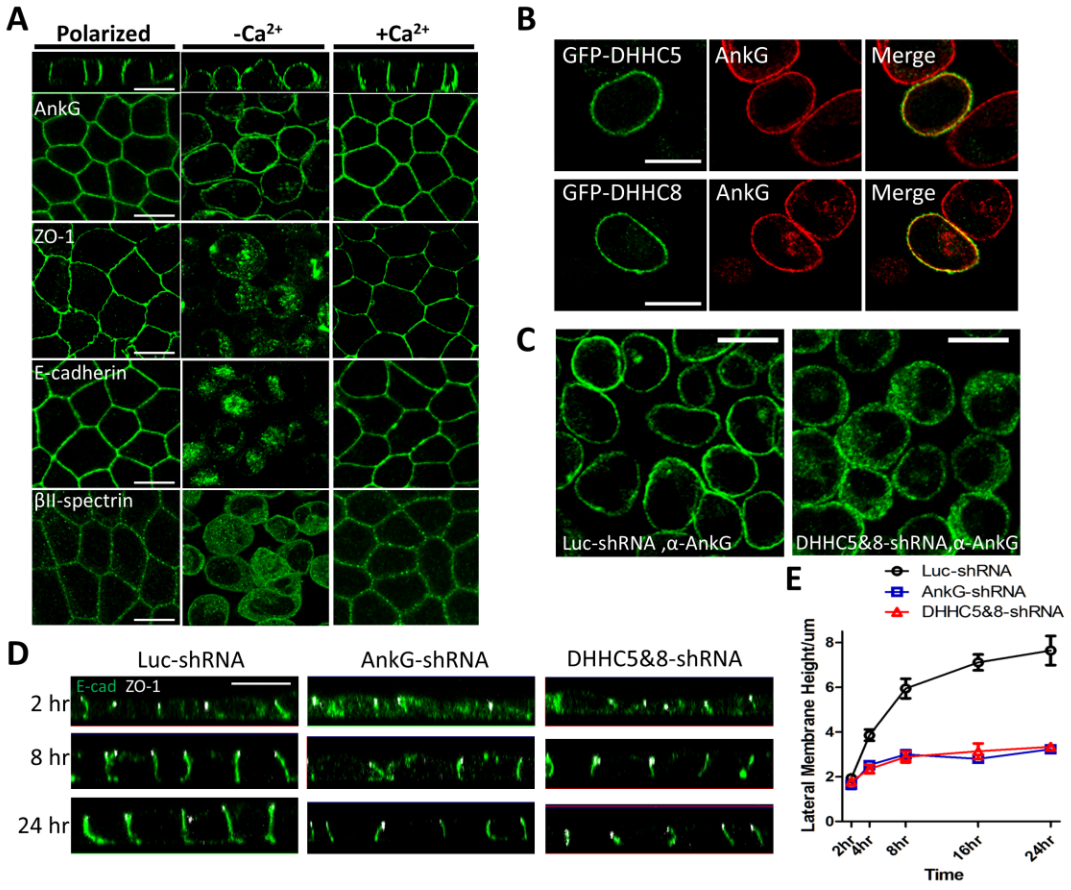

Figure 25: DHHC5/8 and ankyrin-G are required for lateral membrane re-assembly following calcium switch.

(A) Ankyrin-G persists on the plasma membrane in unpolarized MDCK cells. Polarized MDCK cells (Polarized) were trypsinized and grown in Ca2+-depleted medium for 24 hours before fixation (-Ca2+), or switched back to regular medium for another 24 hours (+Ca2+). Samples were stained against Ankyrin-G, ZO-1, E-cadherin or βII-spectrin. Scale bar, 10μm. (B) GFP-DHHC5 and 8 colocalize with ankyrin-G in unpolarized MDCK cells (green, α-GFP; red, α-ankyrin-G), scale bar, 10μm. (C) DHHC5/8-silenced cells or control cells (Luc-shRNA) were plated in Ca2+-depleted medium, and fixed to stain against endogenous ankyrin-G, scale bar, 10μm. (D) DHHC5/8 or ankyrin-G-silenced cells fail to re-assemble the lateral membrane following calcium switch. Luc-shRNA, Ankyrin-G-shRNA and DHHC5/8-shRNA cells were induced by doxycycline to knockdown indicated genes, and then plated in Ca2+-depleted medium. 24 hours later, cells were switched back to regular medium and fixed at different time points, 2 hours, 4 hours, 8 hours, 16 hours and 24 hours (green, α-E-cadherin; white, α-ZO-1), scale bar, 10μm. (E) Quantification of the lateral membrane heights, mean±SEM, n=17-31.

4.3.3 βII-spectrin requires both ankyrin-G and phosphoinositides for lateral membrane targeting

Results so far demonstrate that palmitoylation of ankyrin-G by DHHC5/8 is required for targeting ankyrin-G to the lateral membrane as well as for re-assembly of the lateral membrane following restoration of calcium to un-polarized MDCK cells. We next addressed the role of ankyrin-G in targeting βII-spectrin to the lateral membrane. βII-spectrin potentially can associate with plasma membranes either through its ankyrin-binding site (Davis et al., 2009; Ipsaro et al., 2009), and/or through a pleckstrin homology (PH) domain that preferentially binds to PI(4,5)P2 (Das et al., 2006; Das et al., 2008; Hyvonen et al., 1995; Wang et al., 1996; Wang and Shaw, 1995). Analysis of epistatic relationships between β-spectrin and the two ankyrin genes in Drosophila indicate cell type-specific variations in utilization of PH domains and ankyrin-binding activities (Das et al., 2006; Das et al., 2008; Garbe et al., 2007; Mazock et al., 2010). We therefore wanted to determine how βII-spectrin assembles on the lateral membrane in MDCK cells.

We faced technical challenges in imaging endogenous βII-spectrin and ankyrin-G polypeptides. βII-spectrin antibodies prepared from two different sets of rabbits recognized a large portion of intracellular structures and reacted weakly with the lateral membrane. We do not believe these antibodies accurately represent the localization of endogenous βII-spectrin for the following reasons. GFP-tagged βII-spectrin, which is biologically active since it rescues the loss of lateral membrane height in βII-spectrin knockdown cells, localizes almost entirely to the lateral membrane in cells depleted of

native βII-spectrin (not shown), whether viewed by live imaging or in fixed cells using antibodies against GFP (Figure 27). Antibodies against ankyrin-G recognize a major 210 kDa polypeptide as well as 110 and 120 kDa polypeptides that are likely alternatively spliced variants lacking ANK repeats (Figure 26) (Peters et al., 1995; Hoock et al., 1997). 110 and 120 kDa polypeptides were not depleted by shRNA directed against the ANK repeat region (Figure 26). In order to avoid problems with βII-spectrin antibodies and complications due to multiple ankyrin-G alternative spliced variants, we therefore adopted the strategy of knockdown of endogenous 210 kDa ankyrin-G or βII-spectrin and replacement with GFP-tagged proteins as described next.

We addressed the contributions of spectrin-ankyrin and spectrin-phosphoinositide interactions in MDCK cells by evaluating mutations of ankyrin-G that abolish its binding to βII-spectrin, and mutations of βII-spectrin that abolish either its binding to either ankyrin or to phosphoinositides. In each set of experiments, native 210 kDa ankyrin-G or βII-spectrin were knocked down and replaced with either GFP-tagged wildtype or mutated proteins. GFP-tagged proteins were visualized either using the same antibody against GFP, or by live imaging of native GFP fluorescence. This approach circumvented the problems with antibodies against βII-spectrin as well as complications due to alternatively spliced variants of ankyrin-G noted above. We utilized the same approach of doxycycline-inducible knockdown as employed with DHHC5 and 8 (see above; (Figure 23)) to achieve inducible loss of 80-90 percent of native

210 kDa ankyrin-G or βII-spectrin (Figures 26, 27). Cells induced for shRNA expression were subsequently transfected within 24 hours with GFP-tagged 190 kDa ankyrin-G or βII-spectrin (Methods). 190 kDa ankyrin-G and the native 210 kDa ankyrin-G differ in that 210 kDa ankyrin-G contains additional residues in the C-terminal regulatory domain (WeiChou Tseng and Vann Bennett, unpublished data). However, 190 and 210 kD ankyrin-G do not exhibit any difference in localization or ability to restore the lateral membrane in MDCK cells.

DAR999AAA mutation of ankyrin-G at surface residues of its $ZU5^N$ domain abolishes its binding to spectrin without affecting ankyrin-G expression levels (Ipsaro et al., 2009; Ipsaro and Mondragon, 2010; Kizhatil et al., 2007b). DAR999AAA ankyrin-G lost activity in restoring the lateral membrane in ankyrin-G-silenced cells (Kizhatil et al., 2007b) (Figure 26A and 26B). However, DAR999AAA ankyrin-G still maintained its polarized localization at the residual lateral membrane, presumably due to palmitoylation and/or interaction with E-cadherin (Figure 26B). Ankyrin-G thus does not require βII-spectrin for targeting to the lateral membrane.

Mutation of a highly conserved tyrosine located in a surface-exposed loop within the 15^{th} repeat of β-spectrins disrupts their interaction with ankyrins (Ipsaro et al., 2009; Ipsaro and Mondragon, 2010; Kizhatil et al., 2007b) (Figure 25f). We confirmed that the Y1874A mutation increased the dissociation constant of βII-spectrin for ankyrin-G from 10-20nM to greater than 200nM, and thus reduced the affinity by at least 8 fold (Figure

26F and G). Y1874A βII-spectrin associated equally with both apical and lateral membranes and thus completely lost polarity (Figure 26C and D). Y1874A βII-spectrin also failed to restore the lateral membrane height (Figure 26C and D). The non-polarized plasma membrane association of Y1874A βII-spectrin is likely due to its PH domain, since the βII-spectrin PH domain fused to GFP also associates generically with all plasma membrane surfaces (Figure 27D).

We performed fluorescence recovery after photobleaching (FRAP) experiments to examine whether loss of ankyrin-G interaction affects higher-order assembly of βII-spectrin into stabilized structures. Indeed, the Y1874A GFP-βII-spectrin exhibited a marked increase in dynamics on the lateral membrane compared to the WT GFP-βII-spectrin (Figure 26H), affecting both the extent of recovery (55% for WT, 86% for Y1874A) and half-time required for recovery (36s for WT, 17s for Y1874A). These results indicate that βII-spectrin depends on ankyrin-G for its localization and function in MDCK cells.

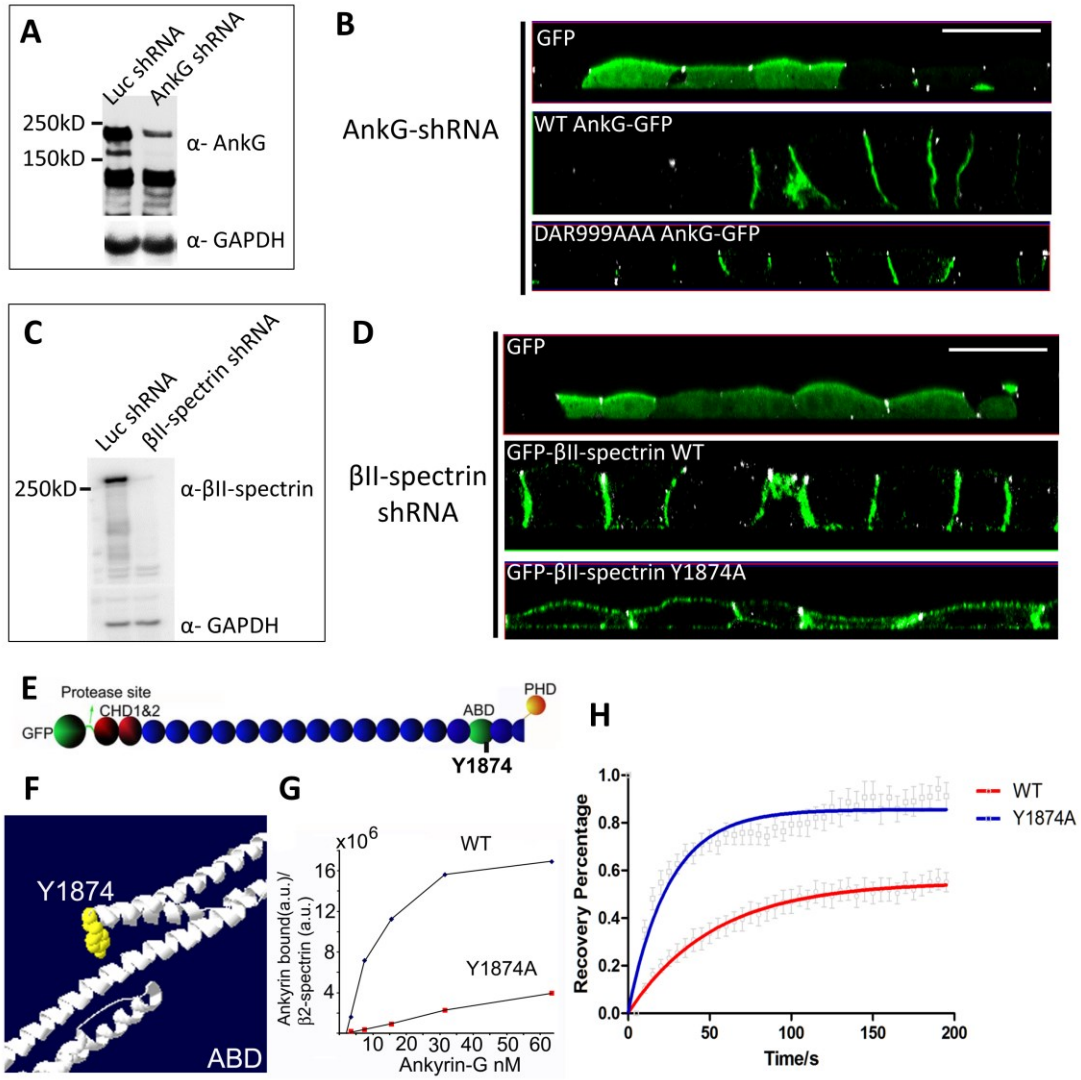

Figure 26: Ankyrin-G determines the polarized recruitment of βII-spectrin to the lateral membrane.

(A) ankyrin-G knockdown efficiency. (B) Ankyrin-G-silenced cells were rescued by GFP, WT Ankyrin-G-GFP or DAR999AAA Ankyrin-G-GFP (green, α-GFP; white, α-ZO-1). Scale bar, 10μm. (C) βII-spectrin knockdown efficiency. (D) BII-spectrin-silenced cells were rescued by GFP, GFP-βII-spectrin WT or GFP-βII-spectrin Y1874A (green, α-GFP; white, α-ZO-1). Scale bar, 10μm. (E) GFP-βII-spectrin construct with precision protease site. (F) βII-spectrin's ankyrin-binding domain, residue Y1874 is highlighted in yellow. (G) The protein binding curve of ankyrin-G with WT βII-spectrin or the Y1874A mutant. (H) The fluorescence recovery after photobleaching (FRAP) showing the dynamics of GFP tagged WT βII-spectrin or the Y1874A mutant on the lateral membrane, n=8-11.

We also confirmed the finding that in MDCK cells βII-spectrin requires ankyrin-G to be polarized at the lateral membrane by examining endogenous proteins. In βII-spectrin knockdown cell, ankyrin-G still localized at the lateral membrane, though the height was significantly reduced. However, in ankyrin-G knockdown cells, βII-spectrin was mislocalized to the apical surface (Figure 27).

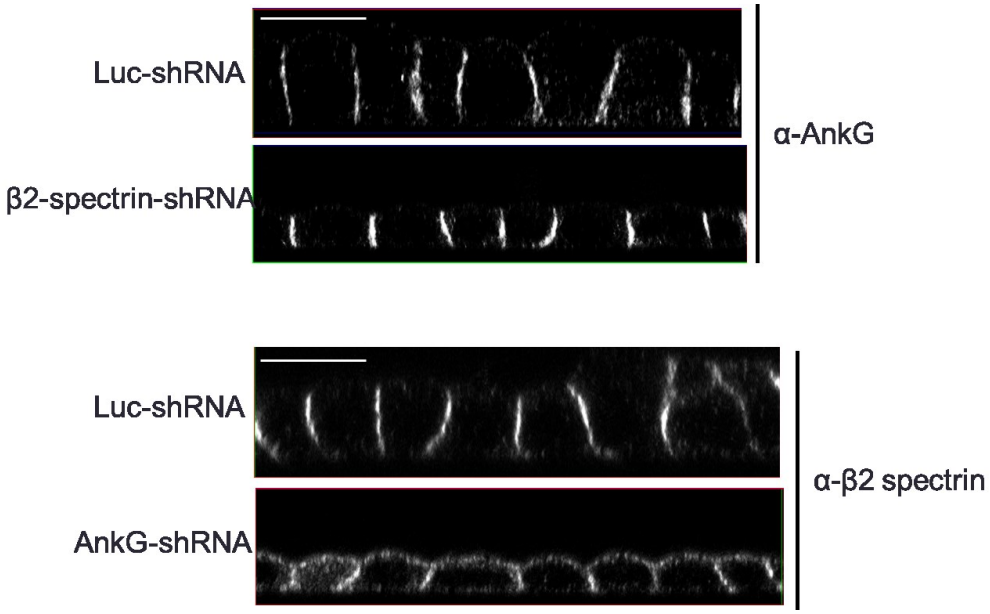

Figure 27: Knockdown of ankyrin-G causes apical mislocalization of βII-spectrin.

We next addressed the role of phosphoinositide recognition by the PH domain of βII-spectrin. Basic residues in the pleckstrin homology domain of β-spectrin required for binding to inositol (1,4,5) P3 have been identified using NMR and other methods (Hyvonen et al., 1995; Rameh et al., 1997). Moreover, mutation of a basic PH domain residue eliminated binding of Drosophila β-spectrin to PI(4,5)P2 (Das et al., 2008). We

confirmed that K2207Q mutation in the PH domain of βII-spectrin abolished binding affinity for phosphoinositides based on loss of interaction with lipid strips and liposomes containing various phosphoinositide lipids (Figure 28C). WT βII-spectrin also associated weakly with PI(3,4)P2 and PI(3,4,5)P3 in addition to PI(4,5)P2, but these interactions were also eliminated by the K2207Q mutation.

The K2207Q βII-spectrin mutant exhibited a striking loss of association with the plasma membrane and remained intracellular (Figure 28E). The K2207Q βII-spectrin mutant also failed to restore the lateral membrane height (Figure 28E and F). This complete loss of plasma membrane targeting by K2207Q βII-spectrin that still retains ankyrin-G binding site is not consistent with a simple linear assembly pathway. Instead, βII-spectrin association with ankyrin-G on the lateral membrane is somehow coupled to interactions of its PH domain with phosphoinositide lipids. The dual requirement of βII-spectrin for both ankyrin and phosphoinositide lipids may explain some of the complexity noted in earlier analysis of relationships between ankyrins and spectrin in Drosophila (Das et al., 2008).

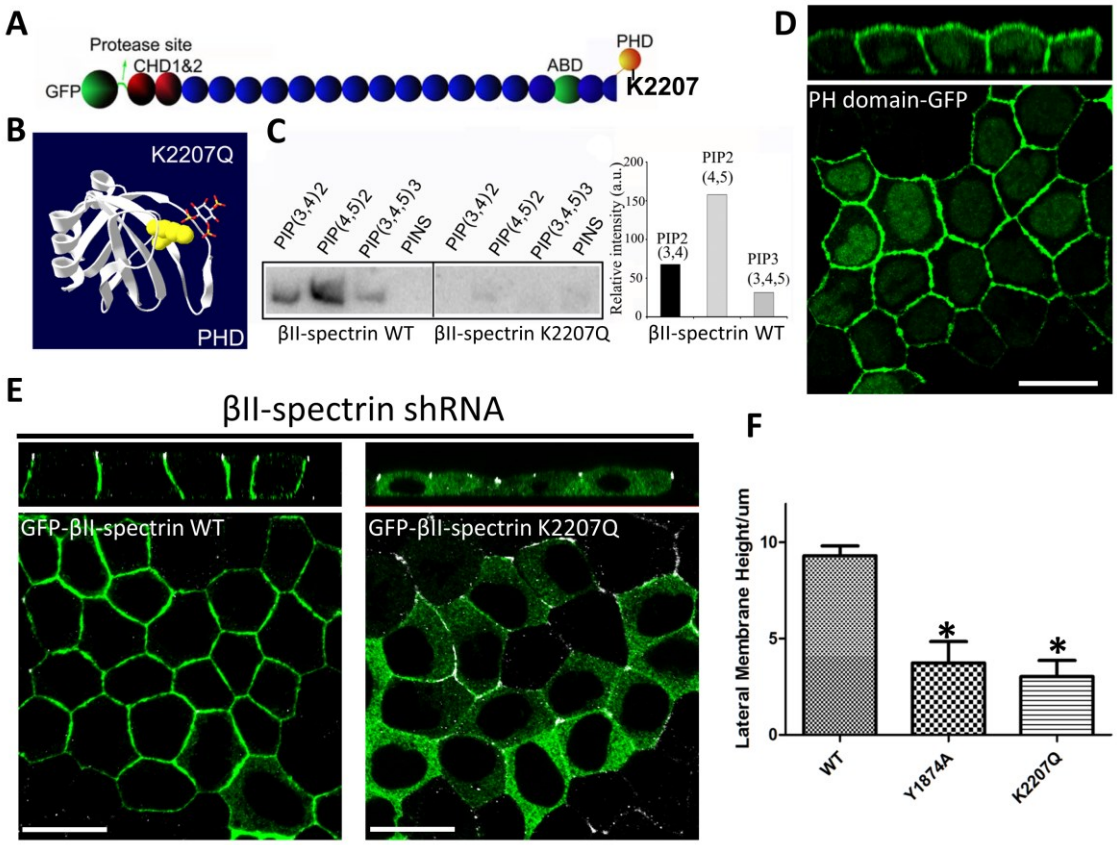

Figure 28: βII-spectrin targets to the plasma membrane through its pleckstrin homology domain by binding to PI (4,5)P2.

(A) The schematic diagram of GFP-βII-spectrin K2207Q. (B) The atomic structure of the pleckstrin homology domain (PHD), the key residue required for phosphoinositides binding is highlighted in yellow. (C) The blots and quantification show the binding affinity of isolated WT βII-spectrin or K2207Q mutant to different phosphatidylinositol labeled liposomes (PI(3,4)P2, PI(4,5)P2, PI(3,4,5)P3 and PIPN(control)). (D) The pleckstrin homology domain (PHD) of βII-spectrin is sufficient to target to the plasma membrane. (Top) the XZ plane, (bottom) the XY plane. Scale bar, 10μm. (E) GFP-βII-spectrin K2207Q fails to target to the plasma membrane or restore the lateral membrane. BII-spectrin-silenced cells were rescued by GFP-βII-spectrin WT or GFP-βII-spectrin K2207Q (green, *α*-GFP; white, *α*-ZO-1), (top) the XZ plane, (bottom) the XY plane. Scale bar, 10μm. (F) Quantification of lateral membrane heights rescued by WT, Y1874A or K2207Q GFP-βII-spectrin. Results were analyzed using one-way ANOVA and Tukey's tests, $p<0.001$, n=27-35.

4.3.4 DHHC5/8, ankyrin-G, and βII-spectrin co-localize in micron-scale membrane subdomains

We next examined the spatial relationships between DHHC5/8, ankyrin-G, and βII-spectrin in the lateral plasma membrane using 3D deconvolution to improve resolution of confocal microscopy (Biggs, 2010; Santangelo et al., 2009; Sibarita, 2005). To evaluate DHHC5/8 and native ankyrin-G at steady state, MDCK cells were transfected with GFP-DHHC5 or 8, fixed, and co-stained with antibodies against GFP and ankyrin-G. After 3D restoration and deconvolution of a selected lateral membrane region, we observed subdomains containing DHHC5/8 or ankyrin-G that ranged in size from 0.5-2 square microns (Figure 29A, top two panels). A substantial population of DHHC5 and 8 are co-patterned into ankyrin-G-positive microdomains based on Pearson coefficients of 0.7 for DHHC5/ankyrin-G, and 0.6 for DHHC8/ankyrin-G (Figure 29A and B). For evaluating the co-localization between ankyrin-G and βII-spectrin, we replaced endogenous βII-spectrin with either WT or Y1874A mutant GFP-βII-spectrin. WT βII-spectrin was also co-patterned into ankyrin-G positive microdomains (Figure 29A, the third panel). This co-localization with ankyrin-G required ankyrin-spectrin interaction since the Y1874A βII-spectrin mutant/ankyrin-G exhibited a markedly reduced Pearson coefficient of 0.3 compared to 0.8 for WT βII-spectrin/ankyrin-G (Figure 29A bottom two panels and 29B). However, this Y1874A βII-spectrin mutant is still patterned into microdomains, probably through its PH domain or other unidentified protein interactions.

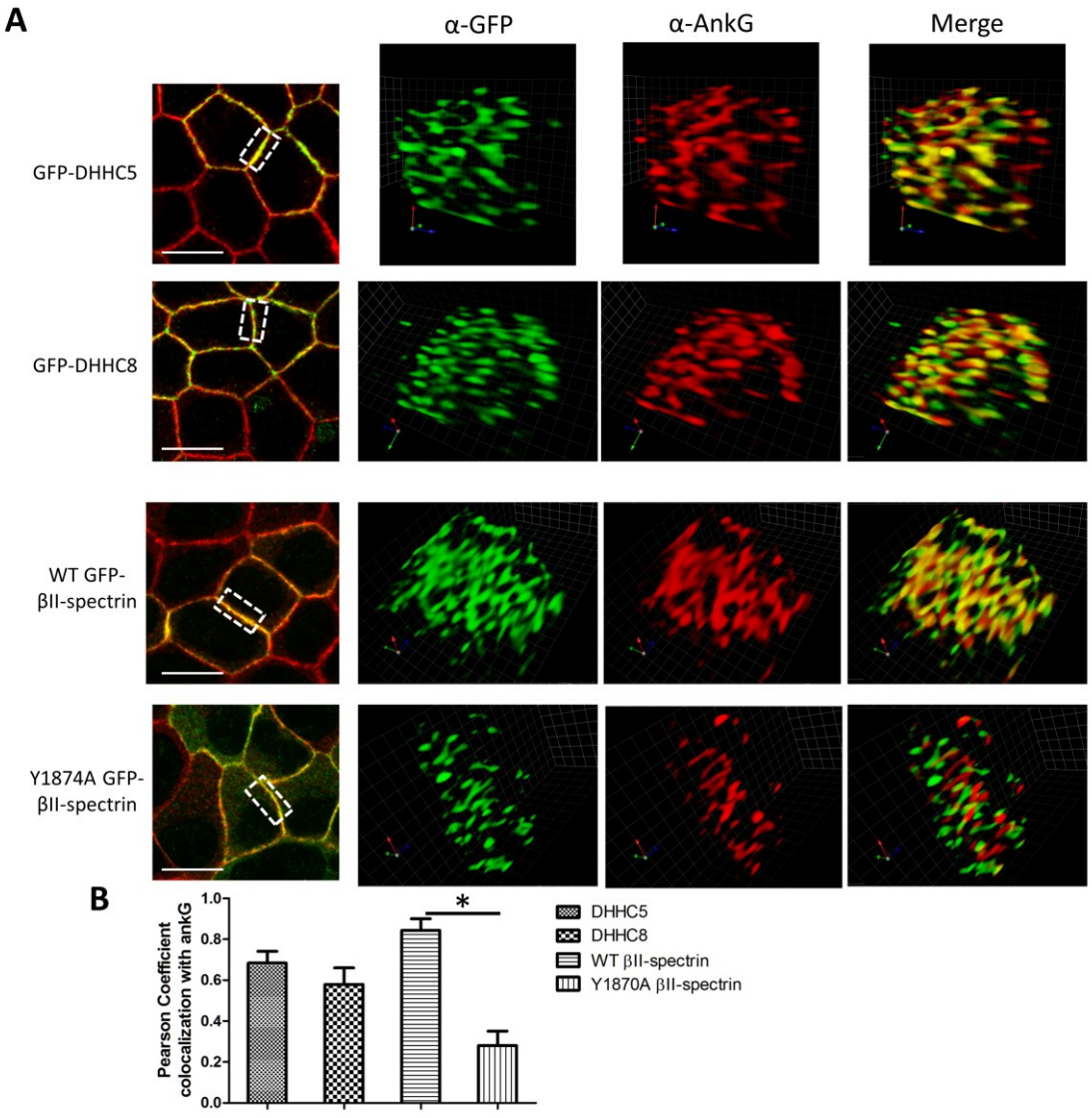

Figure 29: DHHC5/8 and βII-spectrin co-localize with ankyrin-G in microdomains.

(A) A region of interest highlighted in white box was cropped from the lateral membrane, and reconstructed using 3D deconvolution in Volocity Image Analysis Software. Green, α-GFP; red α-ankyrin-G, the unit of the 3D grid is 1um long, scale bar, 10um. (B) Quantification of the co-localization indicated by pearson coefficient. Student t-test was performed for the comparison between WT and Y1874A βII-spectrin, *$p<0.01$, n=4-7.

The finding that DHHC5/8 and βII-spectrin are co-patterned with ankyrin-G into highly organized microdomains suggests a model where ankyrin-G is locally palmitoylated at the lateral membrane, and in turn drives the polarized recruitment of βII-spectrin-phosphoinositide complexes (Figure 30). Loss of ankyrin-G/βII-spectrin binding activity results in loss of ankyrin-G/βII-spectrin co-patterning in those microdomains and failure to restore the epithelial lateral membrane. Thus recruitment of βII-spectrin to ankyrin-G microdomains is essential for its downstream functions in building lateral membranes. The mechanism for polarized targeting of DHHC5/8, which determines the location of ankyrin-G, will be the subject of future investigation.

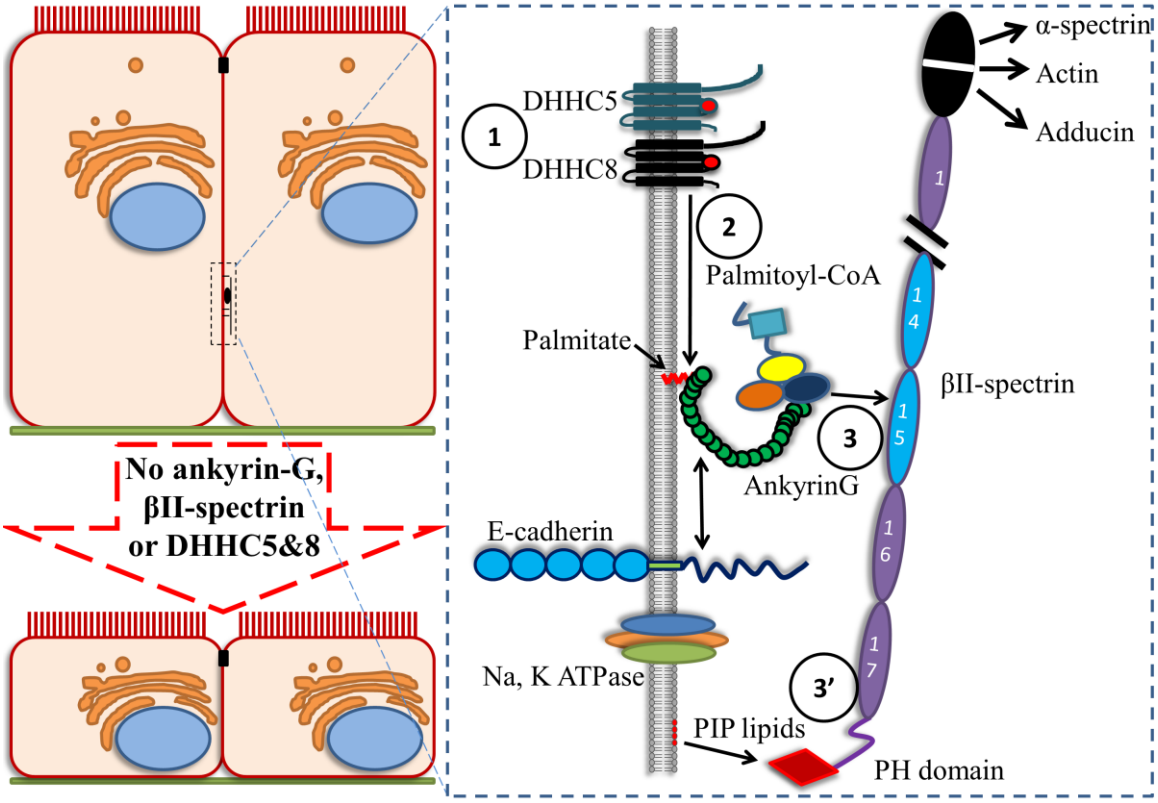

Figure 30: A DHHC5/8-ankyrin-G-βII-spectrin functional network is required to build lateral membranes of polarized MDCK cells.

The schematic view summarizes roles of DHHC5/8, ankyrin-G and βII-spectrin in assembling the lateral membrane of columnar epithelial cells. ○1 DHHC5/8 are localized to the lateral membrane, ○2 where they palmitoylate ankyrin-G. βII-spectrin requires co-incidence detection of ○3 ankyrin-G and ○3` PI(4,5)P2 to ensure its precise lateral membrane localization. Loss of any of the components or the functional relationship results in reduced lateral membrane height.

4.4 Discussion

A core challenge for contemporary biology is to understand how individual molecular partnerships translate into the complex spatial and temporal organization that distinguishes living cells. This is a particularly important issue for ankyrin- and spectrin-based plasma membrane domains whose function critically depends on precise cellular localization of ankyrin-G and beta-2 spectrin. This study identifies two critical inputs from lipids that together provide a rationale for how ankyrin-G and βII-spectrin selectively localize on lateral membranes of MDCK epithelial cells (Figure 30). These experiments began with the observation that ankyrin-G is S-palmitoylated at a single conserved cysteine that is required for ankyrin-G function in assembling lateral membranes and axon initial segments (He et al., 2012). Here, we identified DHHC palmitoyltransferases 5 and 8 as the DHHC family members required for ankyrin-G palmitoylation as well as its localization at the lateral membranes of polarized MDCK cells. We also found that βII-spectrin functions as a co-incidence detector that requires recognition of both palmitoylated ankyrin-G and phosphoinositide lipids as a prerequisite for its localization to the lateral membrane (Figure 29 and 30). DHHC5/8 and phosphoinositides thus ensure that ankyrin-G and βII-spectrin localize only on lateral plasma membranes and not in the cytosol or on other membrane surfaces. Loss of either DHHC5/8, or interactions between ankyrin-G and βII-spectrin, or βII-spectrin

recognition of phosphoinositide lipids all result in failure to build the lateral membrane, which underscores the functional importance of this pathway.

Our findings establish DHHC5 and 8 as critical determinants of polarity for ankyrin-G and βII-spectrin in MDCK cells. However, the mechanisms responsible for polarized localization of DHHC 5 and 8 themselves at the lateral membrane remain to be elucidated. Both proteins are distinguished from other DHHC family members by an extended cytoplasmic domain (Thomas et al., 2012). However, substitution of the C-terminal domain of DHHC14 for that of DHHC5 does not abolish lateral membrane targeting of DHHC5 (Figure 31). Thus important localization information resides in the N-terminal halves of DHHC5 and 8.

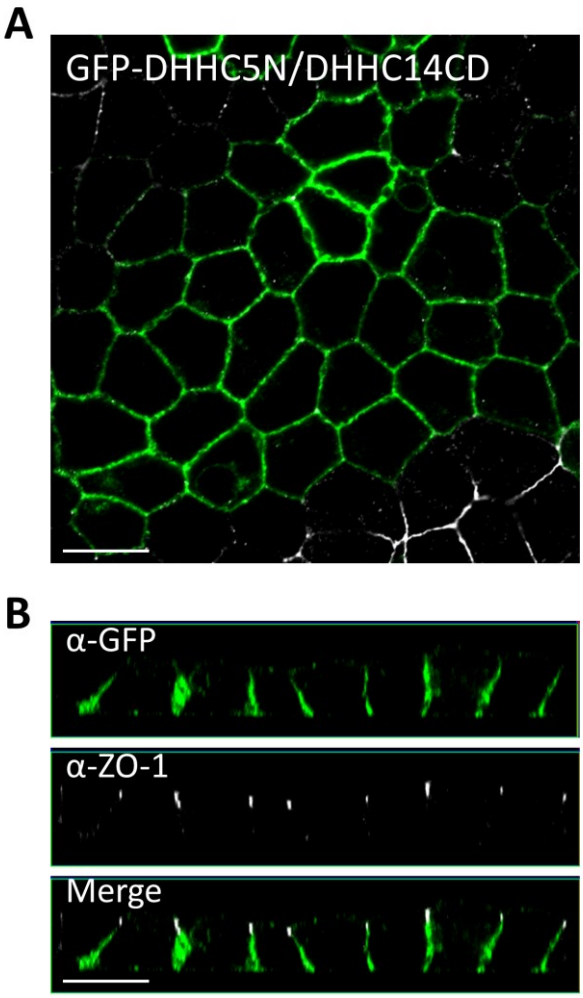

Figure 31: Replacing the C-terminal domain of DHHC5 with that of DHHC14 does not abrogate its polarized localization.

cDNA encoding the C-terminal domain of DHHC14 (amino acids 285-489) was fused to cDNA encoding the N-terminal portion of DHHC5 (amino acids 1-219), and then subcloned into peGFP-C1 vector. Chimeric plasmids were transfected into MDCK cells, followed by immunofluorescence using α-GFP (green) and α-ZO-1 (white) antibody. (A) XY plane, (B) XZ plane, scale bar, 10um.

In initial efforts to learn more about the generality of findings in MDCK cells, we examined localization of DHHC5/8 and ankyrin-G in neurons, human bronchial epithelial (HBE) cells, and the LLC-PK1 line of epithelial cells (Hull et al., 1976). HBE cells resemble MDCK cells in the polarized lateral membrane localization of DHHC5 and 8 with endogenous ankyrin-G (Figure 32B). In contrast, DHHC5 and 8 localize uniformly along neuronal plasma membranes when transfected into cultured hippocampal neurons, and do not exhibit enrichment at axon initial segments where ankyrin-G is concentrated (Figure 33, 34). DHHC5 and 8 also exhibit a non-polarized localization on both apical and lateral plasma membrane surfaces in LLC-PK1 cells (Figure 32C). Surprisingly, we find that LLC-PK1 cells lack the canonical 210 kDa ankyrin-G and instead express a 110 kDa cross-reacting polypeptide, likely a spliced variant lacking ANK repeats that is uniformly associated with all plasma membrane surfaces (Figure 32A and C). LLC-PK1 cells also differ from MDCK cells in lacking the AP1b clathrin adaptor (Ohno et al., 1999) as well as having a cuboidal rather than columnar morphology (Figure 32C). Based on this limited set of examples we conclude that the DHHC5/8-ankyrin-G-βII-spectrin pathway resolved here in MDCK cells may be a specialized feature of columnar epithelial cells.

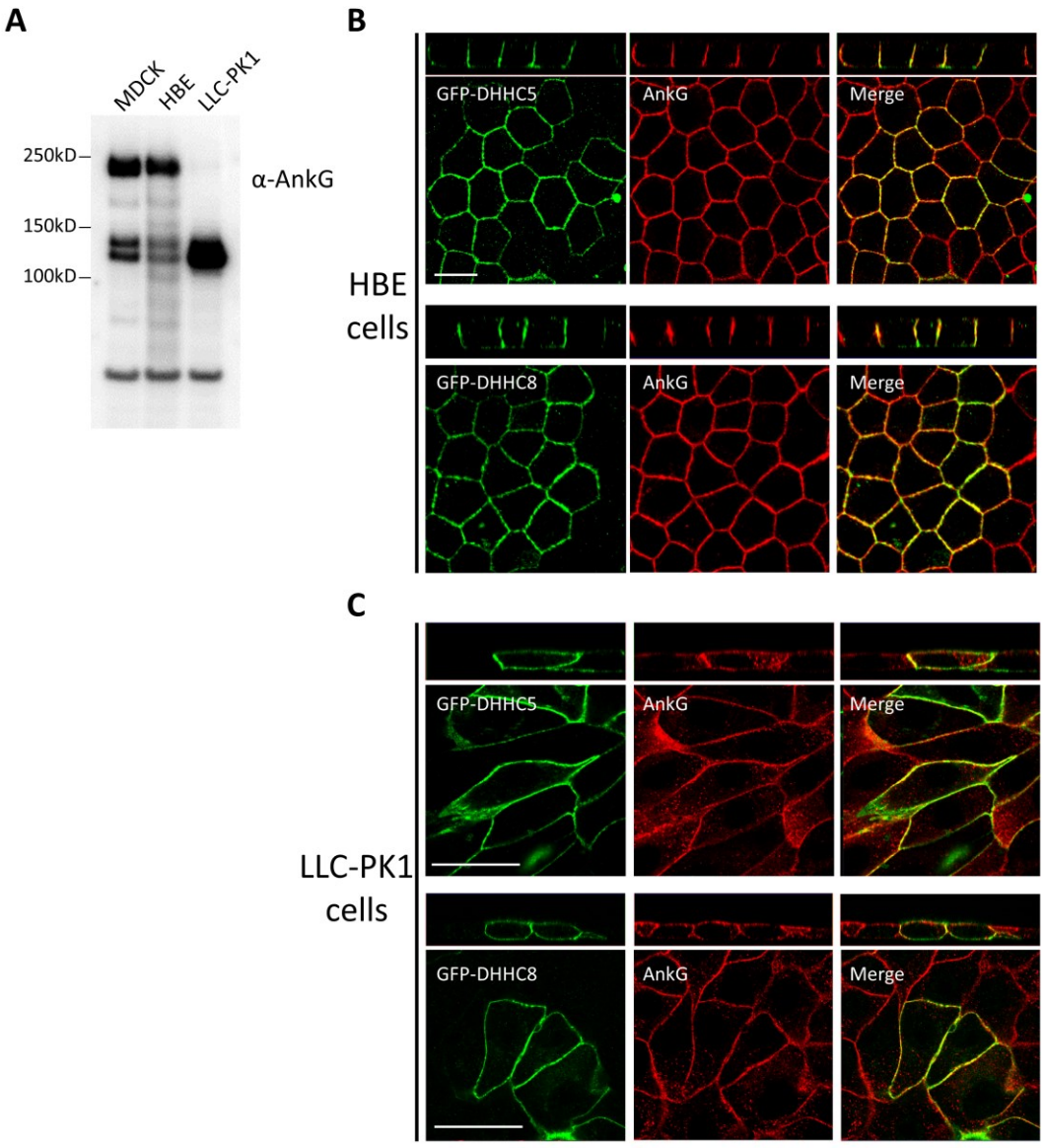

Figure 32: DHHC5/8 and ankyrin-G show polarized localization in columnar epithelial cells (HBE) but not cuboidal epithelial cells (LLC-PK1).

(A) Total cell lysates from cultured MDCK, HBE and LLC-PK1 cells were analyzed by SDS-PAGE and western blotting using α-ankyrin-G antibody. (B) GFP-DHHC5 or 8 were transfected into HBE cells and visualized by immunofluorescence, green, α-GFP; red, α-ankyrin-G, scale bar, 10μm. (C) GFP-DHHC5 or 8 were transfected into LLC-PK1 cells and visualized by immunofluorescence, green, α-GFP; red, α-ankyrin-G, scale bar, 10μm.

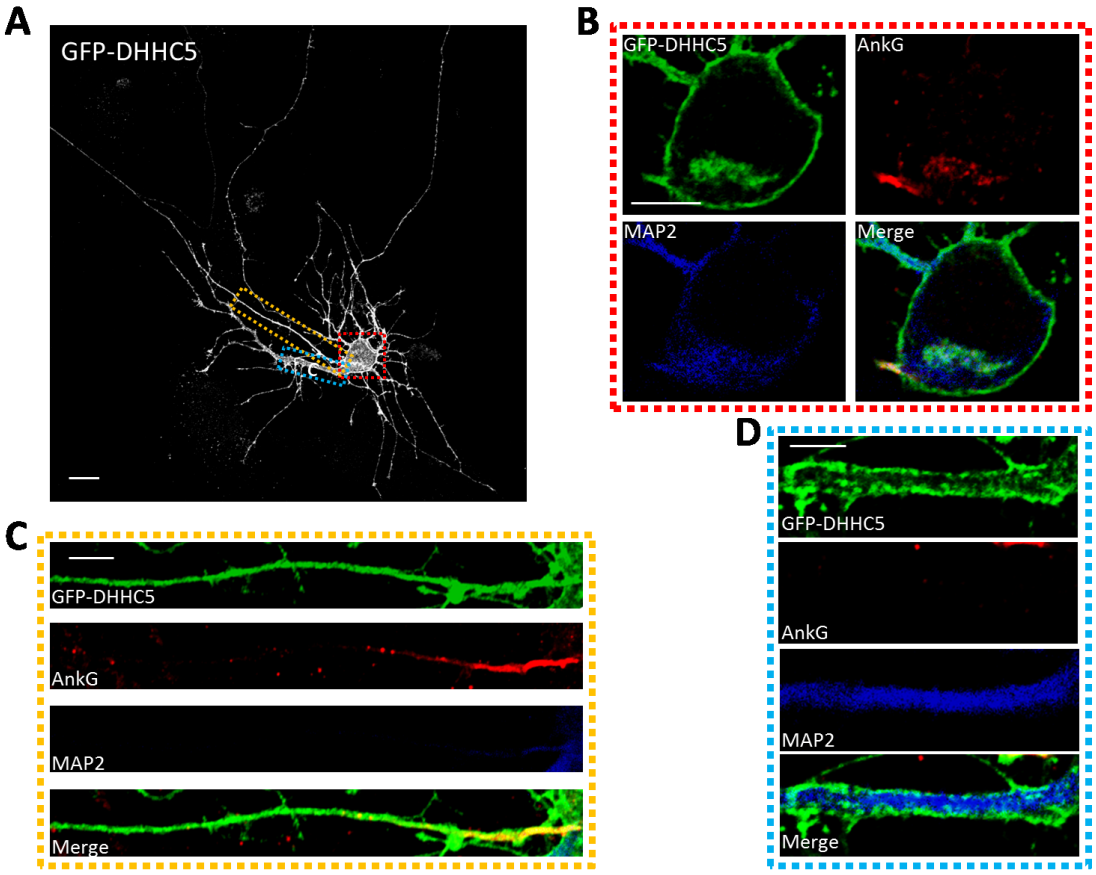

Figure 33: DHHC5 uniformly localize to all neuronal plasma membranes.

GFP-DHHC5 was transfected into cultured hippocampal neurons, and visualized by immunofluorescence. (A) Maximum intensity projection of a transfected neuron, GFP signal was pseudo-colored in white, scale bar, 10μm. (B, C and D) Magnified images to show a single XY plane across the middle of the cell body, axon and primary dendrite highlighted in red, yellow and cyan boxes respectively in (A), green, α-GFP; red, α-ankyrin-G; blue, α-MAP2, scale bar, 5μm.

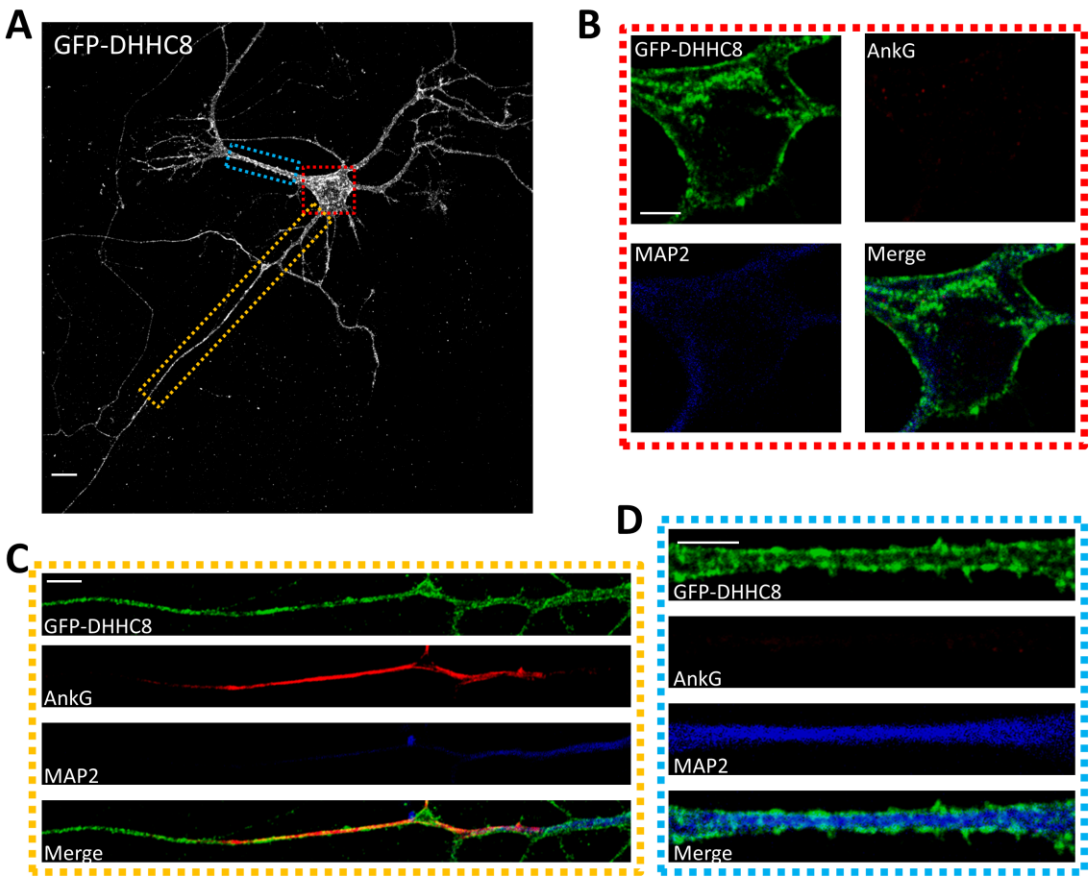

Figure 34: DHHC8 uniformly localize to all neuronal plasma membranes.

GFP-DHHC8 was transfected into cultured hippocampal neurons, and visualized by immunofluorescence. (A) Maximum intensity projection of a transfected neuron, GFP signal was pseudo-colored in white, scale bar, 10μm. (B, C and D) Magnified images to show a single XY plane across the middle of the cell body, axon and primary dendrite highlighted in red, yellow and cyan boxes respectively in (A), green, α-GFP; red, α-ankyrin-G; blue, α-MAP2, scale bar, 5μm.

The finding that βII-spectrin requires both ankyrin-G and phosphoinositides to associate with the lateral membrane was unexpected given the high affinity of the ankyrin-G-βII-spectrin interaction (Figure 26). Moreover, β-spectrin in erythrocytes lacks a PH domain due to alternative splicing but is tightly bound to the plasma membrane through ankyrin (Bennett and Stenbuck, 1979; Byers and Branton, 1985; Winkelmann et al., 1990b). These considerations suggest the possibility of a phosphoinositide-dependent relief of autoinhibition of ankyrin-binding, as occurs with Talin and beta-integrins (Goksoy et al., 2008). Another puzzle is that βII-spectrin preferentially binds to PI(4,5)P2 which is enriched in the apical domain, while PI(3,4,5)P3, confers basolateral membrane identity, at least in some epithelial cell models (Martin-Belmonte et al., 2007; Shewan et al., 2011). Nevertheless, the βII-spectrin PH domain, whether it associates with PI(4,5)P2 or PI(3,4,5)P3, imposes a dual requirement for phosphoinositides in addition to ankyrin-binding that prevents association of β-spectrins with ankyrin at sites other than the plasma membrane. PI(4,5)P2 lipids interact with many effectors including cytoskeletal proteins such as Talin and Arp2/3 as well as small GTPases, and also have several biosynthetic routes (Di Paolo and De Camilli, 2006; Kwiatkowska, 2010). It will be important in future work to resolve other components of the βII-spectrin-dependent membrane microenvironment where PI(4,5)P2 and DHHC5/8 palmitoyltransferases co-reside.

A critical tool that we developed for this study was a method to generate inducible shRNA-mediated knockdown of protein expression in an entire population of MDCK cells. This permitted evaluation of the roles of ankyrin-G and βII-spectrin in assembling lateral membranes, without interference by other cellular defects, including impaired cytokinesis, caused by loss of ankyrin-G or βII-spectrin (Hu et al., 1995). By using this system, we were able to knockdown ankyrin-G or βII-spectrin after cells reached confluence, where mitosis is less frequent. Previous research using a transient siRNA strategy that resulted in a nearly complete loss of ankyrin-G in HBE cells led to a complete loss of the lateral membrane domain and intracellular accumulation of E-cadherin (Kizhatil and Bennett, 2004; Kizhatil et al., 2007a; Kizhatil et al., 2007b). However, we did not observe these phenotypes in MDCK cells with 80-90 percent knockdown achieved with the inducible system. The intracellular accumulation of E-cadherin in these experiments likely was secondary to loss of lateral membranes rather than a failure of post-Golgi transport as originally proposed (Kizhatil et al., 2007a).

An unexpected discovery from our recent studies was that ankyrin-G persists on the plasma membrane together with DHHC5/8 in unpolarized MDCK cells grown in low calcium (Figure 25A, He et al,. 2012). Ankyrin-G so far is the only lateral membrane-localized proteins as we are aware of with this property (Gumbiner et al., 1988; He et al., 2012; Kaiser et al., 1989; Mattey and Garrod, 1986). Re-addition of calcium to calcium-depleted cells results in rapid re-establishment of cell polarity and re-assembly of the

lateral membrane. Using this calcium switch assay, we demonstrated that ankyrin-G and DHHC5/8 are not only required for the maintenance of lateral membranes but also for *de novo* biosynthesis of the lateral membrane following re-addition of calcium (Figure 25D and E). These results suggest that palmitoylated ankyrin-G functions as a core organizer during the assembly of lateral membranes. It remains to be determined whether ankyrin-G affects the biosynthesis and the maintenance of lateral membranes through identical pathways. The calcium switch assay also raises interesting questions whether the re-establishment of apical and lateral membranes is achieved through delivery of newly synthesized membrane components, or through re-arrangements of pre-existing plasma membrane, and how the DHHC5/8/ankyrin-G/βII-spectrin network is incorporated into this process. Therefore future experiments using live imaging to capture the real time distribution of the palmitoyltransferases DHHC5/8, ankyrin-G and βII-spectrin during the re-polarization process may help to address these questions.

While DHHC5/8, ankyrin-G and βII-spectrin are required for columnar morphology of MDCK cells and operate in the same pathway, the mechanism of action of these proteins in expanding the lateral membrane remains to be determined. One possibility is that a lateral membrane-associated spectrin-based actin skeleton provides mechanical support for epithelial monolayers by coupling to membrane-spanning cell adhesion molecules such as E-cadherin, which is an ankyrin-G partner (Kizhatil et al., 2007b; Nelson et al., 1990a; Nelson et al., 1990b). Another possibility is that an ankyrin-

G-spectrin-actin skeleton promotes cell height by enhancing cell-cell contacts through retention of E-cadherin and prevention of its endocytosis. In support of this idea, E-cadherin polarity in MDCK cells depends on a motif in its cytoplasmic domain that contains both ankyrin-binding activity as well as embedded di-leucine residues required to engage clathrin endocytosis (Jenkins et al., 2013). E-cadherin likely can associate with either ankyrin-G or clathrin adaptors but not both at the same time, and thus is restricted to the lateral membrane by the ankyrin-spectrin skeleton. A surprising conclusion of our study is that E-cadherin interaction with ankyrin-G is not sufficient to recruit ankyrin-G to the lateral membrane, which also requires palmitoylation in addition to its protein interactions. However, once ankyrin-G concentrates at the lateral membrane it may be able to prevent participation of E-cadherin in endocytosis through competition for binding to the polarity motif. Interestingly, inhibition of endocytosis of the cell adhesion molecule Fas 2 has been proposed as a mechanism for regulating cell height in Drosophila epithelia (Gomez et al., 2012).

We have observed for the first time that ankyrin-G and βII-spectrin are concentrated in microdomains ranging from 0.5 to 2 square microns in the MDCK cell lateral membrane (Figure 29), which is inconsistent with the conventional view of a uniform ankyrin/spectrin lattice as observed in the plasma membrane of erythrocytes (Baines, 2010; Bennett and Baines, 2001; Liu et al., 1987). We believe that microdomains are not an artifact of cell fixation or deconvolution software, since we observe similar

micro-patterning using live imaging with GFP-ankyrin-G and GFP-βII-spectrin as with fixed cells (Figure 35). In contrast, imaging with a lipid probe reveals uniform label (Figure 35). Moreover, the protein interaction-dependent co-localization between ankyrin-G and βII-spectrin demonstrates specificity in co-segregation of these proteins (Figure 29). The ankyrin-G- and βII-spectrin microdomains revealed by 3D deconvolution microscopy in our study are distinguishable from the membrane "lipid rafts" which normally are much smaller (Lingwood and Simons, 2010; Simons and Gerl, 2010). Segregation of functionally related proteins into microdomains can provide a platform for proteins that interact with moderate affinity and require high local concentration to achieve complexes. The fact that DHHC5/8 colocalize with ankyrin-G in these microdomains suggests localized palmitoylation of ankyrin-G. It will be interesting in future experiments to study the real time dynamics of those microdomains during lateral membrane assembly and their relationship to the clathrin-dependent endocytosis machinery.

In summary, we have identified functional interactions connecting palmitoyltransferases DHHC5/8 with their substrate ankyrin-G, ankyrin-G with its partner βII-spectrin, and βII-spectrin with phosphoinositide lipids that are required to build lateral membranes of MDCK epithelial cells. Given the rapidly reversible nature of palmitoylation (Fukata et al., 2013; Martin et al., 2012; Rocks et al., 2010), as well as PI(4,5)P2 synthesis and degradation (Di Paolo and De Camilli, 2006; Shewan et al., 2011),

these new findings suggest that the ankyrin-G/βII-spectrin-based membrane skeleton is much more dynamic and subject to regulation than previously appreciated. Moreover, the regulatory network properties of this set of interactions in terms of positive and negative feedback and co-incidence circuitry are important areas for future investigation. Finally, our findings reinforce an emerging view of plasma membrane identity determination by a combinatorial code based on highly dynamic protein and lipid variables rather than "hard-wired" stable protein assemblies.

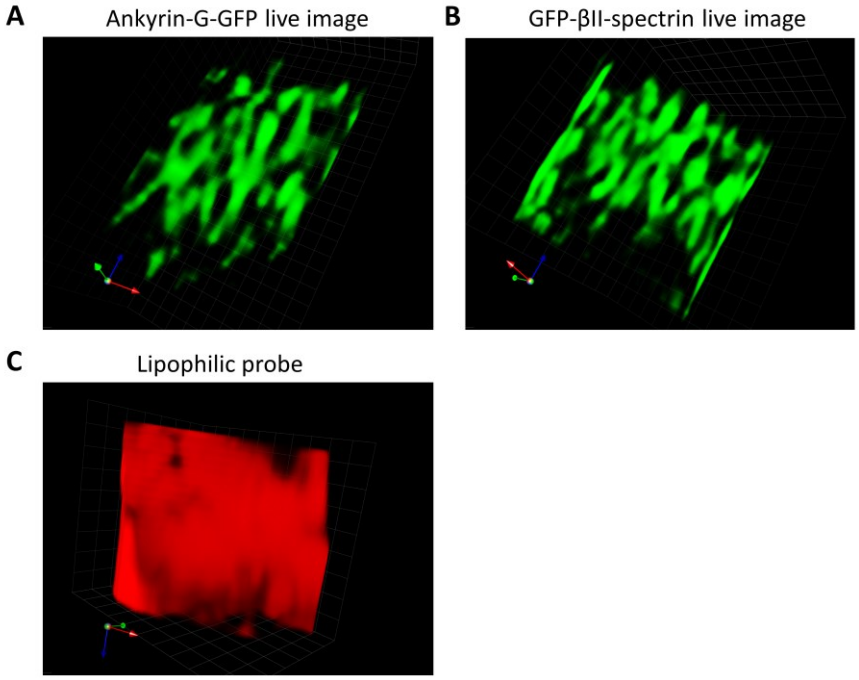

Figure 35: 3D deconvolution of live imaging reveals micro-patterning of GFP-tagged ankyrin-G and βII-spectrin but not lipophilic probes.

(A and B) Endogenous ankyrin-G or βII-spectrin was silenced and replaced with GFP-tagged ankyrin-G or βII-spectrin, native GFP signals were collected from live cells, a shared lateral membrane region was selected and processed for 3D deconvolution, grid unit, 1μm. (C) Live cells were labeled with lipophilic probes (CellMask Orange) and imaged for 3D deconvolution, grid unit, 1μm.

Chapter 5. The Spectrin-Ankyrin Network Assembles Epithelial Lateral Membrane by Opposing Clathrin-Mediated Endocytosis

5.1 Introduction

The previous chapters have provided a mechanism for targeting the spectrin-ankyrin network to those plasma membrane domains, however it is still unclear how this network mechanistically assembles the membrane domains after it is precisely localized. The area of plasma membrane is controlled by the equilibrium between addition and removal of membrane components. Previous work proposed that the spectrin-ankyrin network may be involved in direct transport of new membrane components to the epithelial lateral membrane (Kizhatil et al., 2007a). However, no direct experimental evidence has been observed to support this idea, and at steady state the spectrin-ankyrin network is predominantly localized at the lateral membrane.

A recent study showed that ankyrin-G binds to the cytoplasmic domain of E-cadherin at the same region recognized by the clathrin adaptors (Jenkins et al., 2013). This finding suggests a role of ankyrin-G in regulating the removal of membrane components through clathrin-mediated endocytosis. In this chapter, we provide experimental evidence to demonstrate that the spectrin-ankyrin network plays a role in inhibiting clathrin-mediated endocytosis from the epithelial lateral membrane.

5.2 Methods and Materials

Double Stable cell lines

The ankyrin-G/Clathrin double stable cell line was generated using the improved pLKO-Tet-on lentivector discussed above. Hairpin sequence targeting canis ankyrin-G (gctagaagtagctaatctcct) was first cloned into the pLKO-mCherry vector and used to make the ankyrin-G shRNA stable cell line, then the hairpin sequence targeting canis clathrin heavy chain (aatggatctctttgaatacgg) was cloned into pLKO-tagBFP vector and used to transduce the ankyrin-G shRNA stable cells, which were then sorted for mCherry and tagBFP double positive cells.

Dynasore treatment

Luciferase shRNA control cells, ankyrin-G shRNA cells or beta II spectrin shRNA cells were first induced by 4ug/ml doxycycline for 48 hours to knockdown genes of interest, then $5X10^5$ cells were replated on the 14mm insert of MatTek plates with or without 60uM dynasore for 24 hours. The next day, cells were fixed and stained for E-cadherin to mark the lateral membrane.

Transferrin uptake

Stable cell lines expressing WT ankyrin-binding domain or YA mutated ankyrin-binding domain tagged to the destabilization domain were generated in a way similar to the shRNA stable cell lines. Cells were then induced by Shield-1 to stimulate the rapid expression of ankyrin-binding domain, and labeled with fluorescein isothiocyanate

(FITC)-transferrin from the basolateral surface using filter-grown MDCK cells to measure internalization.

Lipophilic labeling

Cells were grown in the 14mm insert of MatTek plates, and induced to knockdown genes of interest. The CellMask™ Plasma Membrane dye was then added to the medium at 1:1000 dilution, and allow it to incubate with 45 minutes. Then wash the cells with PBS for 3 times, and then add regular medium and applied for live imaging using the LSM 780 confocal microscopy.

5.3 Results

5.3.1 Inhibition of clathrin-mediated endocytosis restores lateral membrane in ankyrin-G depleted MDCK cells.

According to our hypothesis that the spectrin-ankyrin network protects the lateral membrane from being internalized by clathrin-mediated endocytosis, we should observe a restoration of lateral membranes if we inhibit clathrin-mediated endocytosis in ankyrin-G depleted cells. In order to test this, we made shRNA stable cell line which achieved double knockdown of both ankyrin-G and clathrin heavy chain. The knockdown efficiency was verified by western blot (Figure 36A, 91% for ankyrin-G, 84% for clathrin heavy chain), then we measured the height of the lateral membrane by staining endogenous E-cadherin after knocking down both proteins. Loss of clathrin-heavy chain alone resulted in partial mislocalization of E-cadherin (Figure 36B), which is

consistent with previous studies (Deborde et al., 2008; Jenkins et al., 2013). Surprisingly, cells lacking both ankyrin-G and clathrin heavy chain regained their lateral membrane up to the wild type level (Figure 36B and C).

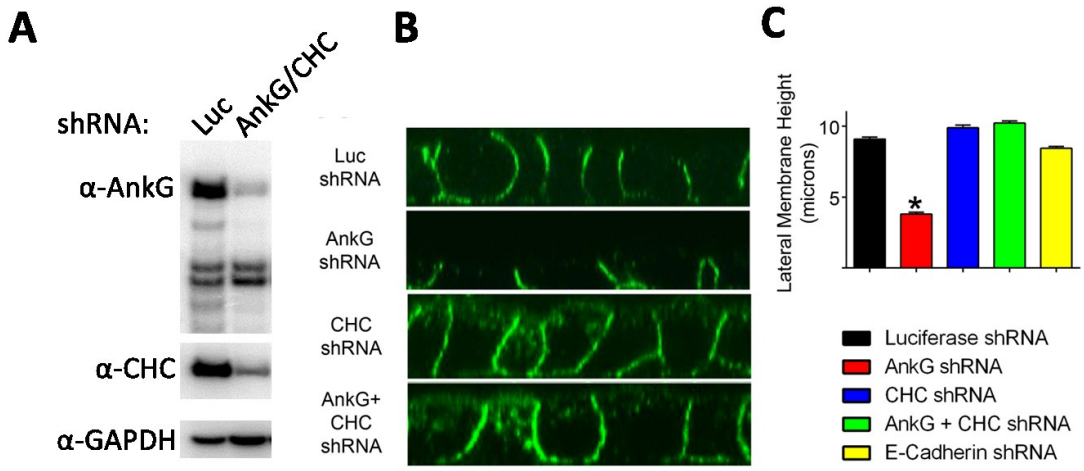

Figure 36: Double knockdown of ankyrin-G and CHC restores MDCK epithelial lateral membranes.

(A) Knockdown efficiency of ankyrin-G and clathrin heavy chain (CHC) in the double shRNA stable cell line. (B) XZ plane of the polarized cell monolayer, green, anti-E-cadherin staining. (C) Quantification of the height of lateral membranes, * indicates $p<0.05$.

Alternatively, we also inhibited endocytosis by using a small inhibitor, dynasore, which blocks all the dynamin-dependent endocytosis (Macia et al., 2006). Similarly, dynasore treatment in cells depleted of ankyrin-G or beta II spectrin also restored the lateral membrane in MDCK cells (Figure 37A and B). These findings are consistent with our hypothesis that the spectrin-ankyrin network plays a role in inhibiting clathrin-

mediated endocytosis, therefore protecting proteins or lipids from being internalized at the lateral membrane by clathrin.

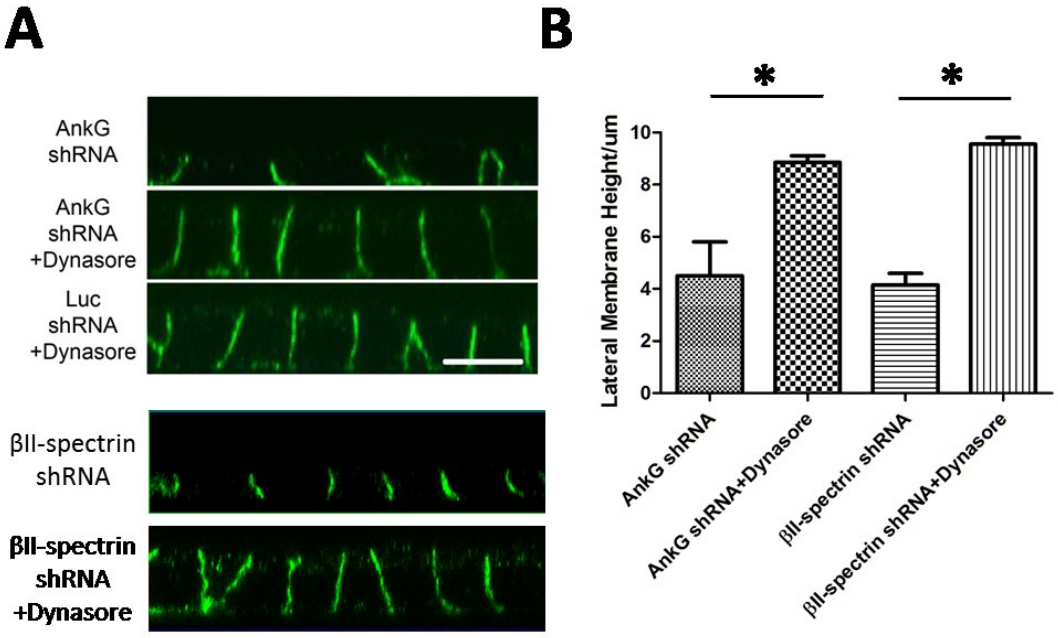

Figure 37: Dynasore treatment restores the lateral membrane in ankyrin-G or beta II spectrin knockdown cells.

(A) XZ plane of the polarized cell monolayer, green, anti-E-cadherin staining. (B) Quantification of the height of lateral membranes, * indicates $p<0.05$.

5.3.2 Disruption of spectrin-ankyrin interaction increases clathrin-mediated uptake of transferrin

Next, we decided to directly examine how the spectrin-ankyrin network affects clathrin-mediated endocytosis. We used an inducible protein expression system previously developed (Banaszynski et al., 2006) to express the ankyrin-binding domain of beta II spectrin. This fragment can disrupt the interaction between ankyrin-G and beta

II spectrin (Hu et al., 1995), thus functions as a dominant negative mutant (Figure 38A). As a control, a tyrosine residue in the peptide critical for ankyrin binding was mutated to alanine (Davis et al., 2009; Ipsaro and Mondragon, 2010).

We used Fluorescein isothiocyanate (FITC) conjugated transferrin as a marker to evaluate clathrin-mediated endocytosis. After rapid induction of the expression of ankyrin-binding domain (WT ABD) but not the control (YA ABD), we observed a significant increase of transferrin uptake (Figure 38B and C.). This finding further supports our hypothesis that the spectrin-ankyrin network inhibits clathrin-mediated endocytosis.

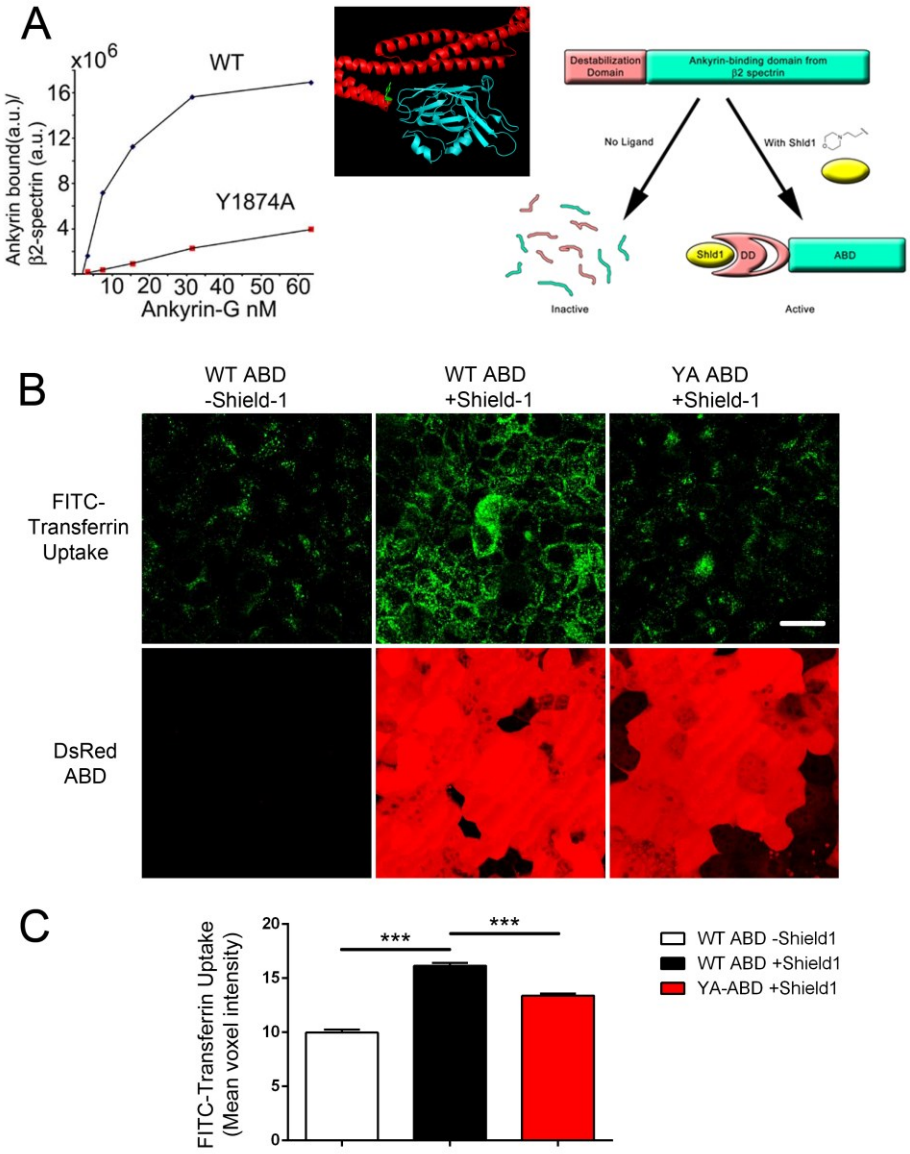

Figure 38: Disruption of spectrin-ankyrin interaction increases clathrin-mediated uptake of transferrin.

(A) Binding curve of the Y1874A mutated beta II spectrin with ankyrin-G and the schematic view of the inducible expression system. (B) Compacted view of Z stacks, FITC-conjugated transferrin (green) was introduced to the cells from the basolateral surface of filter-grown MDCK cells, dsRed marking cells that are expressing ankyrin-binding domain, scale bar, 10um. (C) Quantification of transferrin level, *** indicates $p<0.05$. (Experiments performed by Dr. Paul Jenkins)

5.3.3 Knockdown of ankyrin-G causes massive intracellular accumulation of membrane components.

To further evaluate the role of ankyrin-G in opposing clathrin-mediated endocytosis, we then decided to label plasma membrane using fluorescent lipophilic molecules and study the cellular distribution of the labeled membrane components. The cells that were treated with dynasore or induced to knockdown clathrin heavy chain showed significantly reduced intracellular membrane components compared to control cells (Figure 39A). Surprisingly, the ankyrin-G knockdown cells exhibited a dramatic increase of intracellular membrane components (Figure 39A). To further confirm this accumulation was due to increased activities of endocytosis, we treated the ankyrin-G knockdown cells with dynasore to inhibit dynamin-dependent endocytosis, the cells did not only show an increased lateral membrane height as described above, but also showed markedly reduced intracellular membrane accumulation (Figure 39A).

Additionally, even though the lipophilic molecules were incorporated into the cells from the apical surface, the control cells actually showed a more robust labeling at the lateral membrane than the apical membrane, suggesting that at steady state there is more rapid internalization from the apical than from the basolateral membranes (Figure 39B). This difference may be largely contributed by endocytosis, because when the cells were treated with dynasore or induced to knockdown clathrin heavy chain, they showed evenly labeled apical and lateral membranes. Together these experimental data

demonstrated that ankyrin-G plays an essential role in inhibiting clathrin-mediated endocytosis.

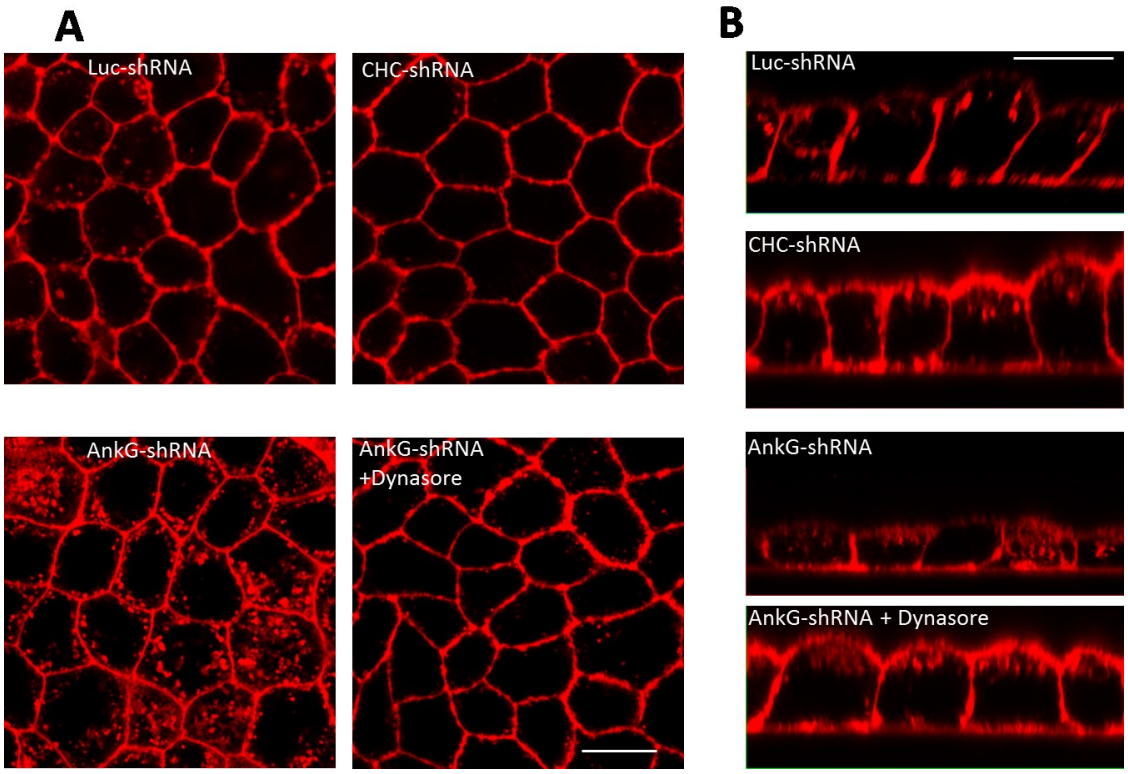

Figure 39: Knockdown of ankyrin-G causes massive intracellular accumulation of membrane components.

(A) Stable MDCK cells were induced to knockdown ankyrin-G or CHC, and then labeled with fluorescent lipophilic dye from the apical surface. Red, cell mask orange dye, scale bar, 10um. (B), XZ plane of the polarized MDCK monolayer, scale bar, 10um.

5.4 Discussion

It has been well recognized that the spectrin-ankyrin network is essential for epithelial cells to establish and maintain their lateral membranes (Kizhatil and Bennett, 2004; Kizhatil et al., 2007a; Kizhatil et al., 2007b). However, the molecular mechanisms

underlying this process are unknown. Here, we identify a mechanism of the spectrin-ankyrin network in assembling epithelial lateral membranes. Instead of being involved in direct membrane delivery, the spectrin-ankyrin network functions as molecular machinery to inhibit clathrin-mediate endocytosis thus protects critical lateral membrane proteins and lipids from being internalized. This spatial and temporary regulation of clathrin-mediate endocytosis may function as a general principal for polarized cells to establish and maintain their specialized membrane domains (Figure 40).

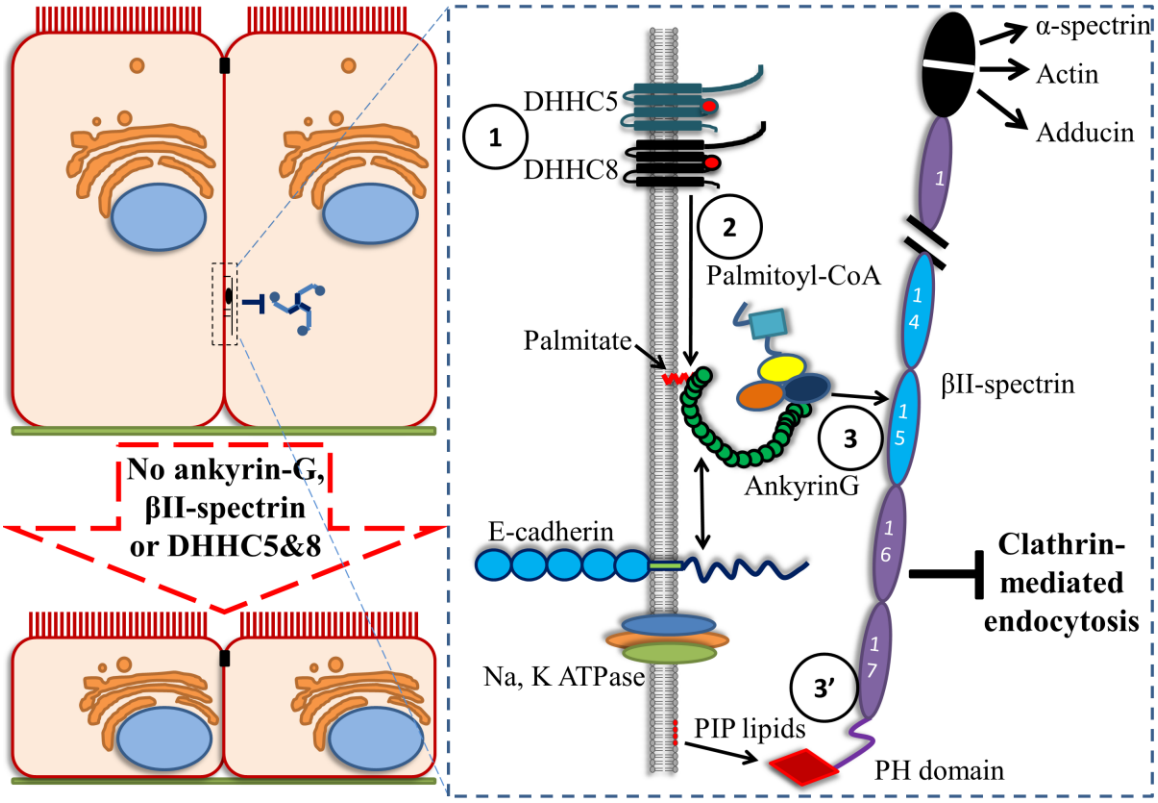

Figure 40: Model of the spectrin-ankyrin networking opposing clathrin-mediated endocytosis.

Membrane components can be internalized from both apical and lateral membranes (Barroso and Sztul, 1994; Thompson et al., 2007; von Bonsdorff et al., 1985; Wang et al., 2000). Here we showed that the spectrin-ankyrin network localized at the lateral membrane is playing a role in regulating clathrin-mediate endocytosis to assemble and maintain this membrane domain. We would hypothesize the existence of a similar protein complex at the apical membrane that may regulate endocytosis to protect specific apical components from being internalized.

We showed here that the spectrin-ankyrin network opposes clathrin-mediated endocytosis, but it is still unclear how this network achieves such inhibition. Based on our knowledge, there may be three different explanations. First, given the finding that ankyrin-G can bind to the cytoplasmic region of E-cadherin which is also recognized by clathrin adaptors (Jenkins et al., 2013), there may be a competitive mechanism between the ankyrin-based protein retention and clathrin-mediate removal. Therefore, it will be interesting in future work to verify whether other sorting signals recognized by clathrin adaptors can also bind to ankyrin-G directly or indirectly. Second, it was shown that clathrin-mediated endocytosis requires PI(4,5)P2 lipids which can recruit the clathrin adaptor AP2 to the plasma membrane and facilitate the formation of endocytic pits (Ford et al., 2001; Gaidarov and Keen, 1999; Motley et al., 2003; Padron et al., 2003; Rohde et al., 2002). Since beta II spectrin also binds to PI(4,5)P2 with the highest affinity as shown above, it may compete with the clathrin adaptor AP2 at the lateral membrane

for PI(4,5)P2, and inhibit the formation of clathrin scaffolds. Third, it was shown that the spectrin-ankyrin network forms a lattice underlying the plasma membrane of erythrocytes (Liu et al., 1987), and the spectrin-actin filaments are also tightly packed into a meshwork that wrap around the circumference of neuronal axons (Xu et al., 2013). These findings also imply that the spectrin-ankyrin network may simply block the access of clathrin machinery to the lateral membrane by forming a highly organized meshwork. However, due to the technical limitation, it still remains challenging to visualize the detailed organization of the spectrin-ankyrin network at epithelial lateral membrane; otherwise it will provide critical information to understand its function.

Chapter 6. Future Directions and Conclusions

6.1 Ankyrin and Phosphoinositide lipids

The structure of the ZU5-UPA-Death domain supermodule of ankyrin-B reveals a binding pocket consisting of several positively-charged residues at the second ZU5 domain (Wang et al., 2012). Those positively-charged residues are extremely conserved among the ankyrin families across different species (Figure 41A). This pocket provides an ideal binding site for lipids, indeed some preliminary data suggest a direct binding between ankyrin-G and phosphatidylinositol 3-phosphate (PI3P) (Figure 41B). To evaluate the functional significance of this binding pocket, we make point mutations to reverse the positively-charged residues into negatively-charged residues, and used this mutant to rescue the lateral membrane in epithelial cells, surprisingly this mutant losses its function to do so (Figure 41C). However, we have not been able to prove that this loss of function is attributed to loss of lipid binding. Therefore it will be very interesting in future experiments to measure the binding of this ankyrin-G mutant with PI3P lipids.

Recently, phosphoinositide lipids are increasingly recognized as critical determinants of plasma membrane organization and identities (Hammond et al., 2012; Johnson et al., 2012; Martin-Belmonte et al., 2007; Nakatsu et al., 2012; Shewan et al., 2011). Since ankyrin-G plays critical roles in assembling plasma membrane domains, this connection between ankyrin-G and phosphoinositide lipids may be of great biological significance in organizing membrane domains. It will be interesting to study how

phosphoinositide lipids affect ankyrin-G function through selective lipid depletion methods.

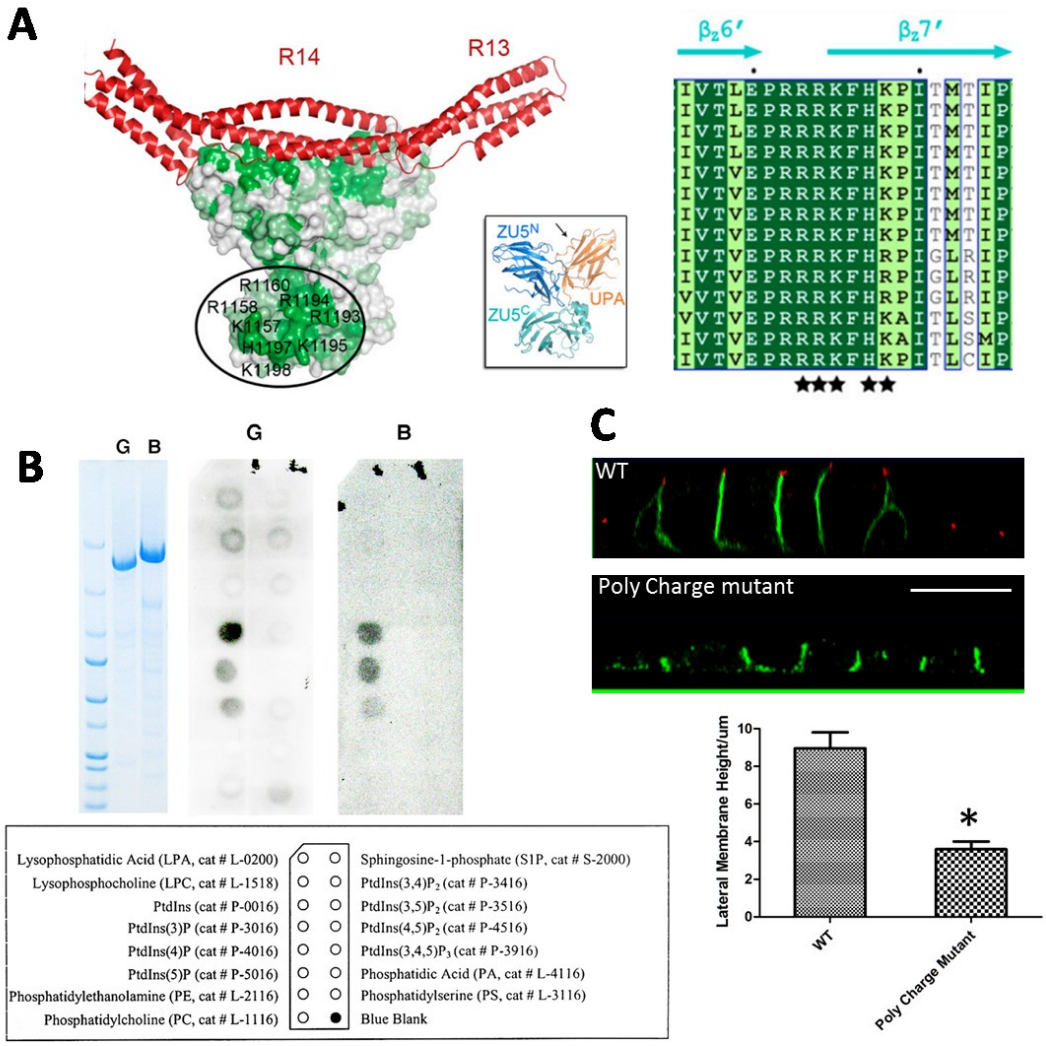

Figure 41: The positively-charged pocket is required for ankyrin-G to restore the lateral membranes in MDCK cells.

(A) From Want et al. 2012. (B) Liposome binding shows that ankyrin-G selectively binds to PI3P lipids (experiment was performed by Jonathan Davis). (C) The poly charge mutant failed to restore the lateral membrane in MDCK cells, green, anti-GFP, red, anti-ZO-1, scale bar, 10um. * indicates $p<0.05$.

6.2 Non-canonical roles of ankyrin-G

6.2.1 Ankyrin-G and cytokinesis

In addition to the well-established function in organizing specialized membrane domains such as axon initial segments and the epithelial lateral membrane (Bennett and Healy, 2009; Bennett and Lorenzo, 2013), ankyrin-G and βII-spectrin are also involved in mitosis. Caco-2 intestinal epithelial cells, transfected with plasmids encoding the actin- or ankyrin-binding domain of βII-spectrin that functions as a dominant negative fragment, became multinucleated which is a sign of mitotic defects (Hu et al., 1995). Immunofluorescence using pan ankyrin antibodies revealed ankyrin analogues that were concentrated in the spindle pole during metaphase and were redistributed to the cleavage furrow in later stages of mitosis (Bennett and Davis, 1981),

We tested how loss of ankyrin-G in MDCK cells affects cell division using our inducible shRNA cell line. First, we confirmed that knockdown of ankyrin-G resulted in multinucleation (Figure 42A and B). Then we did a growth curve to evaluate the overall influence of ankyrin-G on cell division. Surprisingly, loss of ankyrin-G in MDCK cells doubled the average cell cycle time (Figure 42C). We further showed that ankyrin-G functions specifically during the cytokinesis phase using live imaging, the control cells can complete the cytokinesis within a few minutes, whereas the ankyrin-G knockdown cells failed to complete this process even within a few hours.

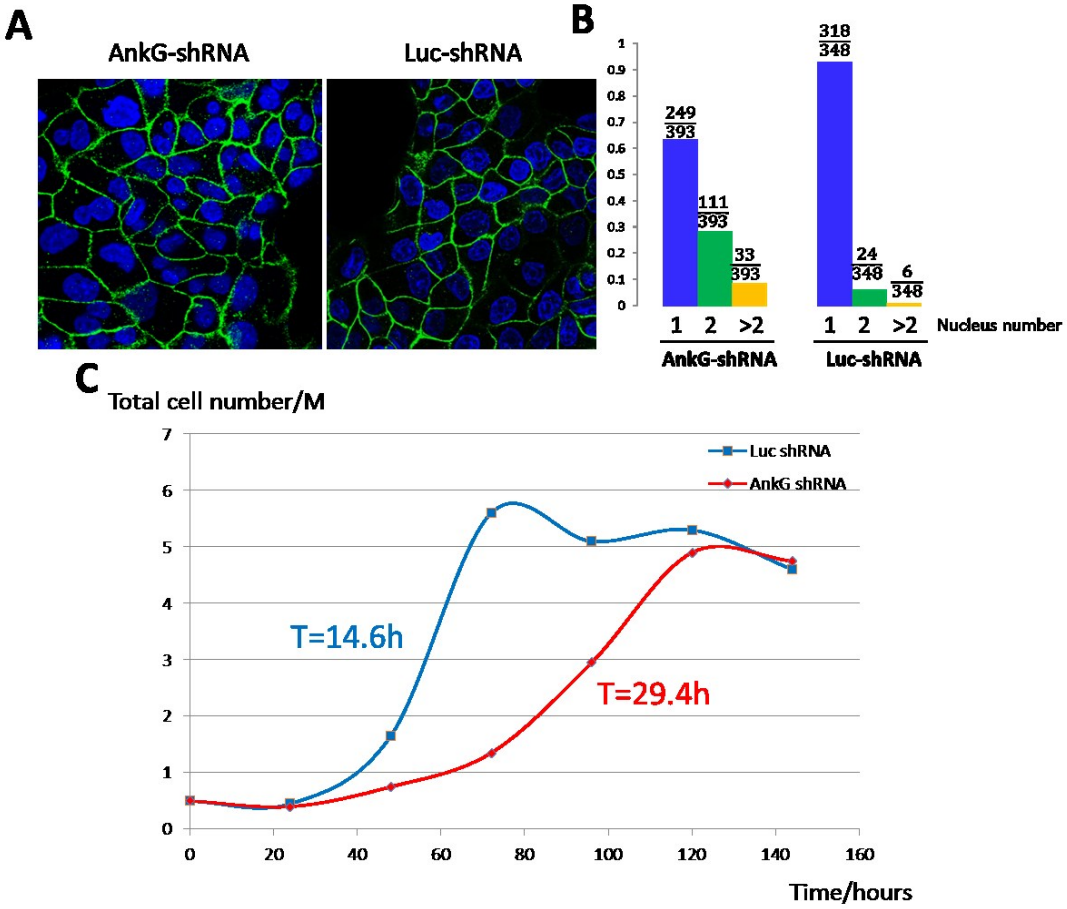

Figure 42: Loss of ankyrin-G leads to delayed cytokinesis and multinucleation.

(A) Ankyrin-G knockdown cells were stained with DAPI (blue) to visualize the nucleus, and NA K ATPase (green) for cell boundaries. (B) Quantification of the number of nucleus. (C) Growth curve of MDCK stable cells that are induced to knockdown ankyrin-G or luciferase as a control (number unit M: million).

The molecular mechanism underlying this phenotype is not known, but it will be interesting to understand how ankyrin-G pays a role in cytokinesis. One of the initial experiments that we tried was to identify potential binding partners in MDCK cells that may function during cytokinesis. Interestingly, in our crosslinking and

immunoprecipitation assay, we identified the non-muscle myosin IIa as a potential binding partner of ankyrin-G (Table 2). It was shown that the non-muscle myosin II accumulates at the cleavage furrow and plays critical roles in cytokinesis and cell migration (Dean et al., 2005; Even-Ram et al., 2007; Straight et al., 2005; Yang et al., 2012). Therefore, it will be important to verify the interaction between ankyrin-G and non-muscle myosin IIa, and examine whether this interaction plays any role in cytokinesis.

Table 2: Mass spectrometry of ankyrin-G immunoprecipitation shows non-muscle myosin IIa as a potential binding partner.

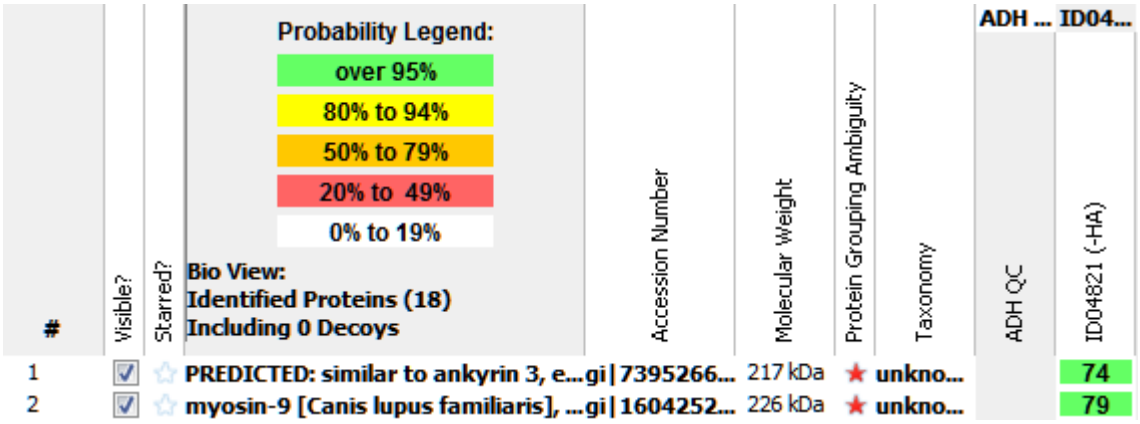

6.2.2 Ankyrin-G and cell migration

When we were characterizing ankyrin-G shRNA cell line, another striking phenotype we observed was that loss of ankyrin-G has a marked influence on cell motility. As demonstrated by wound healing assay and live imaging, the control cells can migrate up to 30 microns per hour, whereas the ankyrin-G knockdown cells showed significantly reduced motility (Figure 43). Interestingly, ankyrin-G knockdown does not

only decrease the migration rate of MDCK cells, but also affect their collective migration pattern. Again, at this point we are not clear about the mechanism how ankyrin-G affects cell migration, and how this may affect development in vivo.

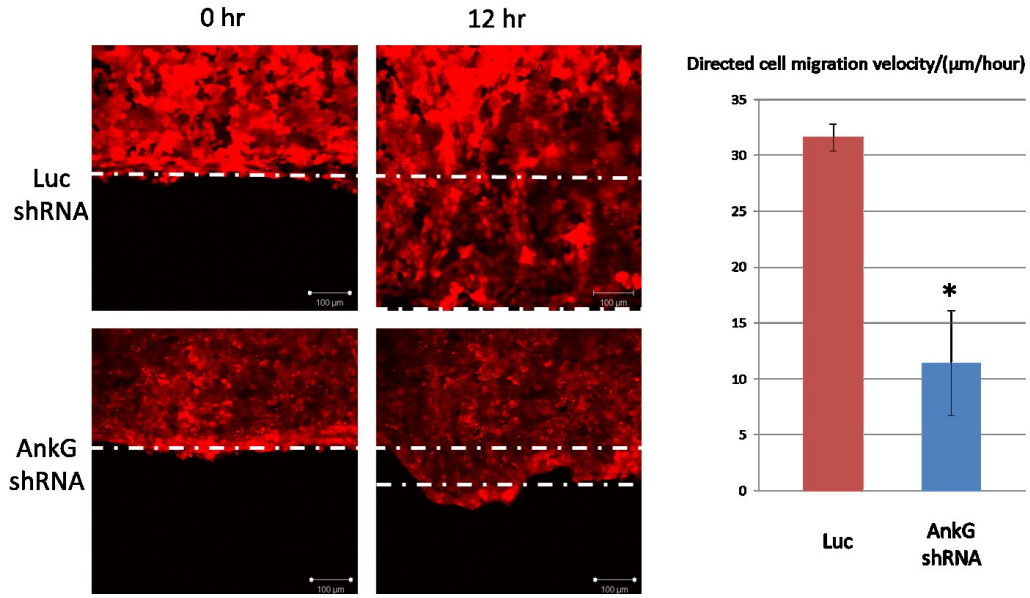

Figure 43: Knockdown of ankyrin-G in MDCK cells results in slower cell mobility.

shRNA stable cell lines were induced to knockdown ankyrin-G, or luciferase as a control, and then plated on MatTek plates. A wound was made across the monolayer, and live imaged for 12 hours, mCherry marking the shRNA expressing cells.

6.3 Conclusions

Even though it has been known for a decade that ankyrin-G localizes to neuronal axon initial segments and epithelial lateral membranes (Kizhatil and Bennett, 2004; Kordeli et al., 1995), it was unclear how it targets to those specialized membrane domains. In this thesis, we characterized ankyrin-G palmitoylation and its significance

in determining ankyrin-G targeting to diverse plasma membrane domains. Our work has solved this long-standing puzzle. Moreover, when ankyrin was first isolated from red blood cells, it exhibited a high level of hydrophobicity as a peripheral membrane protein (Bennett and Stenbuck, 1980), over 30 years after the initial observation, our finding provided a molecular explanation of these biochemical properties.

Following the identification of ankyrin-G palmitoylation, we also identified DHHC5 and DHHC8 as the physiological palmitoyl-transferases of ankyrin-G in MDCK cells. Those two palmitoyltransferases colocalize with ankyrin-G at the lateral membrane of columnar epithelial cells. The identification of DHHC5 and DHHC8 further improved our understanding about how ankyrin-G targeting and function is achieved through dynamic lipid modification. Another lipid input we identified that is critical for targeting beta II spectrin in MDCK cells is the phosphoinositide lipid. This co-incidence detection through protein-protein interaction and protein-lipid interaction further increases the complexity of the spectrin-ankyrin network, and may explain some of the discrepancies that were observed in different systems. Together, these findings expanded our vision about the spectrin-ankyrin network dynamics and how diverse lipid codes may be incorporated into this network to assemble membrane domains.

A striking observation in this thesis is that the palmitoyltransferases, ankyrin-G and beta II spectrin are not only functionally related, but also spatially co-patterned on the epithelial lateral membrane. The existence of such micron scale domains that are

enriched in functionally-related proteins suggests a new mechanism to understand the plasma membrane organization and function, which cannot be fully explained by the "fluid mosaic" model.

Along with the targeting mystery comes the function mystery. The requirement of ankyrin-G to assemble plasma membrane domains has been well-recognized for over a decade, but the molecular mechanism of how ankyrin-G is involved in this process was completely unknown (Bennett and Baines, 2001; Bennett and Healy, 2008; Bennett and Healy, 2009; Bennett and Lorenzo, 2013). Our work in this thesis, for the first time demonstrates the spectrin-ankyrin network maintains epithelial lateral membranes by opposing clathrin-mediated endocytosis. This finding does not only provide a mechanism for the spectrin-ankyrin-based plasma membrane domains, but also suggests a general principle for the cells to organize any plasma membrane domain: Instead of sorting and transporting proteins or lipid components to unique plasma membrane regions, the cells may simply utilize the protein transport pathways to deliver proteins evenly to all plasma membrane regions, and then selectively protect them from being internalized at specific regions to establish a specialized membrane domain.

References

Abdi, K.M., P.J. Mohler, J.Q. Davis, and V. Bennett. 2006. Isoform specificity of ankyrin-B: a site in the divergent C-terminal domain is required for intramolecular association. *The Journal of biological chemistry*. 281:5741-5749.

Agre, P., E.P. Orringer, D.H. Chui, and V. Bennett. 1981. A molecular defect in two families with hemolytic poikilocytic anemia: reduction of high affinity membrane binding sites for ankyrin. *J. Clin. Invest.* 68:1566-1576.

Aicart-Ramos, C., R.A. Valero, and I. Rodriguez-Crespo. 2011. Protein palmitoylation and subcellular trafficking. *Biochim. Biophys. Acta*. 1808:2981-2994.

Anderson, R.G., M.S. Brown, and J.L. Goldstein. 1977. Role of the coated endocytic vesicle in the uptake of receptor-bound low density lipoprotein in human fibroblasts. *Cell*. 10:351-364.

Anderson, R.G., E. Vasile, R.J. Mello, M.S. Brown, and J.L. Goldstein. 1978. Immunocytochemical visualization of coated pits and vesicles in human fibroblasts: relation to low density lipoprotein receptor distribution. *Cell*. 15:919-933.

Armbruster, B.N., S.S. Banik, C. Guo, A.C. Smith, and C.M. Counter. 2001. N-terminal domains of the human telomerase catalytic subunit required for enzyme activity in vivo. *Molecular and cellular biology*. 21:7775-7786.

Ayalon, G., J.Q. Davis, P.B. Scotland, and V. Bennett. 2008. An ankyrin-based mechanism for functional organization of dystrophin and dystroglycan. *Cell*. 135:1189-1200.

Ayalon, G., J.D. Hostettler, J. Hoffman, K. Kizhatil, J.Q. Davis, and V. Bennett. 2011. Ankyrin-B interactions with spectrin and dynactin-4 are required for dystrophin-based protection of skeletal muscle from exercise injury. *J. Biol. Chem.* 286:7370-7378.

Baines, A.J. 2009. Evolution of spectrin function in cytoskeletal and membrane networks. *Biochem. Soc. Trans.* 37:796-803.

Baines, A.J. 2010. The spectrin-ankyrin-4.1-adducin membrane skeleton: adapting eukaryotic cells to the demands of animal life. *Protoplasma*. 244:99-131.

Banaszynski, L.A., L.C. Chen, L.A. Maynard-Smith, A.G. Ooi, and T.J. Wandless. 2006. A rapid, reversible, and tunable method to regulate protein function in living cells using synthetic small molecules. *Cell*. 126:995-1004.

Banik, S.S., C. Guo, A.C. Smith, S.S. Margolis, D.A. Richardson, C.A. Tirado, and C.M. Counter. 2002. C-terminal regions of the human telomerase catalytic subunit essential for in vivo enzyme activity. *Molecular and cellular biology*. 22:6234-6246.

Banuelos, S., M. Saraste, and K. Djinovic Carugo. 1998. Structural comparisons of calponin homology domains: implications for actin binding. *Structure*. 6:1419-1431.

Baranes, D., D. Lederfein, Y.Y. Huang, M. Chen, C.H. Bailey, and E.R. Kandel. 1998. Tissue plasminogen activator contributes to the late phase of LTP and to synaptic growth in the hippocampal mossy fiber pathway. *Neuron*. 21:813-825.

Barroso, M., and E.S. Sztul. 1994. Basolateral to apical transcytosis in polarized cells is indirect and involves BFA and trimeric G protein sensitive passage through the apical endosome. *J. Cell Biol.* 124:83-100.

Bartels, D.J., D.A. Mitchell, X. Dong, and R.J. Deschenes. 1999. Erf2, a novel gene product that affects the localization and palmitoylation of Ras2 in Saccharomyces cerevisiae. *Mol. Cell. Biol.* 19:6775-6787.

Beck, K.A., J.A. Buchanan, V. Malhotra, and W.J. Nelson. 1994. Golgi spectrin: identification of an erythroid beta-spectrin homolog associated with the Golgi complex. *The Journal of cell biology*. 127:707-723.

Bennett, V. 1978. Purification of an active proteolytic fragment of the membrane attachment site for human erythrocyte spectrin. *J. Biol. Chem.* 253:2292-2299.

Bennett, V. 1979. Immunoreactive forms of human erythrocyte ankyrin are present in diverse cells and tissues. *Nature*. 281:597-599.

Bennett, V. 1982. The molecular basis for membrane - cytoskeleton association in human erythrocytes. *J. Cell. Biochem.* 18:49-65.

Bennett, V., and A.J. Baines. 2001. Spectrin and ankyrin-based pathways: metazoan inventions for integrating cells into tissues. *Physiol. Rev.* 81:1353-1392.

Bennett, V., and J. Davis. 1981. Erythrocyte ankyrin: immunoreactive analogues are associated with mitotic structures in cultured cells and with microtubules in brain. *Proc. Natl. Acad. Sci. U. S. A.* 78:7550-7554.

Bennett, V., J. Davis, and W.E. Fowler. 1982. Brain spectrin, a membrane-associated protein related in structure and function to erythrocyte spectrin. *Nature*. 299:126-131.

Bennett, V., and J. Healy. 2008. Organizing the fluid membrane bilayer: diseases linked to spectrin and ankyrin. *Trends Mol. Med.* 14:28-36.

Bennett, V., and J. Healy. 2009. Membrane domains based on ankyrin and spectrin associated with cell-cell interactions. *Cold Spring Harb Perspect Biol*. 1:a003012.

Bennett, V., and D.N. Lorenzo. 2013. Spectrin- and ankyrin-based membrane domains and the evolution of vertebrates. *Current topics in membranes*. 72:1-37.

Bennett, V., and P.J. Stenbuck. 1979. Identification and partial purification of ankyrin, the high affinity membrane attachment site for human erythrocyte spectrin. *J. Biol. Chem.* 254:2533-2541.

Bennett, V., and P.J. Stenbuck. 1980. Human erythrocyte ankyrin. Purification and properties. *J. Biol. Chem.* 255:2540-2548.

Benz, E.J., Jr. 2010. Learning about genomics and disease from the anucleate human red blood cell. *J. Clin. Invest.* 120:4204-4206.

Berchtold, D., and T.C. Walther. 2009. TORC2 plasma membrane localization is essential for cell viability and restricted to a distinct domain. *Mol. Biol. Cell*. 20:1565-1575.

Berghs, S., D. Aggujaro, R. Dirkx, Jr., E. Maksimova, P. Stabach, J.M. Hermel, J.P. Zhang, W. Philbrick, V. Slepnev, T. Ort, and M. Solimena. 2000. betaIV spectrin, a new spectrin localized at axon initial segments and nodes of ranvier in the central and peripheral nervous system. *J. Cell Biol.* 151:985-1002.

Biggs, D.S. 2010. 3D deconvolution microscopy. *Current protocols in cytometry / editorial board, J. Paul Robinson, managing editor ... [et al.]*. Chapter 12:Unit 12 19 11-20.

Boiko, T., M. Vakulenko, H. Ewers, C.C. Yap, C. Norden, and B. Winckler. 2007. Ankyrin-dependent and -independent mechanisms orchestrate axonal compartmentalization of L1 family members neurofascin and L1/neuron-glia cell adhesion molecule. *J Neurosci*. 27:590-603.

Bonifacino, J.S. 2014. Adaptor proteins involved in polarized sorting. *J. Cell Biol.* 204:7-17.

Bonifacino, J.S., and J. Lippincott-Schwartz. 2003. Coat proteins: shaping membrane transport. *Nat. Rev. Mol. Cell Biol.* 4:409-414.

Bonifacino, J.S., and L.M. Traub. 2003. Signals for sorting of transmembrane proteins to endosomes and lysosomes. *Annu. Rev. Biochem.* 72:395-447.

Brameshuber, M., J. Weghuber, V. Ruprecht, I. Gombos, I. Horvath, L. Vigh, P. Eckerstorfer, E. Kiss, H. Stockinger, and G.J. Schutz. 2010. Imaging of mobile long-lived nanoplatforms in the live cell plasma membrane. *J. Biol. Chem.* 285:41765-41771.

Brown, D.A., and E. London. 1998. Functions of lipid rafts in biological membranes. *Annu. Rev. Cell Dev. Biol.* 14:111-136.

Brown, D.A., and J.K. Rose. 1992. Sorting of GPI-anchored proteins to glycolipid-enriched membrane subdomains during transport to the apical cell surface. *Cell*. 68:533-544.

Brown, M.S., and J.L. Goldstein. 1976. Analysis of a mutant strain of human fibroblasts with a defect in the internalization of receptor-bound low density lipoprotein. *Cell*. 9:663-674.

Busche, S., E. Kremmer, and G. Posern. 2010. E-cadherin regulates MAL-SRF-mediated transcription in epithelial cells. *J Cell Sci*. 123:2803-2809.

Byers, T.J., and D. Branton. 1985. Visualization of the protein associations in the erythrocyte membrane skeleton. *Proc. Natl. Acad. Sci. U. S. A.* 82:6153-6157.

Cai, X., and Y. Zhang. 2006. Molecular evolution of the ankyrin gene family. *Mol. Biol. Evol.* 23:550-558.

Casanova, J.E., G. Apodaca, and K.E. Mostov. 1991. An autonomous signal for basolateral sorting in the cytoplasmic domain of the polymeric immunoglobulin receptor. *Cell*. 66:65-75.

Chan, W., E. Kordeli, and V. Bennett. 1993. 440-kD ankyrinB: structure of the major developmentally regulated domain and selective localization in unmyelinated axons. *J. Cell Biol.* 123:1463-1473.

Clarkson, Y.L., E.M. Perkins, C. Cairncross, A.R. Lyndon, P. Skehel, and M. Jackson. 2014. beta-III spectrin underpins ankyrin R function in Purkinje cell dendritic trees: protein complex critical for sodium channel activity is impaired by SCA5-associated mutations. *Hum. Mol. Genet.*

Cunha, S.R., S. Le Scouarnec, J.J. Schott, and P.J. Mohler. 2008. Exon organization and novel alternative splicing of the human ANK2 gene: implications for cardiac function and human cardiac disease. *Journal of molecular and cellular cardiology*. 45:724-734.

Das, A., C. Base, S. Dhulipala, and R.R. Dubreuil. 2006. Spectrin functions upstream of ankyrin in a spectrin cytoskeleton assembly pathway. *J. Cell Biol.* 175:325-335.

Das, A., C. Base, D. Manna, W. Cho, and R.R. Dubreuil. 2008. Unexpected complexity in the mechanisms that target assembly of the spectrin cytoskeleton. *J. Biol. Chem.* 283:12643-12653.

Davis, J.Q., S. Lambert, and V. Bennett. 1996. Molecular composition of the node of Ranvier: identification of ankyrin-binding cell adhesion molecules neurofascin (mucin+/third FNIII domain-) and NrCAM at nodal axon segments. *The Journal of cell biology*. 135:1355-1367.

Davis, L., K. Abdi, M. Machius, C. Brautigam, D.R. Tomchick, V. Bennett, and P. Michaely. 2009. Localization and structure of the ankyrin-binding site on beta2-spectrin. *J. Biol. Chem.* 284:6982-6987.

Davis, L.H., J.Q. Davis, and V. Bennett. 1992. Ankyrin regulation: an alternatively spliced segment of the regulatory domain functions as an intramolecular modulator. *The Journal of biological chemistry*. 267:18966-18972.

Dean, S.O., S.L. Rogers, N. Stuurman, R.D. Vale, and J.A. Spudich. 2005. Distinct pathways control recruitment and maintenance of myosin II at the cleavage furrow during cytokinesis. *Proc. Natl. Acad. Sci. U. S. A.* 102:13473-13478.

Deborde, S., E. Perret, D. Gravotta, A. Deora, S. Salvarezza, R. Schreiner, and E. Rodriguez-Boulan. 2008. Clathrin is a key regulator of basolateral polarity. *Nature*. 452:719-723.

Delint-Ramirez, I., D. Willoughby, G.V. Hammond, L.J. Ayling, and D.M. Cooper. 2011. Palmitoylation targets AKAP79 protein to lipid rafts and promotes its regulation of calcium-sensitive adenylyl cyclase type 8. *J Biol Chem*. 286:32962-32975.

Di Paolo, G., and P. De Camilli. 2006. Phosphoinositides in cell regulation and membrane dynamics. *Nature*. 443:651-657.

Djinovic Carugo, K., S. Banuelos, and M. Saraste. 1997. Crystal structure of a calponin homology domain. *Nat. Struct. Biol.* 4:175-179.

Drisdel, R.C., J.K. Alexander, A. Sayeed, and W.N. Green. 2006. Assays of protein palmitoylation. *Methods*. 40:127-134.

Duffield, A., H. Folsch, I. Mellman, and M.J. Caplan. 2004. Sorting of H,K-ATPase beta-subunit in MDCK and LLC-PK cells is independent of mu 1B adaptin expression. *Traffic*. 5:449-461.

Dzhashiashvili, Y., Y. Zhang, J. Galinska, I. Lam, M. Grumet, and J.L. Salzer. 2007. Nodes of Ranvier and axon initial segments are ankyrin G-dependent domains that assemble by distinct mechanisms. *J Cell Biol*. 177:857-870.

Edelman, E.J., Y. Maksimova, F. Duru, C. Altay, and P.G. Gallagher. 2007. A complex splicing defect associated with homozygous ankyrin-deficient hereditary spherocytosis. *Blood*. 109:5491-5493.

Edidin, M. 2003. The state of lipid rafts: from model membranes to cells. *Annu. Rev. Biophys. Biomol. Struct.* 32:257-283.

Even-Ram, S., A.D. Doyle, M.A. Conti, K. Matsumoto, R.S. Adelstein, and K.M. Yamada. 2007. Myosin IIA regulates cell motility and actomyosin-microtubule crosstalk. *Nat. Cell Biol.* 9:299-309.

Farias, G.G., L. Cuitino, X. Guo, X. Ren, M. Jarnik, R. Mattera, and J.S. Bonifacino. 2012. Signal-mediated, AP-1/clathrin-dependent sorting of transmembrane receptors to the somatodendritic domain of hippocampal neurons. *Neuron*. 75:810-823.

Fernandez-Hernando, C., M. Fukata, P.N. Bernatchez, Y. Fukata, M.I. Lin, D.S. Bredt, and W.C. Sessa. 2006. Identification of Golgi-localized acyl transferases that palmitoylate and regulate endothelial nitric oxide synthase. *J. Cell Biol.* 174:369-377.

Folsch, H., H. Ohno, J.S. Bonifacino, and I. Mellman. 1999. A novel clathrin adaptor complex mediates basolateral targeting in polarized epithelial cells. *Cell*. 99:189-198.

Folsch, H., M. Pypaert, S. Maday, L. Pelletier, and I. Mellman. 2003. The AP-1A and AP-1B clathrin adaptor complexes define biochemically and functionally distinct membrane domains. *J. Cell Biol.* 163:351-362.

Ford, M.G., B.M. Pearse, M.K. Higgins, Y. Vallis, D.J. Owen, A. Gibson, C.R. Hopkins, P.R. Evans, and H.T. McMahon. 2001. Simultaneous binding of PtdIns(4,5)P2 and clathrin by AP180 in the nucleation of clathrin lattices on membranes. *Science*. 291:1051-1055.

Forrester, M.T., D.T. Hess, J.W. Thompson, R. Hultman, M.A. Moseley, J.S. Stamler, and P.J. Casey. 2011. Site-specific analysis of protein S-acylation by resin-assisted capture. *J Lipid Res*. 52:393-398.

Fragoso, R., D. Ren, X. Zhang, M.W. Su, S.J. Burakoff, and Y.J. Jin. 2003. Lipid raft distribution of CD4 depends on its palmitoylation and association with Lck, and evidence for CD4-induced lipid raft aggregation as an additional mechanism to enhance CD3 signaling. *J Immunol*. 170:913-921.

Fukata, M., Y. Fukata, H. Adesnik, R.A. Nicoll, and D.S. Bredt. 2004. Identification of PSD-95 palmitoylating enzymes. *Neuron*. 44:987-996.

Fukata, Y., A. Dimitrov, G. Boncompain, O. Vielemeyer, F. Perez, and M. Fukata. 2013. Local palmitoylation cycles define activity-regulated postsynaptic subdomains. *J. Cell Biol.* 202:145-161.

Fukata, Y., and M. Fukata. 2010. Protein palmitoylation in neuronal development and synaptic plasticity. *Nat. Rev. Neurosci.* 11:161-175.

Fukata, Y., T. Iwanaga, and M. Fukata. 2006. Systematic screening for palmitoyl transferase activity of the DHHC protein family in mammalian cells. *Methods*. 40:177-182.

Gaidarov, I., and J.H. Keen. 1999. Phosphoinositide-AP-2 interactions required for targeting to plasma membrane clathrin-coated pits. *J. Cell Biol.* 146:755-764.

Galiano, M.R., S. Jha, T.S. Ho, C. Zhang, Y. Ogawa, K.J. Chang, M.C. Stankewich, P.J. Mohler, and M.N. Rasband. 2012. A Distal Axonal Cytoskeleton Forms an Intra-Axonal Boundary that Controls Axon Initial Segment Assembly. *Cell*. 149:1125-1139.

Gallagher, P.G., L.A. Steiner, R.I. Liem, A.N. Owen, A.P. Cline, N.E. Seidel, L.J. Garrett, and D.M. Bodine. 2010. Mutation of a barrier insulator in the human ankyrin-1 gene is associated with hereditary spherocytosis. *J. Clin. Invest.* 120:4453-4465.

Garbe, D.S., A. Das, R.R. Dubreuil, and G.J. Bashaw. 2007. beta-Spectrin functions independently of Ankyrin to regulate the establishment and maintenance of axon connections in the Drosophila embryonic CNS. *Development*. 134:273-284.

Glenney, J.R., Jr., P. Glenney, and K. Weber. 1983. The spectrin-related molecule, TW-260/240, cross-links the actin bundles of the microvillus rootlets in the brush borders of intestinal epithelial cells. *J. Cell Biol.* 96:1491-1496.

Goksoy, E., Y.Q. Ma, X. Wang, X. Kong, D. Perera, E.F. Plow, and J. Qin. 2008. Structural basis for the autoinhibition of talin in regulating integrin activation. *Mol. Cell*. 31:124-133.

Goldstein, J.L., and M.S. Brown. 1977. The low-density lipoprotein pathway and its relation to atherosclerosis. *Annu. Rev. Biochem.* 46:897-930.

Gomez, J.M., Y. Wang, and V. Riechmann. 2012. Tao controls epithelial morphogenesis by promoting Fasciclin 2 endocytosis. *J. Cell Biol.* 199:1131-1143.

Gravotta, D., J.M. Carvajal-Gonzalez, R. Mattera, S. Deborde, J.R. Banfelder, J.S. Bonifacino, and E. Rodriguez-Boulan. 2012. The clathrin adaptor AP-1A mediates basolateral polarity. *Dev. Cell*. 22:811-823.

Greaves, J., and L.H. Chamberlain. 2010. S-acylation by the DHHC protein family. *Biochemical Society transactions*. 38:522-524.

Greaves, J., and L.H. Chamberlain. 2011. Differential palmitoylation regulates intracellular patterning of SNAP25. *J. Cell Sci.* 124:1351-1360.

Grubb, M.S., and J. Burrone. 2010. Building and maintaining the axon initial segment. *Curr. Opin. Neurobiol.* 20:481-488.

Gumbiner, B., B. Stevenson, and A. Grimaldi. 1988. The role of the cell adhesion molecule uvomorulin in the formation and maintenance of the epithelial junctional complex. *J. Cell Biol.* 107:1575-1587.

Gundel, F., S. Eber, and A. Heep. 2011. A new ankyrin mutation (ANK1 EXON E9X) causing severe hereditary spherocytosis in the neonatal period. *Ann. Hematol.* 90:231-232.

Hall, T.G., and V. Bennett. 1987. Regulatory domains of erythrocyte ankyrin. *The Journal of biological chemistry*. 262:10537-10545.

Hammond, G.R., M.J. Fischer, K.E. Anderson, J. Holdich, A. Koteci, T. Balla, and R.F. Irvine. 2012. PI4P and PI(4,5)P2 are essential but independent lipid determinants of membrane identity. *Science*. 337:727-730.

Harris, T.J., and C.H. Siu. 2002. Reciprocal raft-receptor interactions and the assembly of adhesion complexes. *Bioessays*. 24:996-1003.

Hase, K., F. Nakatsu, M. Ohmae, K. Sugihara, N. Shioda, D. Takahashi, Y. Obata, Y. Furusawa, Y. Fujimura, T. Yamashita, S. Fukuda, H. Okamoto, M. Asano, S. Yonemura, and H. Ohno. 2013. AP-1B-mediated protein sorting regulates polarity and proliferation of intestinal epithelial cells in mice. *Gastroenterology*. 145:625-635.

He, M., P. Jenkins, and V. Bennett. 2012. Cysteine 70 of ankyrin-G is S-palmitoylated and is required for function of ankyrin-G in membrane domain assembly. *J. Biol. Chem.* 287:43995-44005.

Healy, J.A., K.R. Nilsson, H.E. Hohmeier, J. Berglund, J. Davis, J. Hoffman, M. Kohler, L.S. Li, P.O. Berggren, C.B. Newgard, and V. Bennett. 2010. Cholinergic augmentation of insulin release requires ankyrin-B. *Science signaling*. 3:ra19.

Hedstrom, K.L., Y. Ogawa, and M.N. Rasband. 2008. AnkyrinG is required for maintenance of the axon initial segment and neuronal polarity. *J. Cell Biol.* 183:635-640.

Hedstrom, K.L., X. Xu, Y. Ogawa, R. Frischknecht, C.I. Seidenbecher, P. Shrager, and M.N. Rasband. 2007. Neurofascin assembles a specialized extracellular matrix at the axon initial segment. *J. Cell Biol.* 178:875-886.

Heerklotz, H. 2002. Triton promotes domain formation in lipid raft mixtures. *Biophys. J.* 83:2693-2701.

Henis, Y.I., B. Rotblat, and Y. Kloog. 2006. FRAP beam-size analysis to measure palmitoylation-dependent membrane association dynamics and microdomain partitioning of Ras proteins. *Methods*. 40:183-190.

Hirst, J., and M.S. Robinson. 1998. Clathrin and adaptors. *Biochim. Biophys. Acta*. 1404:173-193.

Hoock, T.C., L.L. Peters, and S.E. Lux. 1997. Isoforms of ankyrin-3 that lack the NH2-terminal repeats associate with mouse macrophage lysosomes. *J. Cell Biol.* 136:1059-1070.

Hu, R.J., S. Moorthy, and V. Bennett. 1995. Expression of functional domains of beta G-spectrin disrupts epithelial morphology in cultured cells. *J. Cell Biol.* 128:1069-1080.

Hu, R.J., M. Watanabe, and V. Bennett. 1992. Characterization of human brain cDNA encoding the general isoform of beta-spectrin. *J. Biol. Chem.* 267:18715-18722.

Huang, H., P. Zhao, K. Arimatsu, K. Tabeta, K. Yamazaki, L. Krieg, E. Fu, T. Zhang, and X. Du. 2013. A deep intronic mutation in the ankyrin-1 gene causes diminished protein expression resulting in hemolytic anemia in mice. *G3*. 3:1687-1695.

Hull, R.N., W.R. Cherry, and G.W. Weaver. 1976. The origin and characteristics of a pig kidney cell strain, LLC-PK. *In Vitro*. 12:670-677.

Hund, T.J., O.M. Koval, J. Li, P.J. Wright, L. Qian, J.S. Snyder, H. Gudmundsson, C.F. Kline, N.P. Davidson, N. Cardona, M.N. Rasband, M.E. Anderson, and P.J. Mohler. 2010. A beta(IV)-spectrin/CaMKII signaling complex is essential for membrane excitability in mice. *J. Clin. Invest.* 120:3508-3519.

Hunziker, W., C. Harter, K. Matter, and I. Mellman. 1991. Basolateral sorting in MDCK cells requires a distinct cytoplasmic domain determinant. *Cell*. 66:907-920.

Hyvonen, M., M.J. Macias, M. Nilges, H. Oschkinat, M. Saraste, and M. Wilmanns. 1995. Structure of the binding site for inositol phosphates in a PH domain. *EMBO J.* 14:4676-4685.

Ipsaro, J.J., L. Huang, and A. Mondragon. 2009. Structures of the spectrin-ankyrin interaction binding domains. *Blood*. 113:5385-5393.

Ipsaro, J.J., and A. Mondragon. 2010. Structural basis for spectrin recognition by ankyrin. *Blood*. 115:4093-4101.

Iwanaga, T., R. Tsutsumi, J. Noritake, Y. Fukata, and M. Fukata. 2009. Dynamic protein palmitoylation in cellular signaling. *Prog. Lipid Res.* 48:117-127.

Jenkins, P.M., C. Vasavda, J. Hostettler, J.Q. Davis, K. Abdi, and V. Bennett. 2013. E-cadherin polarity is determined by a multifunction motif mediating lateral

membrane retention through ankyrin-G and apical-lateral transcytosis through clathrin. *J. Biol. Chem.* 288:14018-14031.

Jenkins, S.M., and V. Bennett. 2001. Ankyrin-G coordinates assembly of the spectrin-based membrane skeleton, voltage-gated sodium channels, and L1 CAMs at Purkinje neuron initial segments. *J. Cell Biol.* 155:739-746.

Jenkins, S.M., and V. Bennett. 2002. Developing nodes of Ranvier are defined by ankyrin-G clustering and are independent of paranodal axoglial adhesion. *Proceedings of the National Academy of Sciences of the United States of America*. 99:2303-2308.

Jennings, B.C., and M.E. Linder. 2012. DHHC protein S-acyltransferases use similar ping-pong kinetic mechanisms but display different acyl-CoA specificities. *J. Biol. Chem.* 287:7236-7245.

Johnson, J.L., J.W. Erickson, and R.A. Cerione. 2012. C-terminal di-arginine motif of Cdc42 protein is essential for binding to phosphatidylinositol 4,5-bisphosphate-containing membranes and inducing cellular transformation. *J. Biol. Chem.* 287:5764-5774.

Kaiser, H.W., E. O'Keefe, and V. Bennett. 1989. Adducin: Ca++-dependent association with sites of cell-cell contact. *J. Cell Biol.* 109:557-569.

Kalthoff, C., J. Alves, C. Urbanke, R. Knorr, and E.J. Ungewickell. 2002a. Unusual structural organization of the endocytic proteins AP180 and epsin 1. *J. Biol. Chem.* 277:8209-8216.

Kalthoff, C., S. Groos, R. Kohl, S. Mahrhold, and E.J. Ungewickell. 2002b. Clint: a novel clathrin-binding ENTH-domain protein at the Golgi. *Mol. Biol. Cell*. 13:4060-4073.

Kennedy, S.P., S.L. Warren, B.G. Forget, and J.S. Morrow. 1991. Ankyrin binds to the 15th repetitive unit of erythroid and nonerythroid beta-spectrin. *J. Cell Biol.* 115:267-277.

Kirchhausen, T. 1999. Adaptors for clathrin-mediated traffic. *Annu. Rev. Cell Dev. Biol.* 15:705-732.

Kizhatil, K., S.A. Baker, V.Y. Arshavsky, and V. Bennett. 2009a. Ankyrin-G promotes cyclic nucleotide-gated channel transport to rod photoreceptor sensory cilia. *Science*. 323:1614-1617.

Kizhatil, K., and V. Bennett. 2004. Lateral membrane biogenesis in human bronchial epithelial cells requires 190-kDa ankyrin-G. *J Biol Chem*. 279:16706-16714.

Kizhatil, K., J.Q. Davis, L. Davis, J. Hoffman, B.L. Hogan, and V. Bennett. 2007a. Ankyrin-G is a molecular partner of E-cadherin in epithelial cells and early embryos. *J Biol Chem*. 282:26552-26561.

Kizhatil, K., N.K. Sandhu, N.S. Peachey, and V. Bennett. 2009b. Ankyrin-B is required for coordinated expression of beta-2-spectrin, the Na/K-ATPase and the Na/Ca exchanger in the inner segment of rod photoreceptors. *Exp. Eye Res.* 88:57-64.

Kizhatil, K., W. Yoon, P.J. Mohler, L.H. Davis, J.A. Hoffman, and V. Bennett. 2007b. Ankyrin-G and beta2-spectrin collaborate in biogenesis of lateral membrane of human bronchial epithelial cells. *J. Biol. Chem.* 282:2029-2037.

Komada, M., and P. Soriano. 2002. [Beta]IV-spectrin regulates sodium channel clustering through ankyrin-G at axon initial segments and nodes of Ranvier. *J. Cell Biol.* 156:337-348.

Kordeli, E., J. Davis, B. Trapp, and V. Bennett. 1990. An isoform of ankyrin is localized at nodes of Ranvier in myelinated axons of central and peripheral nerves. *J. Cell Biol.* 110:1341-1352.

Kordeli, E., S. Lambert, and V. Bennett. 1995. AnkyrinG. A new ankyrin gene with neural-specific isoforms localized at the axonal initial segment and node of Ranvier. *J. Biol. Chem.* 270:2352-2359.

Koticha, D., P. Maurel, G. Zanazzi, N. Kane-Goldsmith, S. Basak, J. Babiarz, J. Salzer, and M. Grumet. 2006. Neurofascin interactions play a critical role in clustering sodium channels, ankyrin G and beta IV spectrin at peripheral nodes of Ranvier. *Dev. Biol.* 293:1-12.

Kunimoto, M. 1995. A neuron-specific isoform of brain ankyrin, 440-kD ankyrinB, is targeted to the axons of rat cerebellar neurons. *J. Cell Biol.* 131:1821-1829.

Kunimoto, M., E. Otto, and V. Bennett. 1991. A new 440-kD isoform is the major ankyrin in neonatal rat brain. *J. Cell Biol.* 115:1319-1331.

Kusumi, A., I. Koyama-Honda, and K. Suzuki. 2004. Molecular dynamics and interactions for creation of stimulation-induced stabilized rafts from small unstable steady-state rafts. *Traffic*. 5:213-230.

Kwiatkowska, K. 2010. One lipid, multiple functions: how various pools of PI(4,5)P(2) are created in the plasma membrane. *Cell. Mol. Life Sci.* 67:3927-3946.

Legendre, K., S. Safieddine, P. Kussel-Andermann, C. Petit, and A. El-Amraoui. 2008. alphaII-betaV spectrin bridges the plasma membrane and cortical lattice in the lateral wall of the auditory outer hair cells. *J. Cell Sci.* 121:3347-3356.

Lentz, B.R., D.A. Barrow, and M. Hoechli. 1980. Cholesterol-phosphatidylcholine interactions in multilamellar vesicles. *Biochemistry (Mosc.)*. 19:1943-1954.

Levental, I., M. Grzybek, and K. Simons. 2010. Greasing their way: lipid modifications determine protein association with membrane rafts. *Biochemistry*. 49:6305-6316.

Levine, J., and M. Willard. 1981. Fodrin: axonally transported polypeptides associated with the internal periphery of many cells. *The Journal of cell biology*. 90:631-642.

Li, Y., B.R. Martin, B.F. Cravatt, and S.L. Hofmann. 2012. DHHC5 protein palmitoylates flotillin-2 and is rapidly degraded on induction of neuronal differentiation in cultured cells. *J. Biol. Chem.* 287:523-530.

Lim, J.A., H.J. Baek, M.S. Jang, E.K. Choi, Y.M. Lee, S.J. Lee, S.C. Lim, J.Y. Kim, T.H. Kim, H.S. Kim, L. Mishra, and S.S. Kim. 2014. Loss of beta2-spectrin prevents cardiomyocyte differentiation and heart development. *Cardiovasc. Res.* 101:39-47.

Lin, H., L. Yue, and A.C. Spradling. 1994. The Drosophila fusome, a germline-specific organelle, contains membrane skeletal proteins and functions in cyst formation. *Development*. 120:947-956.

Linder, M.E., and R.J. Deschenes. 2007. Palmitoylation: policing protein stability and traffic. *Nat Rev Mol Cell Biol*. 8:74-84.

Lingwood, D., and K. Simons. 2010. Lipid rafts as a membrane-organizing principle. *Science*. 327:46-50.

Lise, S., Y. Clarkson, E. Perkins, A. Kwasniewska, E. Sadighi Akha, R.P. Schnekenberg, D. Suminaite, J. Hope, I. Baker, L. Gregory, A. Green, C. Allan, S. Lamble, S. Jayawant, G. Quaghebeur, M.Z. Cader, S. Hughes, R.J. Armstrong, A. Kanapin, A. Rimmer, G. Lunter, I. Mathieson, J.B. Cazier, D. Buck, J.C. Taylor, D. Bentley, G. McVean, P. Donnelly, S.J. Knight, M. Jackson, J. Ragoussis, and A.H. Nemeth. 2012. Recessive mutations in SPTBN2 implicate beta-III spectrin in both cognitive and motor development. *PLoS Genet.* 8:e1003074.

Liu, S.C., L.H. Derick, and J. Palek. 1987. Visualization of the hexagonal lattice in the erythrocyte membrane skeleton. *J. Cell Biol.* 104:527-536.

Lonergan, K.M., O. Iliopoulos, M. Ohh, T. Kamura, R.C. Conaway, J.W. Conaway, and W.G. Kaelin, Jr. 1998. Regulation of hypoxia-inducible mRNAs by the von Hippel-Lindau tumor suppressor protein requires binding to complexes containing elongins B/C and Cul2. *Molecular and cellular biology*. 18:732-741.

Lowe, J.S., O. Palygin, N. Bhasin, T.J. Hund, P.A. Boyden, E. Shibata, M.E. Anderson, and P.J. Mohler. 2008. Voltage-gated Nav channel targeting in the heart requires an ankyrin-G dependent cellular pathway. *J. Cell Biol.* 180:173-186.

Macia, E., M. Ehrlich, R. Massol, E. Boucrot, C. Brunner, and T. Kirchhausen. 2006. Dynasore, a cell-permeable inhibitor of dynamin. *Dev. Cell*. 10:839-850.

Macias, M.J., A. Musacchio, H. Ponstingl, M. Nilges, M. Saraste, and H. Oschkinat. 1994. Structure of the pleckstrin homology domain from beta-spectrin. *Nature*. 369:675-677.

Marsilio, E., S.H. Cheng, B. Schaffhausen, E. Paucha, and D.M. Livingston. 1991. The T/t common region of simian virus 40 large T antigen contains a distinct transformation-governing sequence. *Journal of virology*. 65:5647-5652.

Martin-Belmonte, F., A. Gassama, A. Datta, W. Yu, U. Rescher, V. Gerke, and K. Mostov. 2007. PTEN-mediated apical segregation of phosphoinositides controls epithelial morphogenesis through Cdc42. *Cell*. 128:383-397.

Martin, B.R., C. Wang, A. Adibekian, S.E. Tully, and B.F. Cravatt. 2012. Global profiling of dynamic protein palmitoylation. *Nat. Methods*. 9:84-89.

Martinez-Palomo, A., I. Meza, G. Beaty, and M. Cereijido. 1980. Experimental modulation of occluding junctions in a cultured transporting epithelium. *J. Cell Biol.* 87:736-745.

Mattey, D.L., and D.R. Garrod. 1986. Calcium-induced desmosome formation in cultured kidney epithelial cells. *J. Cell Sci.* 85:95-111.

Mazock, G.H., A. Das, C. Base, and R.R. Dubreuil. 2010. Transgene rescue identifies an essential function for Drosophila beta spectrin in the nervous system and a selective requirement for ankyrin-2-binding activity. *Mol. Biol. Cell*. 21:2860-2868.

Michaely, P., D.R. Tomchick, M. Machius, and R.G. Anderson. 2002. Crystal structure of a 12 ANK repeat stack from human ankyrinR. *EMBO J.* 21:6387-6396.

Miranda, K.C., T. Khromykh, P. Christy, T.L. Le, C.J. Gottardi, A.S. Yap, J.L. Stow, and R.D. Teasdale. 2001. A dileucine motif targets E-cadherin to the basolateral cell surface in Madin-Darby canine kidney and LLC-PK1 epithelial cells. *J. Biol. Chem.* 276:22565-22572.

Mohler, P.J., J.Q. Davis, and V. Bennett. 2005. Ankyrin-B coordinates the Na/K ATPase, Na/Ca exchanger, and InsP3 receptor in a cardiac T-tubule/SR microdomain. *PLoS Biol.* 3:e423.

Mohler, P.J., J.Q. Davis, L.H. Davis, J.A. Hoffman, P. Michaely, and V. Bennett. 2004a. Inositol 1,4,5-trisphosphate receptor localization and stability in neonatal cardiomyocytes requires interaction with ankyrin-B. *The Journal of biological chemistry*. 279:12980-12987.

Mohler, P.J., A.O. Gramolini, and V. Bennett. 2002a. The ankyrin-B C-terminal domain determines activity of ankyrin-B/G chimeras in rescue of abnormal inositol 1,4,5-trisphosphate and ryanodine receptor distribution in ankyrin-B (-/-) neonatal cardiomyocytes. *The Journal of biological chemistry*. 277:10599-10607.

Mohler, P.J., A.O. Gramolini, and V. Bennett. 2002b. The -B C-terminal domain determines activity of ankyrin-B/G chimeras in rescue of abnormal inositol 1,4,5-trisphosphate and ryanodine receptor distribution in ankyrin-B (-/-) neonatal cardiomyocytes. *The Journal of biological chemistry*. 277:10599-10607.

Mohler, P.J., J.A. Healy, H. Xue, A.A. Puca, C.F. Kline, R.R. Allingham, E.G. Kranias, H.A. Rockman, and V. Bennett. 2007a. Ankyrin-B syndrome: enhanced cardiac function balanced by risk of cardiac death and premature senescence. *PloS one*. 2:e1051.

Mohler, P.J., J.A. Hoffman, J.Q. Davis, K.M. Abdi, C.R. Kim, S.K. Jones, L.H. Davis, K.F. Roberts, and V. Bennett. 2004b. Isoform specificity among ankyrins. An amphipathic alpha-helix in the divergent regulatory domain of ankyrin-b interacts with the molecular co-chaperone Hdj1/Hsp40. *The Journal of biological chemistry*. 279:25798-25804.

Mohler, P.J., S. Le Scouarnec, I. Denjoy, J.S. Lowe, P. Guicheney, L. Caron, I.M. Driskell, J.J. Schott, K. Norris, A. Leenhardt, R.B. Kim, D. Escande, and D.M. Roden. 2007b. Defining the cellular phenotype of "ankyrin-B syndrome" variants: human

ANK2 variants associated with clinical phenotypes display a spectrum of activities in cardiomyocytes. *Circulation*. 115:432-441.

Mohler, P.J., I. Rivolta, C. Napolitano, G. LeMaillet, S. Lambert, S.G. Priori, and V. Bennett. 2004c. Nav1.5 E1053K mutation causing Brugada syndrome blocks binding to ankyrin-G and expression of Nav1.5 on the surface of cardiomyocytes. *Proc. Natl. Acad. Sci. U. S. A.* 101:17533-17538.

Mohler, P.J., J.J. Schott, A.O. Gramolini, K.W. Dilly, S. Guatimosim, W.H. duBell, L.S. Song, K. Haurogne, F. Kyndt, M.E. Ali, T.B. Rogers, W.J. Lederer, D. Escande, H. Le Marec, and V. Bennett. 2003. Ankyrin-B mutation causes type 4 long-QT cardiac arrhythmia and sudden cardiac death. *Nature*. 421:634-639.

Mohler, P.J., I. Splawski, C. Napolitano, G. Bottelli, L. Sharpe, K. Timothy, S.G. Priori, M.T. Keating, and V. Bennett. 2004d. A cardiac arrhythmia syndrome caused by loss of ankyrin-B function. *Proceedings of the National Academy of Sciences of the United States of America*. 101:9137-9142.

Mohler, P.J., W. Yoon, and V. Bennett. 2004e. Ankyrin-B targets beta2-spectrin to an intracellular compartment in neonatal cardiomyocytes. *The Journal of biological chemistry*. 279:40185-40193.

Mosher, R.A., W.E. Durrant, D. Wang, J. Song, and X. Dong. 2006. A comprehensive structure-function analysis of Arabidopsis SNI1 defines essential regions and transcriptional repressor activity. *The Plant cell*. 18:1750-1765.

Mostov, K.E., A. de Bruyn Kops, and D.L. Deitcher. 1986. Deletion of the cytoplasmic domain of the polymeric immunoglobulin receptor prevents basolateral localization and endocytosis. *Cell*. 47:359-364.

Motley, A., N.A. Bright, M.N. Seaman, and M.S. Robinson. 2003. Clathrin-mediated endocytosis in AP-2-depleted cells. *J. Cell Biol.* 162:909-918.

Mousavi, S.A., L. Malerod, T. Berg, and R. Kjeken. 2004. Clathrin-dependent endocytosis. *Biochem. J.* 377:1-16.

Munro, S. 2003. Lipid rafts: elusive or illusive? *Cell*. 115:377-388.

Nakatsu, F., J.M. Baskin, J. Chung, L.B. Tanner, G. Shui, S.Y. Lee, M. Pirruccello, M. Hao, N.T. Ingolia, M.R. Wenk, and P. De Camilli. 2012. PtdIns4P synthesis by PI4KIIIalpha at the plasma membrane and its impact on plasma membrane identity. *J. Cell Biol.* 199:1003-1016.

Nejsum, L.N., and W.J. Nelson. 2009. Epithelial cell surface polarity: the early steps. *Front Biosci (Landmark Ed)*. 14:1088-1098.

Nelson, W.J., R.W. Hammerton, A.Z. Wang, and E.M. Shore. 1990a. Involvement of the membrane-cytoskeleton in development of epithelial cell polarity. *Semin. Cell Biol.* 1:359-371.

Nelson, W.J., E.M. Shore, A.Z. Wang, and R.W. Hammerton. 1990b. Identification of a membrane-cytoskeletal complex containing the cell adhesion molecule uvomorulin (E-cadherin), ankyrin, and fodrin in Madin-Darby canine kidney epithelial cells. *J. Cell Biol.* 110:349-357.

Nelson, W.J., and P.J. Veshnock. 1987. Ankyrin binding to (Na+ + K+)ATPase and implications for the organization of membrane domains in polarized cells. *Nature*. 328:533-536.

Ohara, O., R. Ohara, H. Yamakawa, D. Nakajima, and M. Nakayama. 1998. Characterization of a new beta-spectrin gene which is predominantly expressed in brain. *Brain Res. Mol. Brain Res.* 57:181-192.

Ohno, H., T. Tomemori, F. Nakatsu, Y. Okazaki, R.C. Aguilar, H. Foelsch, I. Mellman, T. Saito, T. Shirasawa, and J.S. Bonifacino. 1999. Mu1B, a novel adaptor medium chain expressed in polarized epithelial cells. *FEBS Lett.* 449:215-220.

Ohno, Y., A. Kihara, T. Sano, and Y. Igarashi. 2006. Intracellular localization and tissue-specific distribution of human and yeast DHHC cysteine-rich domain-containing proteins. *Biochim. Biophys. Acta*. 1761:474-483.

Padron, D., Y.J. Wang, M. Yamamoto, H. Yin, and M.G. Roth. 2003. Phosphatidylinositol phosphate 5-kinase Ibeta recruits AP-2 to the plasma membrane and regulates rates of constitutive endocytosis. *J. Cell Biol.* 162:693-701.

Papal, S., M. Cortese, K. Legendre, N. Sorusch, J. Dragavon, I. Sahly, S. Shorte, U. Wolfrum, C. Petit, and A. El-Amraoui. 2013. The giant spectrin betaV couples the molecular motors to phototransduction and Usher syndrome type I proteins along their trafficking route. *Hum. Mol. Genet.* 22:3773-3788.

Parkinson, N.J., C.L. Olsson, J.L. Hallows, J. McKee-Johnson, B.P. Keogh, K. Noben-Trauth, S.G. Kujawa, and B.L. Tempel. 2001. Mutant beta-spectrin 4 causes auditory and motor neuropathies in quivering mice. *Nat. Genet.* 29:61-65.

Pearse, B.M. 1975. Coated vesicles from pig brain: purification and biochemical characterization. *J. Mol. Biol.* 97:93-98.

Peters, L.L., K.M. John, F.M. Lu, E.M. Eicher, A. Higgins, M. Yialamas, L.C. Turtzo, A.J. Otsuka, and S.E. Lux. 1995. Ank3 (epithelial ankyrin), a widely distributed new member of the ankyrin gene family and the major ankyrin in kidney, is expressed in alternatively spliced forms, including forms that lack the repeat domain. *J. Cell Biol.* 130:313-330.

Pizzo, P., E. Giurisato, M. Tassi, A. Benedetti, T. Pozzan, and A. Viola. 2002. Lipid rafts and T cell receptor signaling: a critical re-evaluation. *Eur. J. Immunol.* 32:3082-3091.

Rameh, L.E., A. Arvidsson, K.L. Carraway, 3rd, A.D. Couvillon, G. Rathbun, A. Crompton, B. VanRenterghem, M.P. Czech, K.S. Ravichandran, S.J. Burakoff, D.S. Wang, C.S. Chen, and L.C. Cantley. 1997. A comparative analysis of the phosphoinositide binding specificity of pleckstrin homology domains. *J. Biol. Chem.* 272:22059-22066.

Rasband, M.N. 2011. Composition, assembly, and maintenance of excitable membrane domains in myelinated axons. *Semin. Cell Dev. Biol.* 22:178-184.

Ren, Q., and V. Bennett. 1998. Palmitoylation of neurofascin at a site in the membrane-spanning domain highly conserved among the L1 family of cell adhesion molecules. *J Neurochem*. 70:1839-1849.

Rocks, O., M. Gerauer, N. Vartak, S. Koch, Z.P. Huang, M. Pechlivanis, J. Kuhlmann, L. Brunsveld, A. Chandra, B. Ellinger, H. Waldmann, and P.I. Bastiaens. 2010. The palmitoylation machinery is a spatially organizing system for peripheral membrane proteins. *Cell*. 141:458-471.

Rodriguez Boulan, E., and D.D. Sabatini. 1978. Asymmetric budding of viruses in epithelial monlayers: a model system for study of epithelial polarity. *Proc. Natl. Acad. Sci. U. S. A.* 75:5071-5075.

Roduit, C., F.G. van der Goot, P. De Los Rios, A. Yersin, P. Steiner, G. Dietler, S. Catsicas, F. Lafont, and S. Kasas. 2008. Elastic membrane heterogeneity of living cells revealed by stiff nanoscale membrane domains. *Biophys. J.* 94:1521-1532.

Rohde, G., D. Wenzel, and V. Haucke. 2002. A phosphatidylinositol (4,5)-bisphosphate binding site within mu2-adaptin regulates clathrin-mediated endocytosis. *J. Cell Biol.* 158:209-214.

Roth, A.F., Y. Feng, L. Chen, and N.G. Davis. 2002. The yeast DHHC cysteine-rich domain protein Akr1p is a palmitoyl transferase. *J. Cell Biol.* 159:23-28.

Salaun, C., J. Greaves, and L.H. Chamberlain. 2010. The intracellular dynamic of protein palmitoylation. *J Cell Biol*. 191:1229-1238.

Salle, L., and F. Brette. 2007. T-tubules: a key structure of cardiac function and dysfunction. *Arch. Mal. Coeur Vaiss.* 100:225-230.

Sangerman, J., Y. Maksimova, E.J. Edelman, J.S. Morrow, B.G. Forget, and P.G. Gallagher. 2008. Ankyrin-linked hereditary spherocytosis in an African-American kindred. *Am. J. Hematol.* 83:789-794.

Santangelo, P.J., A.W. Lifland, P. Curt, Y. Sasaki, G.J. Bassell, M.E. Lindquist, and J.E. Crowe, Jr. 2009. Single molecule-sensitive probes for imaging RNA in live cells. *Nat. Methods*. 6:347-349.

Sato, T., S. Mushiake, Y. Kato, K. Sato, M. Sato, N. Takeda, K. Ozono, K. Miki, Y. Kubo, A. Tsuji, R. Harada, and A. Harada. 2007. The Rab8 GTPase regulates apical protein localization in intestinal cells. *Nature*. 448:366-369.

Scotland, P., D. Zhou, H. Benveniste, and V. Bennett. 1998. Nervous system defects of AnkyrinB (-/-) mice suggest functional overlap between the cell adhesion molecule L1 and 440-kD AnkyrinB in premyelinated axons. *The Journal of cell biology*. 143:1305-1315.

Sellers, W.R., B.G. Novitch, S. Miyake, A. Heith, G.A. Otterson, F.J. Kaye, A.B. Lassar, and W.G. Kaelin, Jr. 1998. Stable binding to E2F is not required for the retinoblastoma protein to activate transcription, promote differentiation, and suppress tumor cell growth. *Genes & development*. 12:95-106.

Sezgin, E., and P. Schwille. 2011. Fluorescence techniques to study lipid dynamics. *Cold Spring Harb. Perspect. Biol.* 3:a009803.

Shafaq-Zadah, M., L. Brocard, F. Solari, and G. Michaux. 2012. AP-1 is required for the maintenance of apico-basal polarity in the C. elegans intestine. *Development*. 139:2061-2070.

Shewan, A., D.J. Eastburn, and K. Mostov. 2011. Phosphoinositides in cell architecture. *Cold Spring Harb. Perspect. Biol.* 3:a004796.

Shotton, D.M., B.E. Burke, and D. Branton. 1979. The molecular structure of human erythrocyte spectrin. Biophysical and electron microscopic studies. *J. Mol. Biol.* 131:303-329.

Sibarita, J.B. 2005. Deconvolution microscopy. *Adv. Biochem. Eng. Biotechnol.* 95:201-243.

Siliciano, J.D., and D.A. Goodenough. 1988. Localization of the tight junction protein, ZO-1, is modulated by extracellular calcium and cell-cell contact in Madin-Darby canine kidney epithelial cells. *J Cell Biol*. 107:2389-2399.

Simons, K., and M.J. Gerl. 2010. Revitalizing membrane rafts: new tools and insights. *Nat. Rev. Mol. Cell Biol.* 11:688-699.

Simons, K., and J.L. Sampaio. 2011. Membrane organization and lipid rafts. *Cold Spring Harb. Perspect. Biol.* 3:a004697.

Simons, K., and D. Toomre. 2000. Lipid rafts and signal transduction. *Nat. Rev. Mol. Cell Biol.* 1:31-39.

Simons, K., and G. van Meer. 1988. Lipid sorting in epithelial cells. *Biochemistry (Mosc.).* 27:6197-6202.

Simons, K., and W.L. Vaz. 2004. Model systems, lipid rafts, and cell membranes. *Annu. Rev. Biophys. Biomol. Struct.* 33:269-295.

Singer, S.J., and G.L. Nicolson. 1972. The fluid mosaic model of the structure of cell membranes. *Science*. 175:720-731.

Sobotzik, J.M., J.M. Sie, C. Politi, D. Del Turco, V. Bennett, T. Deller, and C. Schultz. 2009. AnkyrinG is required to maintain axo-dendritic polarity in vivo. *Proceedings of the National Academy of Sciences of the United States of America*. 106:17564-17569.

Spira, F., N.S. Mueller, G. Beck, P. von Olshausen, J. Beig, and R. Wedlich-Soldner. 2012. Patchwork organization of the yeast plasma membrane into numerous coexisting domains. *Nat. Cell Biol.* 14:640-648.

Stabach, P.R., and J.S. Morrow. 2000. Identification and characterization of beta V spectrin, a mammalian ortholog of Drosophila beta H spectrin. *J. Biol. Chem.* 275:21385-21395.

Stabach, P.R., I. Simonovic, M.A. Ranieri, M.S. Aboodi, T.A. Steitz, M. Simonovic, and J.S. Morrow. 2009. The structure of the ankyrin-binding site of beta-spectrin

reveals how tandem spectrin-repeats generate unique ligand-binding properties. *Blood*. 113:5377-5384.

Stankewich, M.C., W.T. Tse, L.L. Peters, Y. Ch'ng, K.M. John, P.R. Stabach, P. Devarajan, J.S. Morrow, and S.E. Lux. 1998. A widely expressed betaIII spectrin associated with Golgi and cytoplasmic vesicles. *Proc. Natl. Acad. Sci. U. S. A.* 95:14158-14163.

Staufenbiel, M. 1987. Ankyrin-bound fatty acid turns over rapidly at the erythrocyte plasma membrane. *Mol Cell Biol*. 7:2981-2984.

Staufenbiel, M. 1988. Fatty acids covalently bound to erythrocyte proteins undergo a differential turnover in vivo. *J Biol Chem*. 263:13615-13622.

Straight, A.F., C.M. Field, and T.J. Mitchison. 2005. Anillin binds nonmuscle myosin II and regulates the contractile ring. *Mol. Biol. Cell*. 16:193-201.

Susuki, K., K.J. Chang, D.R. Zollinger, Y. Liu, Y. Ogawa, Y. Eshed-Eisenbach, M.T. Dours-Zimmermann, J.A. Oses-Prieto, A.L. Burlingame, C.I. Seidenbecher, D.R. Zimmermann, T. Oohashi, E. Peles, and M.N. Rasband. 2013. Three mechanisms assemble central nervous system nodes of Ranvier. *Neuron*. 78:469-482.

Takahashi, D., K. Hase, S. Kimura, F. Nakatsu, M. Ohmae, Y. Mandai, T. Sato, Y. Date, M. Ebisawa, T. Kato, Y. Obata, S. Fukuda, Y.I. Kawamura, T. Dohi, T. Katsuno, O. Yokosuka, S. Waguri, and H. Ohno. 2011. The epithelia-specific membrane trafficking factor AP-1B controls gut immune homeostasis in mice. *Gastroenterology*. 141:621-632.

Takei, K., and V. Haucke. 2001. Clathrin-mediated endocytosis: membrane factors pull the trigger. *Trends Cell Biol.* 11:385-391.

Tang, Y., V. Katuri, A. Dillner, B. Mishra, C.X. Deng, and L. Mishra. 2003. Disruption of transforming growth factor-beta signaling in ELF beta-spectrin-deficient mice. *Science*. 299:574-577.

Tang, Y., V. Katuri, R. Srinivasan, F. Fogt, R. Redman, G. Anand, A. Said, T. Fishbein, M. Zasloff, E.P. Reddy, B. Mishra, and L. Mishra. 2005. Transforming growth factor-beta suppresses nonmetastatic colon cancer through Smad4 and adaptor protein ELF at an early stage of tumorigenesis. *Cancer Res.* 65:4228-4237.

Thomas, G.M., T. Hayashi, S.L. Chiu, C.M. Chen, and R.L. Huganir. 2012. Palmitoylation by DHHC5/8 targets GRIP1 to dendritic endosomes to regulate AMPA-R trafficking. *Neuron*. 73:482-496.

Thompson, A., R. Nessler, D. Wisco, E. Anderson, B. Winckler, and D. Sheff. 2007. Recycling endosomes of polarized epithelial cells actively sort apical and basolateral cargos into separate subdomains. *Mol. Biol. Cell*. 18:2687-2697.

Trave, G., A. Pastore, M. Hyvonen, and M. Saraste. 1995. The C-terminal domain of alpha-spectrin is structurally related to calmodulin. *Eur. J. Biochem.* 227:35-42.

Tsui-Pierchala, B.A., M. Encinas, J. Milbrandt, and E.M. Johnson, Jr. 2002. Lipid rafts in neuronal signaling and function. *Trends Neurosci.* 25:412-417.

Tsutsumi, R., Y. Fukata, J. Noritake, T. Iwanaga, F. Perez, and M. Fukata. 2009. Identification of G protein alpha subunit-palmitoylating enzyme. *Mol. Cell. Biol.* 29:435-447.

von Bonsdorff, C.H., S.D. Fuller, and K. Simons. 1985. Apical and basolateral endocytosis in Madin-Darby canine kidney (MDCK) cells grown on nitrocellulose filters. *EMBO J.* 4:2781-2792.

Wang, C., C. Yu, F. Ye, Z. Wei, and M. Zhang. 2012. Structure of the ZU5-ZU5-UPA-DD tandem of ankyrin-B reveals interaction surfaces necessary for ankyrin function. *Proceedings of the National Academy of Sciences of the United States of America*. 109:4822-4827.

Wang, D.S., R. Miller, R. Shaw, and G. Shaw. 1996. The pleckstrin homology domain of human beta I sigma II spectrin is targeted to the plasma membrane in vivo. *Biochem. Biophys. Res. Commun.* 225:420-426.

Wang, D.S., and G. Shaw. 1995. The association of the C-terminal region of beta I sigma II spectrin to brain membranes is mediated by a PH domain, does not require membrane proteins, and coincides with a inositol-1,4,5 triphosphate binding site. *Biochem. Biophys. Res. Commun.* 217:608-615.

Wang, E., P.S. Brown, B. Aroeti, S.J. Chapin, K.E. Mostov, and K.W. Dunn. 2000. Apical and basolateral endocytic pathways of MDCK cells meet in acidic common endosomes distinct from a nearly-neutral apical recycling endosome. *Traffic*. 1:480-493.

Wiederschain, D., S. Wee, L. Chen, A. Loo, G. Yang, A. Huang, Y. Chen, G. Caponigro, Y.M. Yao, C. Lengauer, W.R. Sellers, and J.D. Benson. 2009. Single-vector inducible lentiviral RNAi system for oncology target validation. *Cell Cycle*. 8:498-504.

Wilson, I.A., D.H. Haft, E.D. Getzoff, J.A. Tainer, R.A. Lerner, and S. Brenner. 1985. Identical short peptide sequences in unrelated proteins can have different conformations: a testing ground for theories of immune recognition. *Proceedings of the National Academy of Sciences of the United States of America*. 82:5255-5259.

Winkelmann, J.C., J.G. Chang, W.T. Tse, A.L. Scarpa, V.T. Marchesi, and B.G. Forget. 1990a. Full-length sequence of the cDNA for human erythroid beta-spectrin. *J. Biol. Chem.* 265:11827-11832.

Winkelmann, J.C., F.F. Costa, B.L. Linzie, and B.G. Forget. 1990b. Beta spectrin in human skeletal muscle. Tissue-specific differential processing of 3' beta spectrin pre-mRNA generates a beta spectrin isoform with a unique carboxyl terminus. *J. Biol. Chem.* 265:20449-20454.

Winkelmann, J.C., and B.G. Forget. 1993. Erythroid and nonerythroid spectrins. *Blood*. 81:3173-3185.

Xu, K., G. Zhong, and X. Zhuang. 2013. Actin, spectrin, and associated proteins form a periodic cytoskeletal structure in axons. *Science*. 339:452-456.

Yang, F., Q. Wei, R.S. Adelstein, and P.J. Wang. 2012. Non-muscle myosin IIB is essential for cytokinesis during male meiotic cell divisions. *Dev. Biol.* 369:356-361.

Yang, Y., Y. Ogawa, K.L. Hedstrom, and M.N. Rasband. 2007. betaIV spectrin is recruited to axon initial segments and nodes of Ranvier by ankyrinG. *J. Cell Biol.* 176:509-519.

Yu, J., D.A. Fischman, and T.L. Steck. 1973. Selective solubilization of proteins and phospholipids from red blood cell membranes by nonionic detergents. *J. Supramol. Struct.* 1:233-248.

Zhang, C., K. Susuki, D.R. Zollinger, J.L. Dupree, and M.N. Rasband. 2013. Membrane domain organization of myelinated axons requires betaII spectrin. *J. Cell Biol.* 203:437-443.

Zhang, H., A. Kim, N. Abraham, L.A. Khan, D.H. Hall, J.T. Fleming, and V. Gobel. 2012. Clathrin and AP-1 regulate apical polarity and lumen formation during C. elegans tubulogenesis. *Development*. 139:2071-2083.

Zhang, X., and V. Bennett. 1998. Restriction of 480/270-kD ankyrin G to axon proximal segments requires multiple ankyrin G-specific domains. *J. Cell Biol.* 142:1571-1581.

Zhang, X., J.Q. Davis, S. Carpenter, and V. Bennett. 1998. Structural requirements for association of neurofascin with ankyrin. *The Journal of biological chemistry*. 273:30785-30794.

Zhou, D., S. Lambert, P.L. Malen, S. Carpenter, L.M. Boland, and V. Bennett. 1998. AnkyrinG is required for clustering of voltage-gated Na channels at axon initial segments and for normal action potential firing. *J. Cell Biol.* 143:1295-1304.

Biography

Meng He was born in the city of Bozhou, Anhui Province, China on March 10th, 1986. He received his bachelor degree from the Department of Biological Science and Biotechnology at Tsinghua University in Beijing in July, 2009. He then decided to pursue a PhD degree in biomedical science, and was admitted to the Molecular Cancer Biology Program at Duke University in 2009. He finished his PhD training with Dr. Vann Bennett in 2014.

Membership

- American Society for Cell Biology, 2011-2012
- American Association for the Advancement of Science, 2011-present

Publications

- Jenkins, P., **He, M. (co-first author)**, and V. Bennett. 2014. Ankyrin-G and βII-spectrin control MDCK cell lateral membrane height by opposing clathrin-mediated endocytosis. (In submission)

- **He, M.,** K. M. Abdi, and V. Bennett. 2014. Ankyrin-G palmitoylation and βII-spectrin binding to PI(4,5)P2 drive lateral membrane assembly. Journal of Cell Biology. (Under peer review)

- **He, M.,** W.C. Tseng, and V. Bennett. 2013. A single divergent exon inhibits ankyrin-B association with the plasma membrane. Journal of Biological Chemistry. 288:14769-14779.

- **He, M.,** P. Jenkins, and V. Bennett. 2012. Cysteine 70 of ankyrin-G is S-palmitoylated and is required for function of ankyrin-G in membrane domain assembly. Journal of Biological Chemistry. 287:43995-44005.